Global Sea Level Budget 1993-Present

WCRP Global Sea Level Budget Group*

*A full list of authors and their affiliations appears at the end of the paper

Revised version
23 July 2018

Corresponding author: Anny Cazenave, LEGOS, 18 Avenue Edouard Belin, 31401 Toulouse, Cedex 9, France; anny.cazenave@legos.obs-mip.fr

Abstract

Global mean sea level is an integral of changes occurring in the climate system in response to unforced climate variability as well as natural and anthropogenic forcing factors. Its temporal evolution allows detecting changes (e.g., acceleration) in one or more components. Study of the sea level budget provides constraints on missing or poorly known contributions, such as the unsurveyed deep ocean or the still uncertain land water component. In the context of the World Climate Research Programme Grand Challenge entitled "Regional Sea Level and Coastal Impacts", an international effort involving the sea level community worldwide has been recently initiated with the objective of assessing the various data sets used to estimate components of the sea level budget during the altimetry era (1993 to present). These data sets are based on the combination of a broad range of space-based and in situ observations, model estimates and algorithms. Evaluating their quality, quantifying uncertainties and identifying sources of discrepancies between component estimates is extremely useful for various applications in climate research. This effort involves several tens of scientists from about fifty research teams/institutions worldwide (www.wcrp-climate.org/grand-challenges/gc-sea-level). The results presented in this paper are a synthesis of the first assessment performed during 2017-2018. We present estimates of the altimetry-based global mean sea level (average rate of 3.1 +/- 0.3 mm/yr and acceleration of 0.1 mm/yr^2 over 1993-present), as well as of the different components of the sea level budget (http://doi.org/10.17882/54854). We further examine closure of the sea level budget, comparing the observed global mean sea level with the sum of components. Ocean thermal expansion, glaciers, Greenland and Antarctica contribute by 42%, 21%, 15% and 8% to the global mean sea level over the 1993-present. We also study the sea level budget over 2005-present, using GRACE-based ocean mass estimates instead of sum of individual mass components. Our results demonstrate that the global mean sea level can be closed to within 0.3 mm/yr (one sigma). Substantial uncertainty remains for the land water storage component, as shown in examining individual mass contributions to sea level.

1. Introduction

Global warming has already several visible consequences, in particular increase of the Earth's mean surface temperature and ocean heat content (Rhein et al., 2013, Stocker et al., 2013), melting of sea ice, loss of mass of glaciers (Gardner et al., 2013), and ice mass loss from the Greenland and Antarctica ice sheets (Rignot et al., 2011, Shepherd et al., 2012). On average over the last 50 years, about 93% of heat excess accumulated in the climate system because of greenhouse gas emissions has been stored in the ocean, and the remaining 7% has been warming the atmosphere and continents, and melting sea and land ice (von Schuckmann et al., 2016). Because of ocean warming and land ice mass loss, sea level rises. Since the end of the last deglaciation about 3000 years ago, sea level remained nearly constant (e.g., Lambeck et al., 2010, Kemp et al., 2011, Kopp et al. 2014). However, direct observations from in situ tide gauges available since the mid-to-late 19th century show that the 20th century global mean sea level has started to rise again at a rate of 1.2 mm/yr to 1.9 mm/yr (Church and White, 2011, Jevrejeva et al., 2014a, Hay et al., 2015, Dangendorf et al., 2017). Since the early 1990s sea level rise is measured by high-precision altimeter satellites and the rate has increased to ~3 mm/yr on average (Legeais et al., 2018, Nerem et al., 2018).

Accurate assessment of present-day global mean sea level variations and its components (ocean thermal expansion, ice sheet mass loss, glaciers mass change, changes in land water storage, etc.) is important for many reasons. The global mean sea level is an integral of changes occurring in the Earth's climate system in response to unforced climate variability as well as natural and anthropogenic forcing factors e.g., net contribution of ocean warming, land ice mass loss, and changes in water storage in continental river basins. Temporal changes of the components are directly reflected in the global mean sea level curve. If accurate enough, study of the sea level budget provides constraints on missing or poorly known contributions, e.g., the deep ocean or polar regions under sampled by current observing systems, or still uncertain changes in water storage on land due to human activities (e.g. ground water depletion in aquifers). Global mean sea level corrected for ocean mass change in principle allows one to independently estimate temporal changes in total ocean heat content, from which the Earth's energy imbalance can be deduced (von Schuckmann et al., 2016). The sea level and/or ocean mass budget approach can also be used to constrain models of Glacial Isostatic Adjustment (GIA). The GIA phenomenon has significant impact on the interpretation of GRACE-based space gravimetry data over the oceans (for ocean mass change) and over Antarctica (for ice sheet mass balance). However, there is still incomplete

consensus on best estimates, a result of uncertainties in deglaciation models and mantle viscosity structure. Finally, observed changes of the global mean sea level and its components are fundamental for validating climate models used for projections.

In the context of the Grand Challenge entitled "Regional Sea Level and Coastal Impacts" of the World Climate Research Programme (WCRP), an international effort involving the sea level community worldwide has been recently initiated with the objective of assessing the sea level budget during the altimetry era (1993 to present). To estimate the different components of the sea level budget, different data sets are used. These are based on the combination of a broad range of space-based and in situ observations. Evaluating their quality, quantifying their uncertainties, and identifying the sources of discrepancies between component estimates, including the altimetry-based sea level time series, are extremely useful for various applications in climate research.

Several previous studies have addressed the sea level budget over different time spans and using different data sets. For example, Munk (2002) found that the 20th century sea-level rise could not be closed with the data available at that time and showed that if the missing contribution were due to polar ice melt, this would be in conflict with external astronomical constraints. The enigma has been resolved in two ways. Firstly, an improved theory of rotational stability of the Earth (Mitrovica et al., 2006) effectively removed the constraints proposed by Munk (2002), and allows a polar ice sheet contribution to 20th century sea-level rise of as much as ~1.1 mm/yr, with about 0.8 mm/yr beginning in the 20th century. In addition, more recent studies by Gregory et al. (2013) and Slangen et al. (2017), combining observations with model estimates, showed that it was possible to effectively close the 20th century sea level budget within uncertainties. For the altimetry era, many studies have investigated closure of the sea level budget (e.g., Cazenave et al., 2009, Leuliette and Willis, 2010, Church and White, 2011, Chambers et al., 2017, Dieng et al., 2017, Chen et al., 2017, Nerem et al., 2018). Assessments of the published literature have also been performed in past IPCC (Intergovernmental Panel on Climate Change) reports (e.g., Church et al., 2013). Building on these previous works, here we intend to provide a collective update of the global mean sea level budget, involving the many groups worldwide interested in present-day sea level rise and its components. We focus on observations rather than model-based estimates and consider the high-precision altimetry era starting in 1993 that includes the period since the mid-2000s where new observing systems, like the Argo float project (Roemmich et al., 2012) and the GRACE space gravimetry mission (Tapley et al., 2004) that provide improved

data sets of high value for such a study. Only the global mean budget is considered here. Regional budget will be the focus of a future assessment.

Section 2 describes for each component of the sea level budget equation the different data sets used to estimate the corresponding contribution to sea level, discusses associated errors and provides trend estimates for the two periods. Section 3 addresses the mass and sea level budgets over the study periods. A discussion is provided in Section 4, followed by a conclusion.

2. Methods and Data

In this section, we briefly present the global mean sea level budget (sub section 2.1), then provide, for each term of the budget equation, an assessment of the most up-to-date published results. Multiple organizations and research groups routinely generate the basic measurements as well as the derived data sets and products used to study the sea level budget. Sub-sections 2.2 to 2.7 summarize the measurements and methodologies used to derive observed sea level, as well as steric and mass components. In most cases, we focus on observations but in some instances (e.g., for GIA corrections applied to the data), model-based estimates are the only available information.

2.1 Sea level budget equation

Global mean sea level (GMSL) change as a function of time t is usually expressed by the sea level budget equation:

$$GMSL(t) = GMSL(t)_{steric +} GMSL(t)_{ocean\ mass} \quad (1)$$

where $GMSL(t)_{steric}$ refers to the contributions of ocean thermal expansion and salinity to sea level change, and $GMSL(t)_{\ oceanmass}$ refers to the change in mass of the oceans. Due to water conservation in the climate system, the ocean mass term (also noted as $M(t)_{ocean}$) can further be expressed as:

$$M(t)_{ocean} + M(t)_{glaciers} + M(t)_{Greenland} + M(t)_{Antarctica} + M(t)_{TWS} + M(t)_{WV} + M(t)_{Snow} + \text{uncertainty} = 0 \quad (2)$$

where $M(t)_{glaciers}$, $M(t)_{Greenland}$, $M(t)_{Antarctica,}$ $M(t)_{TWS,}$ $M(t)_{WV,}$ $M(t)_{Snow}$ represent temporal changes in mass of glaciers, Greenland and Antarctica ice sheets, terrestrial water storage (TWS), atmospheric water vapor (WV), and snow mass changes. The uncertainty is a result of

uncertainties in all of the estimates and potentially missing mass terms, for example, permafrost melting.

From equation (2), we deduce:

$$GMSL(t)_{ocean\ mass} = -[M(t)_{glaciers} + M(t)_{Greenland} + M(t)_{Antarctica} + M(t)_{TWS} + M(t)_{WV} + M(t)_{Snow} + \text{missing mass terms}] \quad (3)$$

In the next subsections, we successively discuss the different terms of the budget (equations 1 and 2) and how they are estimated from observations. We do not consider the atmospheric water vapor and snow components, assumed to be small. Two periods are considered: (1) 1993-present (i.e. the entire altimetry era), and (2) 2005-present (i.e. the period covered by both Argo and GRACE).

2.2 Altimetry-based global mean sea level over 1993-present

The launch of the TOPEX/Poseidon (T/P) altimeter satellite in 1992 led to a new paradigm for measuring sea level from space, providing for the first time precise and globally distributed sea level measurements at 10-day intervals. At the time of the launch of T/P, the measurements were not expected to have sufficient accuracy for measuring GMSL changes. However, as the radial orbit error decreased from ~10 cm at launch to ~1 cm presently, and other instrumental and geophysical corrections applied to altimetry system improved (e.g., Stammer and Cazenave, 2017), several groups regularly provided an altimetry-based GMSL time series (e.g., Nerem et al. 2010, Church et al. 2011, Ablain et al., 2015, Legeais et al., 2018). The initial T/P GMSL time series was extended with the launch of Jason-1 (2001), Jason-2 (2008) and Jason-3 (2016). By design, each of these missions has an overlap period with the previous one in order to inter-compare the sea level measurements and estimate instrument biases (e.g., Nerem et al., 2010; Ablain et al., 2015). This has allowed the construction of an uninterrupted GMSL time series that is currently 25-year long.

2.2.1 Global mean sea level datasets

Six groups (AVISO/CNES, SL_cci/ESA, University of Colorado, CSIRO, NASA/GSFC, NOAA) provide altimetry-based GMSL time series. All of them use 1-Hz altimetry measurements derived from T/P, Jason-1, Jason-2 and Jason-3 as reference missions. These

missions provide the most accurate long-term stability at global and regional scales (Ablain et al. 2009, 2017a), and are all on the same historical T/P ground track. This allows computation of a long-term record of the GMSL from 1993 to present. In addition, complementary missions (ERS-1, ERS-2, Envisat, Geosat Follow-on, CryoSat-2, SARAL/AltiKa and Sentinel-3A) provide increased spatial resolution and coverage of high latitude ocean areas, pole-ward of 66°N/S latitude (e.g. the European Space Agency/ESA Climate Change Initiative/CCI sea level data set; Legeais et al. 2018).

The above groups adopt different approaches when processing satellite altimetry data. The most important differences concern the geophysical corrections needed to account for various physical phenomena such as atmospheric propagation delays, sea state bias, ocean tides, and the ocean response to atmospheric wind and pressure forcing. Other differences come from data editing, methods to spatially average individual measurements during orbital cycles and link between successive missions (Masters et al. 2012; Henry et al. 2014).

Overall, the quality of the different GMSL time series is similar. Long-term trends agree well to within 6% of the signal, approximately 0.2 mm/yr (see Figure 1) within the GMSL trend uncertainty range (~ 0.3 mm/yr; see next section). The largest differences are observed at interannual time scales and during the first years (before 1999; see below). Here we use an ensemble mean GMSL based on averaging all individual GMSL time series.

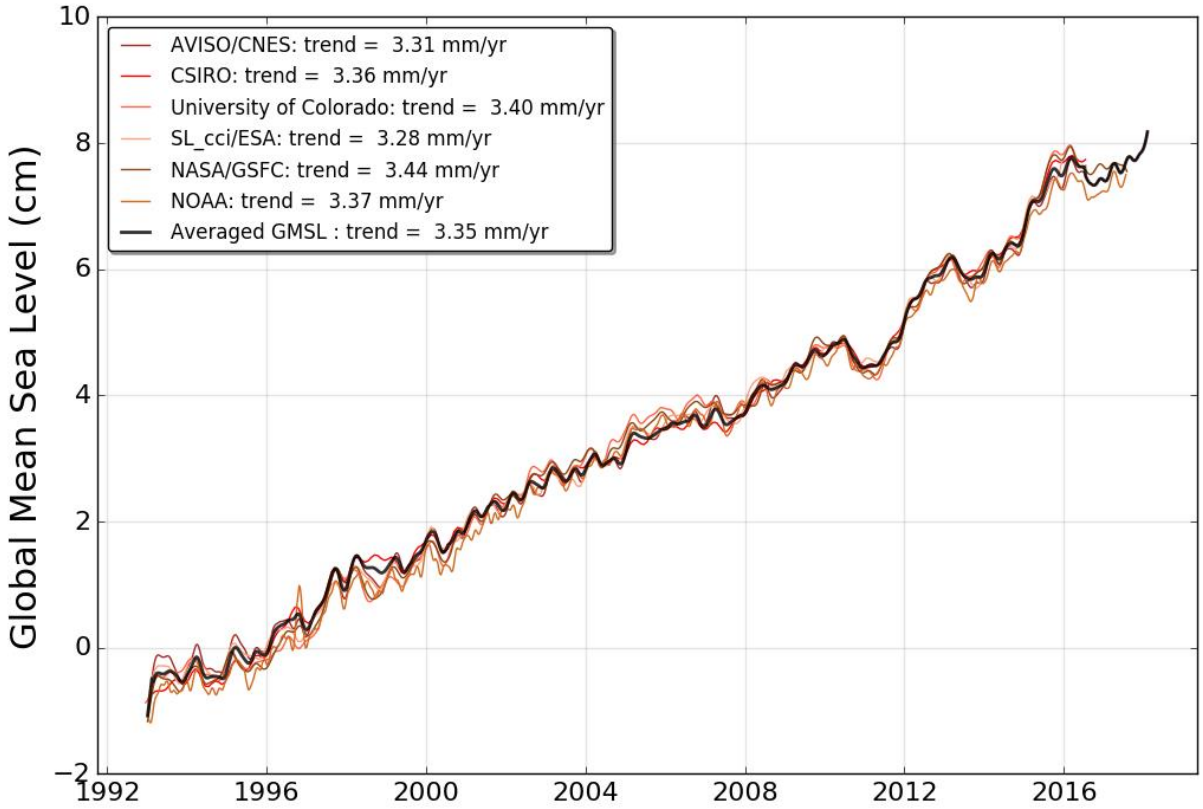

Figure 1: Evolution of GMSL time series from 6 different groups (AVISO/CNES, SL_cci/ESA, University of Colorado, CSIRO, NASA/GSFC, NOAA) products. Annual signals are removed and 6-month smoothing applied. All GMSL time series are centered in 1993 with zero mean. A GIA correction of -0.3 mm/yr has been subtracted to each data set.

2.2.2 Global mean sea level uncertainties and TOPEX-A drift

Based on an assessment of all sources or uncertainties affecting satellite altimetry (Ablain et al. 2017), the GMSL trend uncertainty (90% confidence interval) is estimated as ~0.4 mm/yr over the whole altimetry era (1993-2017). The main contribution to the uncertainty is the wet tropospheric correction with a drift uncertainty in the range of 0.2-0.3 mm/yr (Legeais et al. 2018) over a 10-year period. To a lesser extent, the orbit error (Couhert et al. 2015; Escudier et al., 2017) and the altimeter parameters' (range, sigma-0 and significant wave height/SWH) instability (Ablain et al., 2012) also contribute to the GMSL trend uncertainty, at the level of 0.1 mm/yr. Furthermore, imperfect links between successive altimetry missions lead to another trend uncertainty of about 0.15 mm/yr over the 1993-2017 period (Zawadzki and Ablain, 2016).

Uncertainties are higher during the first decade (1993-2002) where T/P measurements display larger errors at climatic scales. For instance, the orbit solutions are much more uncertain due

to gravity field solutions calculated without GRACE data. Furthermore, the switch from TOPEX-A to TOPEX-B in February 1999 (with no overlap between the two instrumental observations) leads to an error of ~ 3 mm in the GMSL time series (Escudier et al., 2017).

However, the most significant error that affects the first 6 years (January-1993 to February 1999) of the T/P GMSL measurements is due to an instrumental drift of the TOPEX-A altimeter, not included in the formal uncertainty estimates discussed above. This effect on the GMSL time series was recently highlighted via comparisons with tide gauges (Valladeau et al. 2012; Watson et al. 2015; Chen et al. 2017; Ablain et al. 2017), via a sea level budget approach (i.e., comparison with the sum of mass and steric components; Dieng et al., 2017) and by comparing with Poseidon-1 measurements (Zawadsky, personal communication). In a recent study, Beckley et al. (2017) asserted that the corresponding error on the 1993-1998 GMSL resulted from incorrect onboard calibration parameters.

All three approaches conclude that during the period January 1993 to February 1999, the altimetry-based GMSL was overestimated. TOPEX-A drift correction was estimated close to 1.5 mm/yr (in terms of sea level trend) with an uncertainty of ±0.5 to ±1.0 mm/yr (Watson et al. 2015; Chen et al. 2017; Dieng et al. 2017). Beckley et al. (2017) proposed to not apply the suspect onboard calibration correction on TOPEX-A measurements. The impact of this approach is similar to the TOPEX-A drift correction estimated by Dieng et al. (2017) and Ablain et al. (2017b). In the latter study, accurate comparison between TOPEX A-based GMSL and tide gauge measurements leads to a drift correction to about -1.0 mm/yr between January 1993 and July 1995, and +3.0 mm/yr between August 1995 and February 1999, with an uncertainty of 1.0 mm/yr (with a 68% confidence level, see Table 1).

TOPEX-A drift correction	**to be subtracted from the first 6-years (Jan. 1993 to Feb. 1999) of the uncorrected GMSL record**
Watson et al. (2015)	1.5 +/- 0.5 mm/yr over Jan.1993/ Feb.1999
Chen et al. (2017); Dieng et al. (2017)	1.5 +/- 0.5 mm/yr over Jan.1993/ Feb.1999
Beckley et al. (2017)	No onboard calibration applied
Ablain et al. (2017b)	-1.0 +/- 1.0 mm/yr over Jan.1993/ Jul.1995

	+3.0 +/-1.0 mm/yr over Aug.1995- Feb.1999

Table 1. TOPEX-A GMSL drift corrections proposed by different studies

2.2.3 Global Mean Sea Level variations

The ensemble mean GMSL rate after correcting for the TOPEX-A drift (for all of the proposed corrections) amounts to 3.1 mm/yr over 1993-2017 (Figure 2). This corresponds to a mean sea level rise of about 7.5 cm over the whole altimetry period. More importantly, the GMSL curve shows a net acceleration, estimated at 0.08 mm/yr² (Chen et al. 2017; Dieng et al. 2017) and 0.084 +/- 0.025 mm/yr² (Nerem et al., 2018) (Note Watson et al. found a smaller acceleration after correcting for the instrumental bias over a shorter period up to the end of 2014.). GMSL trends calculated over 10-year moving windows illustrate this acceleration (Figure 3). GMSL trends are close to 2.5 mm/yr over 1993-2002 and 3.0 mm/yr over 1996-2005. After a slightly smaller trend over 2002-2011, the 2008-2017 trend reaches 4.2 mm/yr. Uncertainties (90% confidence interval) associated to these 10-year trends regularly decrease through time from 1.3 mm/yr over 1993-2002 (corresponding to T/P data) to 0.65 mm/yr for 2008-2017 (corresponding to Jason-2 and Jason-3 data).

Removing the trend from the GMSL time series highlights inter-annual variations (not shown). Their magnitudes depend on the period (+3 mm in 1998-1999, -5 mm in 2011-2012, and +10 mm in 2015-2016) and are well correlated in time with El Niño and La Niña events (Nerem et al. 2010; Cazenave et al. 2014, Nerem et al., 2018). However, substantial differences (of 1-3 mm) exist between the six de-trended GMSL time series. This issue needs further investigation.

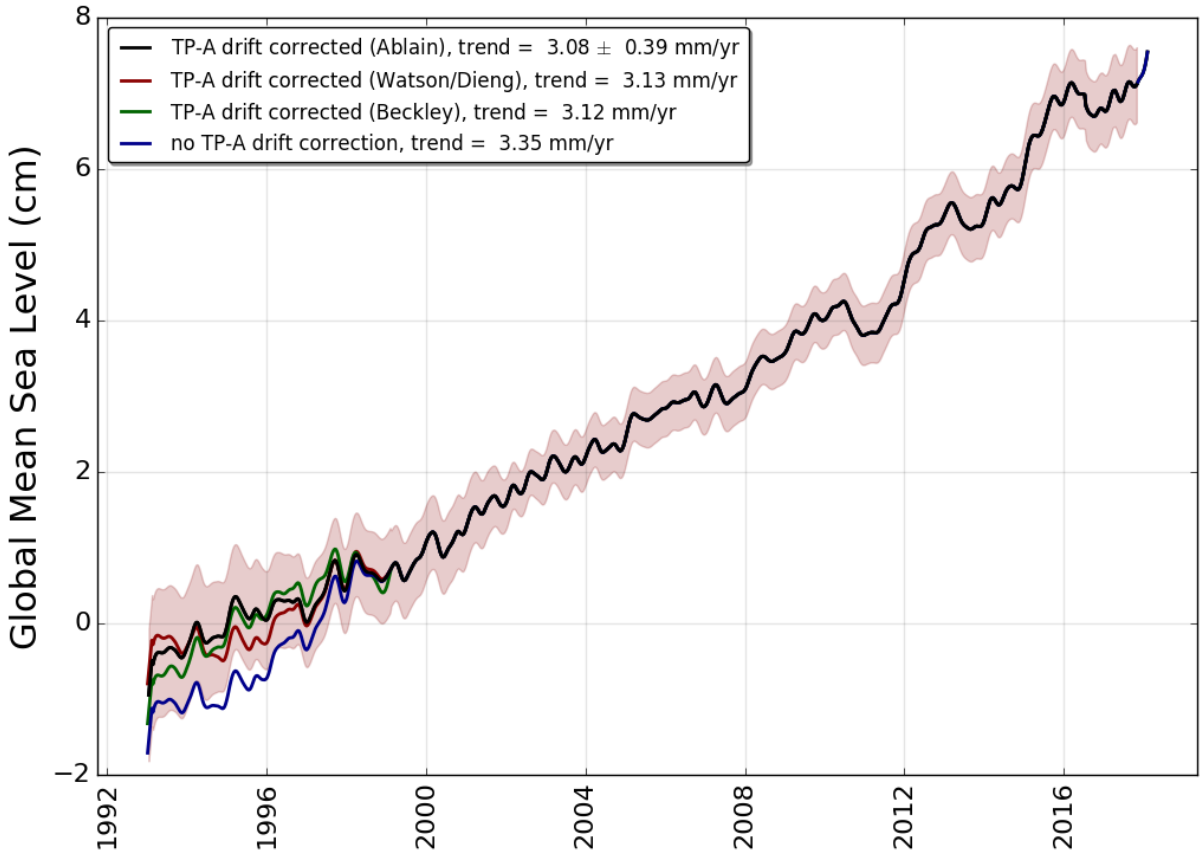

Figure 2: Evolution of ensemble mean GMSL time series (average of the 6 GMSL products from AVISO/CNES, SL_cci/ESA, University of Colorado, CSIRO, NASA/GSFC, and NOAA). On the black, red and green curves, the TOPEX-A drift correction is applied respectively based on (Ablain et al, 2017b), (Watson et al. 2015; Dieng et al. 2017) and Beckley et al., 2017). Annual signal removed and 6-month smoothing applied; GIA correction also applied. Uncertainties (90% confidence interval) of correlated errors over a 1-year period are superimposed for each individual measurement (shaded area).

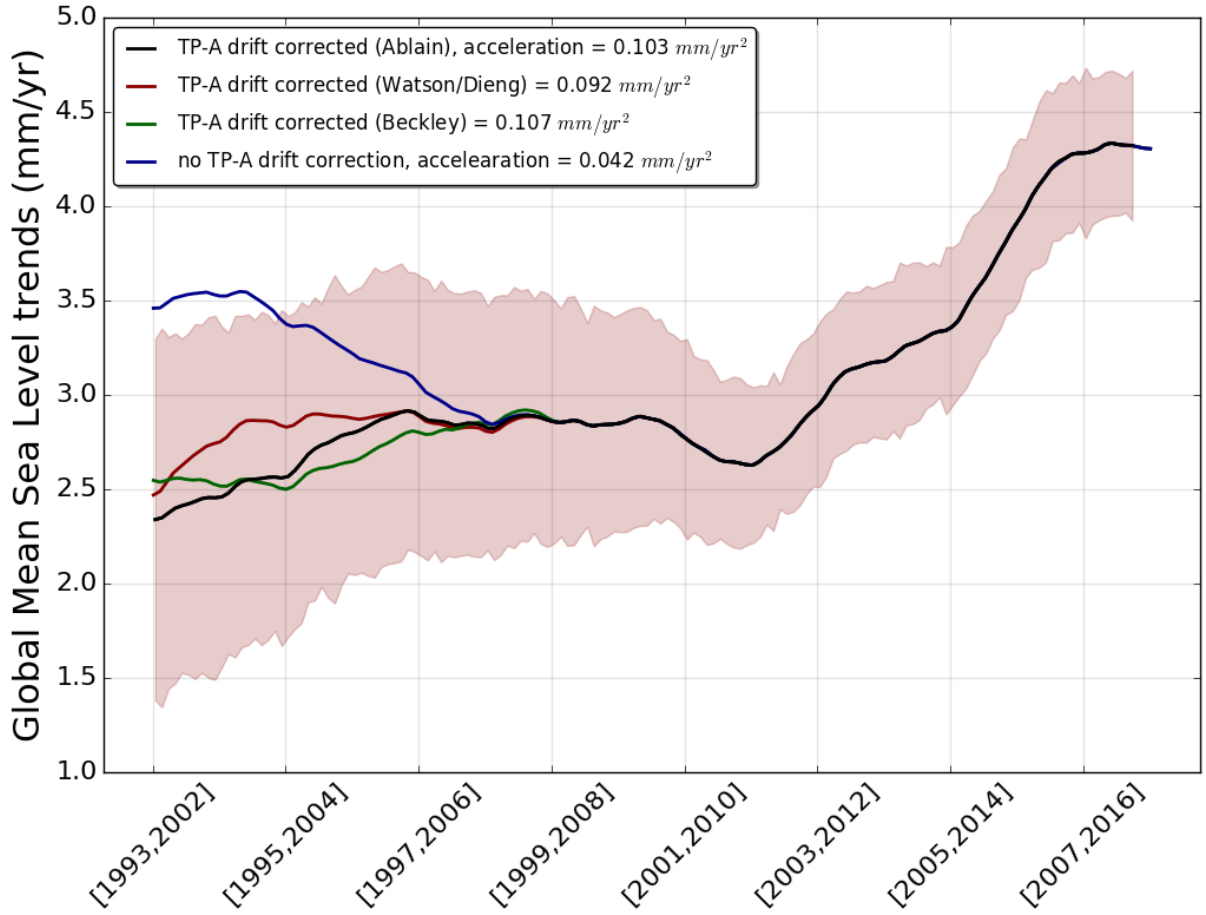

Figure 3: Ensemble mean GMSL trends calculated over 10-year moving windows. On the black, red and green curves, the TOPEX-A drift correction is applied respectively based on (Ablain et al, 2017b), and Beckley et al., 2017). Uncorrected GMSL trends are shown by the blue curve. The shaded area represents trend uncertainty over 10-year periods (90% confidence interval).

For the sea level budget assessment (section 3), we will use the ensemble mean GMSL time series corrected for the TOPEX A drift using the Ablain et al. (2017b) correction.

2.2.4. Comparison with tide gauges

Prior to 1992 global sea level rise estimates rely on the tide gauge measurements, and it is worth mentioning past attempts to produce global sea level reconstructions utilizing these measurements (e.g. Gornitz et al. 1982; Bartnett 1984; Douglas 1991, 1997, 2001). Here we focus on global sea level reconstructions that overlap with satellite altimetry data over a substantial common time span. Some of these reconstructions rely on tide gauge data only

(Jevrejeva et al. 2006, 2014; Merrifield et al. 2009; Wenzel and Schroter 2010; Ray and Douglas 2011; Hamlington et al. 2011, Spada and Galassi 2012; Thompson and Merrifield 2014; Dangendorf et al. 2017; Frederikse et al. 2017). In addition, there are reconstructions that jointly use satellite altimetry and tide gauge records (Church and White 2006, 2011) and reconstructions which combines tide gauge records with ocean models (Meyssignac et al. 2011) or physics-based and model-derived geometries of the contributing processes (Hay et al. 2015).

For the period since 1993, with most of the world coastlines densely sampled, the rates of sea level rise from all tide gauge based reconstructions and estimates from satellite altimetry agree within their specific uncertainties, e.g., rates of 3.0 ± 0.7 mm· yr^{-1} (Hay et al. 2015); 2.8 ± 0.5 mm· yr^{-1} (Church and White 2011; Rhein et al. 2013); 3.1 ± 0.6 mm·yr^{-1} (Jevrejeva et al, 2014); 3.1 ± 1.4 mm·yr^{-1} (Dangendorf et al. 2017) and the estimate from satellite altimetry 3.2 ± 0.4 mm· yr^{-1} (Nerem et al. 2010; Rhein et al. 2013). However, classical tide gauge-based reconstructions still tend to overestimate the inter-annual to decadal variability of global mean sea level (e.g. Calafat et al., 2012; Dangendorf et al. 2015; Natarov et al. 2017) compared to global mean sea level from satellite altimetry, due to limited and uneven spatial sampling of the global ocean afforded by the tide gauge network. Sea level rise being non uniform, spatial variability of sea-level measured at tide gauges is evidenced by 2D reconstruction methods. The most widely used approach is the use of empirical orthogonal functions (EOF) calibrated with the satellite altimetry data (e.g. Church and White, 2004). Alternatively, Choblet et al. (2014) implemented a Bayesian inference method based on a Voronoi tessellation of the Earth's surface to reconstruct sea level during the twentieth century. Considerable uncertainties remain however in long term assessments due to poorly sampled ocean basins such as the South Atlantic, or regions which are significantly influenced by open-ocean circulation (e.g. Subtropical North Atlantic) (Frederikse et al. 2017). Uncertainties involved in specifying vertical land motion corrections at tide gauges also impact tide gauge reconstructions (Jevrejeva et al. 2014; Woppelmann and Marcos 2016; Hamlington et al. 2016). Frederikse et al. (2017) recently also demonstrated that both global mean sea level reconstructed from tide gauges and the sum of steric and mass contributors show a good agreement with altimetry estimates for the overlapping period 1993-2014.

2.3 Steric sea level

Steric sea level variations result from temperature (T) and salinity (S) related density changes of sea water associated to volume expansion and contraction. These are referred to as thermosteric and halosteric components. Despite clear detection of regional salinity changes and the dominance of the salinity effect on density changes at high latitudes (Rhein et al., 2013), the halosteric contribution to present-day global mean steric sea level rise is negligible, as the ocean's total salt content is essentially constant over multidecadal timescales (Gregory and Lowe, 2000). Hence in this study, we essentially consider the thermosteric sea level component.

Averaged over the 20th century, ocean thermal expansion associated with ocean warming has been the largest contribution to global mean sea level rise (Church et al., 2013). This remains true for the altimetry period starting in the year 1993 (e.g., Chen et al. 2017; Dieng et al., 2017, Nerem et al., 2018). But total land ice mass loss (from glaciers, Greenland and Antarctica) during this period, now dominates the sea level budget (see section 3).

Until the mid-2000s, the majority of ocean temperature data have been retrieved from shipboard measurements. These include vertical temperature profiles along research cruise tracks from the surface sometimes all the way down to the bottom layer (e.g. Purkey and Johnson, 2010) and upper-ocean broad-scale measurements from ships of opportunity (Abraham et al., 2013). These upper-ocean in situ temperature measurements however are limited to the upper 700 m depth due to common use of expandable bathy thermographs (XBTs). Although the coverage has been improved through time, large regions characterized by difficult meteorological conditions remained under-sampled, in particular the southern hemisphere oceans and the Arctic area.

2.3.1 Thermosteric data sets

Over the altimetry era, several research groups have produced gridded time series of temperature data for different depth levels, based on XBTs (with additional data from mechanical bathythermographs -MBTs- and conductivity-temperature-depth (CTD) devices and moorings) and Argo float measurements. The temperature data have further been used to provide thermosteric sea level products. These differ because of different strategies adopted for data editing, temporal and spatial data gaps filling, mapping methods, baseline climatology and instrument bias corrections (in particular the time-to-depth correction for XBT data, Boyer et al., 2016).

The global ocean in situ observing system has been dramatically improved through the implementation of the international Argo program of autonomous floats, delivering a unique

insight of the interior ocean from the surface down to 2000 m depth of the ice-free global ocean (Roemmich et al., 2012, Riser et al., 2016). More than 80% of initially planned full deployment of Argo float program was achieved during the year 2005, with quasi- global coverage of the ice-free ocean by the start of 2006. At present, more than 3800 floats provide systematic T/S data, with quasi (60°S-60°N latitude) global coverage down to 2000 m depth. A full overview on in situ ocean temperature measurements is given for example in Abraham et al. (2013).

In this section, we consider a set of 11 direct (in situ) estimates, publically available over the entire altimetry era, to review global mean thermosteric sea level rise and, ultimately, to construct an ensemble mean time series. These data sets are:

1. CORA = Coriolis Ocean database for ReAnalysis, Copernicus Service, France marine.copernicus.eu/, product name : INSITU_GLO_TS_OA_REP_OBSERVATIONS_013_002_b
2. CSIRO (RSOI) = Commonwealth Scientific and Industrial Research Organisation/Reduced-Space Optimal Interpolation, Australia
3. ACECRC/IMAS-UTAS = Antarctic Climate and Ecosystem Cooperative Research Centre/Institute for Marine and Antarctic Studies-University of Tasmania, Australia http://www.cmar.csiro.au/sealevel/thermal_expansion_ocean_heat_timeseries.html
4. ICCES = International Center for Climate and Environment Sciences, Institute of Atmospheric Physics, China http://ddl.escience.cn/f/PKFR
5. ICDC = Integrated Climate Data Center, Universit of Hamburg, Germany
6. IPRC = International Pacific Research Center, University of Hawaii, USA http://apdrc.soest.hawaii.edu/projects/Argo/data/gridded/On_standard_levels/index-1.html
7. JAMSTEC = Japan Agency for Marine-Earth Science and Technology, Japan ftp://ftp2.jamstec.go.jp/pub/argo/MOAA_GPV/Glb_PRS/OI/
8. MRI/JMA = Meteorological Resarch Institute/Japan Meteorological Agency, Japan https://climate.mri-jma.go.jp/~ishii/.wcrp/
9. NCEI/NOAA = National Centers for Environmental Information/National Oceanic and Atmospheric Adinistration, USA
10. SIO = Scripps Institution of Oceanography, USA Deep/abyssal: https://cchdo.ucsd.edu/
11. SIO = Scripps Institution of Oceanography, USA Deep/abyssal: https://cchdo.ucsd.edu/ (for the abyssal ocean)

Their characteristics are presented in Table 2.

424

425

426

427

Product/Institution		Period	Depth-integration (m)				Temporal resolution / Latitudinal range	Reference
			0-700	700-2000	0-2000	≥2000		
1	**CORA**	1993-2016	Y	Y	Y	- - -	Monthly 60°S-60°N	http://marine.copernicus.eu/services-portfolio/access-to-products/
2	**CSIRO (RSOI)**	2004-2017	Y/E (0-300)	Y/E	Y/E	- - -	Monthly 65°S-65°N	Roemmich et al. (2015); Wijffels et al. (2016)
3	**CSIRO/ACECRC/ IMAS-UTAS**	1970-2017	Y/E (0-300)	- - -	- - -	- - -	Yearly (3-yr run. mean) 65°S-65°N	Domingues et al. (2008); Church et al. (2011)
4	**ICCES**	1970-2016	Y/E (0-300)	Y/E	Y/E	- - -	Yearly 89°S-89°N	Cheng and Zhu (2016); Cheng et al. (2017)
5	**ICDC**	1993-2016	Y (1993)	- - -	Y (2005)	- - -	Monthly	Gouretzki and Koltermann (2007)
6	**IPRC**	2005-2016	- - -	- - -	Y	- - -	Monthly	http://apdrc.soest.hawaii.edu/projects/argo
7	**JAMSTEC**	2005-2016	- - -	- - -	Y	- - -	Monthly	Hosoda et al. (2008)
8	**MRI/JMA**	1970-2016 (rel. to 1961-1990 averages)	Y/E (0-300)	Y/E	Y/E	- - -	Yearly 89°S-89°N	Ishii et al. (2017)
9	**NCEI/NOAA**	1970-2016	Y/E	Y/E	Y/E	- - -	Yearly 89°S-89°N	Antonov et al. (2005)
10	**SIO**	2005-2016	- - -	- - -	Y	- - -	Monthly	Roemmich and Gilson (2009)
11	**SIO**	1990-2010	- - -	- - -	- - -	Y/E	Linear	Purkey and

1	**(Deep/abyssal)**	(as of 01/2018)					trend 89°S-89°N, as an aggregation of 32 deep ocean basins	Johnson (2010)

Table 2: Compilation of available in situ datasets from different originators and/or contributors.The table indicates the time span covered by the data, the depth of integration, as well as the temporal resolution and latitude coverage.

2.3.2 Individual estimates

All in situ estimates compiled in this study show a steady rise in global mean thermosteric sea level, independent of depth-integration and decadal/multidecadal periods (Figure 4 and 5, left panels). As the deep/abyssal ocean estimate only illustrates the updated version of the linear trend from Purkey and Johnson (2010) for 1990-2010 extrapolated to 2016, it does not have any variability superimposed.

Interannual to decadal variability during the Altimeter era (since 1993) is similar for both 0-700 m and 700-2000 m, with larger amplitude in the upper ocean (Figure 4 and 5, right panels). For the 0-700 m, there is an apparent change in amplitude before/after the Argo era (since 2005), mostly due to a maximum (2-4 mm) around 2001-2004, except for one estimate. Higher amplitude and larger spread in variability between estimates before the Argo era is a symptom of the much sparser in situ coverage of the global ocean. Interannual variability over the Argo era (Figures 4 and 5, right panels) is mainly modulated by El Niño Southern Oscillation (ENSO) phases in the upper 500 m ocean, particularly for the Pacific, the largest ocean basin (Roemmich et al., 2011; Johnson and Birnbaum, 2017).

In terms of depth contribution, on average, the upper 300 m explains the same percentage (almost 70%) of the 0-700 m linear rate over both altimetry and Argo eras, but the contribution from the 0-700 m to 0-2000 m varies: about 75% for 1993-2016 and 65% for 2005-2016. Thus, the 700-2000 m contribution m increases by 10% during the Argo decade, when the number of observations within 700-2000 m has significantly increased.

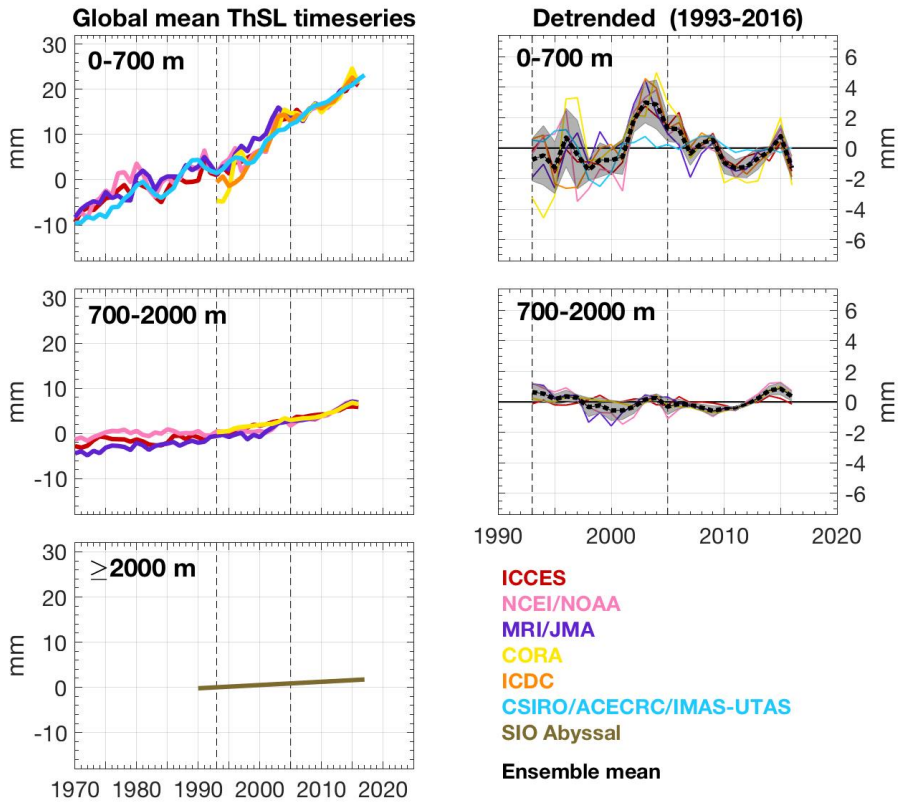

Figure 4. *Left- panels. Annual mean global mean thermosteric anomaly Time-series since 1970, from various research groups (color) and for three depth-integrations: 0-700 m (top), 700-2000 m (middle), and below 2000 m (bottom). Vertical dashed lines are plotted along 1993 and 2005. For comparison, all time-series were offset arbitrarily. Right panels. Respective linearly de-trended time-series for 1993-2016. Black bold dashed line is the ensemble mean and gray shadow bar the ensemble spread (1-standard deviation). Units are mm.*

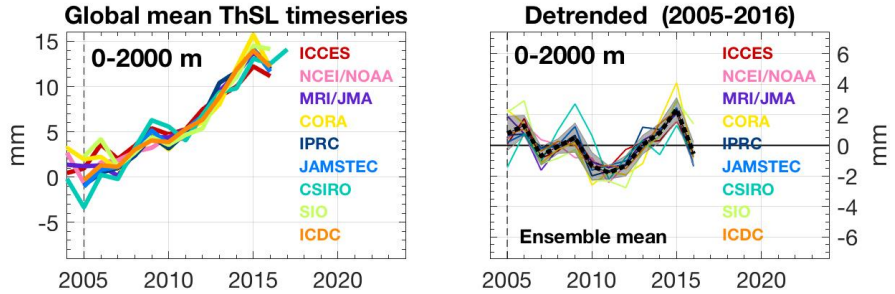

Figure 5. Left- panel. Annual mean global mean thermosteric anomaly time-series since 2004, from various research groups (color) in the upper 2000 m. A vertical dashed line is plotted along 2005. For comparison, all time-series were offset arbitrarily. Right panel. Respective linearly de-trended time series for 2005-2016. Black bold dashed line is the ensemble mean and gray shadow bar the ensemble spread (1-standard deviation). Units are mm.

2.3.3. Ensemble mean thermosteric sea level

Given that the global mean thermosteric sea level anomaly estimates compiled for this study are not necessarily referenced to the same baseline climatology, they cannot be directly averaged together to create an ensemble mean. To circumvent this limitation, we created an ensemble mean in three steps, as explained below.

Firstly, we de-trended the individual time-series by removing a linear trend for 1993-2016 and averaged together to obtain an "ensemble mean variability time-series". Secondly, we averaged together the corresponding linear trends of the individual estimates to obtain an "ensemble mean linear rate". Thirdly, we combined this "ensemble mean linear rate" with the "ensemble mean variability time-series" to obtain the final ensemble mean time-series. We applied the same steps for the Argo era (2005-2016).

To maximise the number of individual estimates used in the final full-depth ensemble mean time-series, the three steps above were actually divided into depth-integrations and then summed. For the Argo era, we summed 0-2000 m (9 estimates) and ≥2000 m (1 estimate). For the altimetry era, we summed 0-700 m (6 estimates), 700-2000 (4 estimates) and ≥2000 m (1 estimate), although there is no statistical difference if the calculation was only based on the sum of 0-2000 m (4 estimates) and ≥2000 m (1 estimate). There is also no statistical difference between the full-depth ensemble mean time-series created for the Altimeter and Argo eras during their overlapping years (since 2005).

Figure 6 shows the full-depth ensemble mean time series over 1993-2016 and 2005-2016. It reveals a global mean thermosteric sea level rise of about 30 mm over 1993-2016 (24 years) or about 18 mm over 2005-2016 (12 years) , with a record high in 2015. These thermosteric changes are equivalent to a linear rate of 1.32 +/- 0.4 mm/yr and 1.31 +/- 0.4 mm/yr respectively.

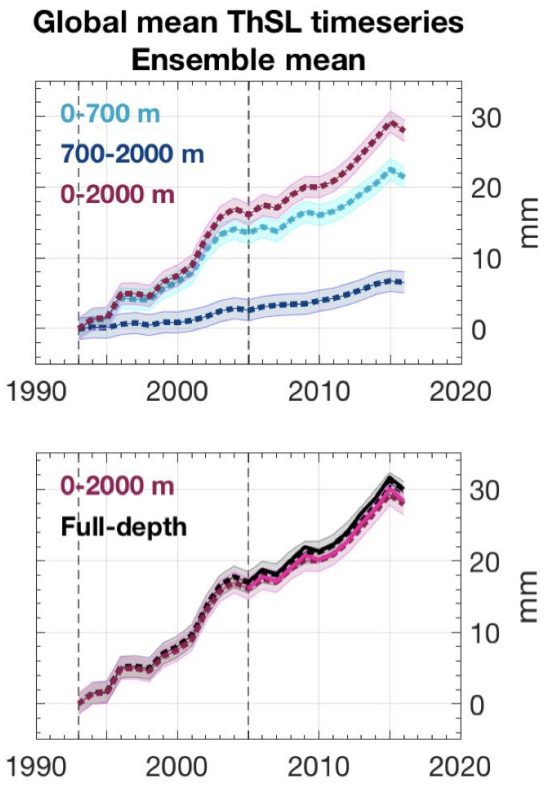

Figure 6: *Ensemble mean time-series for global mean thermosteric anomaly, for three-depth integrations (top) and for 0-2000 m and f3ull-depth (bottom). In the bottom panel, dashed lines are for the 1993-2016 period whereas solid lines are for 2005-2016. Error bars represent the ensemble spread (standard deviation). Units are mm.*

Figure 7 shows thermosteric sea level trends for each of the data sets used over the 1993-2016 (left panel) and 2005-2016 (right panel) time spans and different depth ranges (including full depth), as well as associated ensemble mean trends. The full depth ensemble mean trend amounts to 1.3 +/- 0.4 mm/yr over 2005-2016. It is similar to the 1993-2016 ensemble mean trend, suggesting negligible acceleration of the thermosteric component over the altimetry era.

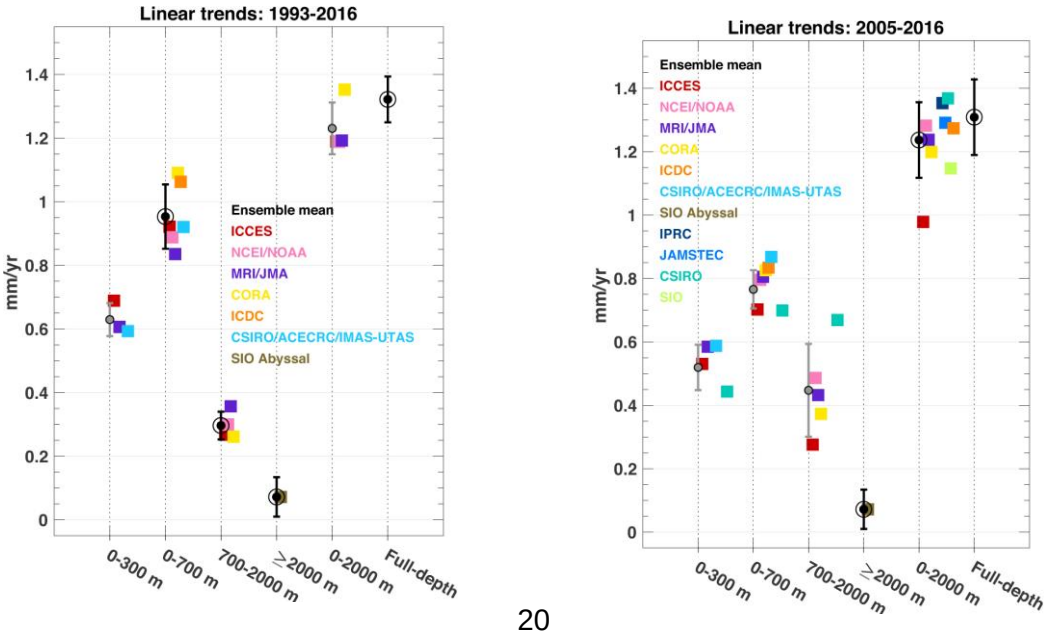

Figure 7: Linear rates of global mean thermosteric sea level for depth-integrations (x-axis), for individual estimates and ensemble means, over 1993-2016 (left) and 2005-2016 (right). Ensemble mean rates with a black circle were used in the estimation of the time-series described in Section 2.3.4. Error bars are standard deviation due to spread of the estimates except for ≥2000 m. Units are mm/yr.

2.4 Glaciers

Glaciers have strongly contributed to sea-level rise during the 20th century – around 40% - and will continue to be an important part of the projected sea-level change during the 21st century – around 30% (Kaser et al., 2006, Church et al., 2013, Gardner et al., 2013, Marzeion et al., 2014, Zemp et al., 2015; Huss and Hock, 2015). Because glaciers are time-integrated dynamic systems, a response lag of at least 10 years to a few hundred years is observed between changes in climate forcing and glacier shape, mainly depending on glacier length and slope (Johannesson et al., 1989, Bahr et al., 1998). Today, glaciers are globally (a notable exception is the Karakoram/Kunlun Shan region, e.g. Brun et al., 2017) in a strong disequilibrium with the current climate and are loosing mass, due essentially to the global warming in the second half of the 20th century (Marzeion et al., 2018).

Global glacier mass changes are derived from in situ measurements of glacier mass changes or glacier length changes. Remote sensing methods measure elevation changes over entire glaciers based on differencing digital elevation models (DEMs) from satellite imagery between two epochs (or at points from repeat altimetry), surface flow velocities for determination of mass fluxes, and glacier mass changes from space-based gravimetry. Mass balance modeling driven by climate observations is also used (Marzeion et al., 2017 provide a review of these different methods).

Glacier contribution to sea level is primarily the result of their surface mass balance and dynamic adjustment, plus iceberg discharge and frontal ablation (below sea level) in the case of marine-terminating glaciers. The sum of worldwide glacier mass balances (MBs) does not correspond to the total glacier contribution to sea-level change for the following reasons:

- Glacier ice below sea level does not contribute to sea-level change, apart from a small lowering when replacing ice with seawater of a higher density. Total volume of glacier ice below sea level is estimated to be 10 – 60 mm sea-level equivalent (SLE, Huss and Farinotti, 2012, Haeberli and Linsbauer, 2013, Huss and Hock, 2015).

- Incomplete transfer of melting ice from glaciers to the ocean: meltwater stored in lakes or wetlands, meltwater intercepted by natural processes and human activities (e.g.

drainage to lakes and aquifers in endorheic basins, impoundment in reservoirs, agriculture use of freshwater, Loriaux and Casassa, 2013, Käab et al., 2015).

Despite considerable progress in observing methods and spatial coverage (Marzeion et al., 2017), estimating glacier contribution to sea-level change remains challenging due to the following reasons:

- Number of regularly observed glaciers (in the field) remains very low (0.25% of the 200 000 glaciers of the world have at least one observation and only 37 glaciers have multi decade-long observations, Zemp et al. 2015).

- Uncertainty of the total glacier ice mass remains high (Figure 8, Grinsted et al., 2013, Pfeffer et al., 2014, Farinotti et al., 2017, Frey et al. 2014).

- Uncertainties in glacier inventories and DEMs are not negligible. Sources of uncertainties include debris-covered glaciers, disappearance of small glaciers, positional uncertainties, wrongly mapped seasonal snow, rock glaciers, voids and artifacts in DEMs (Paul et al., 2004, Bahr and Radić, 2012).

- Uncertainties of satellite retrieval algorithms from space-based gravimetry and regional DEM differencing are still high, especially for global estimates (Gardner et al. 2013, Marzeion et al., 2017, Chambers et al., 2017).

- Uncertainties of global glacier modeling (e.g. initial conditions, model assumptions and simplifications, local climate conditions, Marzeion et al., 2012).

- Knowledge about some processes governing mass balance (e.g. wind redistribution and metamorphism, sublimation, refreezing, basal melting) and dynamic processes (e.g. basal hydrology, fracking, surging) remains limited (Farinotti et al., 2017).

An annual assessment of glacier contribution to sea-level change is difficult to perform from ground-based or space-based observations except space-based gravimetry, due to the sparse and irregular observation of glaciers, and the difficulty of assessing accurately the annual mass balance variability. Global annual averages are highly uncertain because of the sparse coverage, but successive annual balances are uncorrelated and therefore averages over several years are known with greater confidence.

2.4.1 Glacier datasets

The following datasets are considered, with a focus on the trends of annual mass changes:

1. Update of Gardner et al., 2013 (Reager et al., 2016), from satellite gravimetry and altimetry, and glaciological records, called G16.

2. Update of Marzeion et al, 2012 (Marzeion et al., 2017), from global glacier modeling and mass balance observations, called M17.

3. Update of Cogley (2009) (Marzeion et al., 2017), from geodetic and direct mass-balance measurements, called C17.

4. Update of Leclercq et al., 2011 (Marzeion et al., 2017), from glacier length changes, called L17.

5. Average of GRACE-based estimates of Marzeion et al. (2017), from spatial gravimetry measurements, called M17-G.

In general it is not possible to align measurements of glacier mass balance with the calendar. Most in-situ measurements are for glaciological years that extend between successive annual minima of the glacier mass at the end of the summer melt season. Geodetic measurements have start and end dates several years apart and are distributed irregularly through the calendar year; some are corrected to align with annual mass minima but most are not. Consequently, measurements discussed here for 1993-2016 (the altimetry era) and 2005-2016 (the GRACE and Argo era) are offset by up to a few months from the nominal calendar years.

Peripheral glaciers around the Greenland and Antarctic ice sheets are not treated in detail in this section (see sections 2.5 and 2.6 for mass-change estimates that combine the peripheral glaciers with the Greenland Ice Sheet and Antarctic Ice Sheet respectively). This is primarily because of the lack of observations (especially ground-based measurements) and also because of the high spatial variability of mass balance in those regions, and the slightly different climate (e.g. precipitation regime) and processes (e.g. refreezing). In the past, these regions have often been neglected. However, Radić and Hock (2010) estimated the total ice mass of peripheral glaciers around Greenland and Antarctica as 191 +/- 70 mm SLE, with an actual contribution to sea-level rise of around 0.23 +/- 0.04 mm/yr (Radić and Hock, 2011). Gardner et al. (2013) found a contribution from Greenland and Antarctic peripheral glaciers equal to 0.12 +/- 0.05 mm/yr.

Note that some new or updated datasets for peripheral glaciers surrounding polar ice sheets are under development and would hopefully be available in coming years in order to incorporate Greenland and Antarctic peripheral glaciers in the estimates of global glacier mass changes.

2.4.2 Methods

No globally complete observational dataset exists for glacier mass changes (except GRACE estimates, see below). Any calculation of the global glacier contribution to sea-level change

has to rely on spatial interpolation or extrapolation or both, or to consider limited knowledge of responses to climate change (due to the heterogeneous spatial distribution of glaciers around the world). Consequently, most observational methods to derive glacier sea-level contribution must extend local observations (in situ or satellite) to a larger region. Thanks to the recent global glacier outline inventory (Randolph Glacier Inventory – RGI – first release in 2012) as well as global climate observations, glacier modeling can now also be used to estimate the contribution of glaciers to sea level (Marzeion et al., 2012, Huss and Hock, 2015, Maussion et al., 2018, subm.). Still, those global modeling methods need to globalize local observations and glacier processes which require fundamental assumptions and simplifications. Only GRACE-based gravimetric estimates are global but they suffer from large uncertainties in retrieval algorithms (signal leakage from hydrology, GIA correction) and coarse spatial resolution, not resolving smaller glaciated mountain ranges or those peripheral to the Greenland ice sheet.

DEM differencing method is not yet global, but regional, and can hopefully in the near future be applied globally. This method needs also to convert elevation changes to mass changes (using assumptions on snow and ice densities). In contrast, very detailed glacier surface mass balance and glacier dynamic models are today far from being applicable globally, mainly due to the lack of crucial observations (e.g., meteorological data, glacier surface velocity and thickness) and of computational power for the more demanding theoretical models. However, somewhat simplified approaches are currently developed to make best use of the steadily increasing datasets. Modeling-based estimates suffer also from the large spread in estimates of the actual global glacier ice mass (Figure 8). The mean value is 469 +/- 146 mm SLE, with recent studies converging towards a range of values between 400 and 500 mm SLE global glacier ice mass. But as mentioned above, a part of this ice mass will not contribute to sea level.

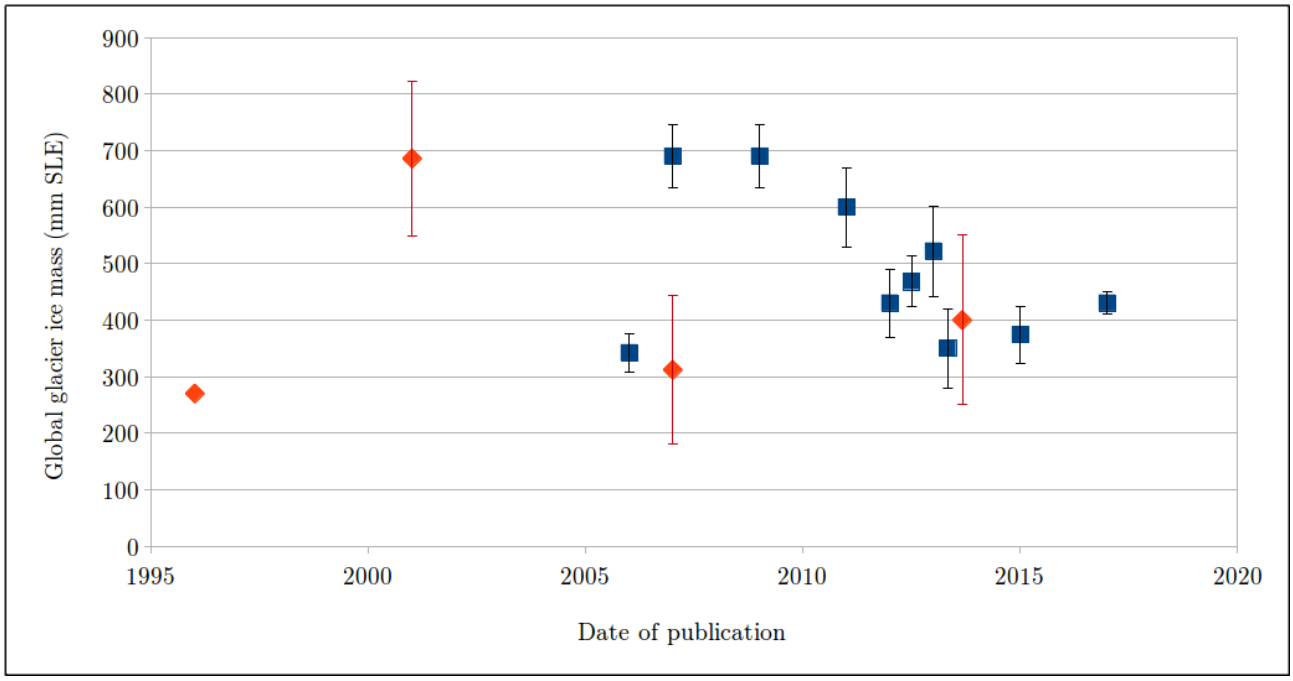

Fig 8. Evolution of global glacier ice mass estimates from different studies published over the past two decades, based on different observations and methods. The red marks correspond to IPCC reports. We clearly see the most recent publications lead to less scattered results. Note that Antarctica and Greenland peripheral glaciers are taken into account in this figure.

2.4.3 Results (trends)

Table 3 presents most recent estimates of trends in global glacier mass balances.

	1993 – 2016 mm/yr SLE	**2005 – 2016 mm/yr SLE**
G16		0.70 +- 0.070[a]
M17	0.68 +- 0.032	0.80 +- 0.048
C17	0.63 +- 0.070	0.75 +- 0.070[b]
L17		0.84 +- 0.640[c]
M17-G		0.61 +- 0.070[d]

Table 3: All data are in mm/yr SLE. [a] The time period of G16 is 2002 – 2014. [b] The time period of C17 is 2003 – 2009. [c] The time period of L17 is 2003 – 2009. [d] The time period of M17-G is 2002/2005 – 2013/2015 because this value is an average of different estimates.

The ensemble mean contribution of glaciers to sea-level rise for the time period 1993 – 2016 is 0.65 +/- 0.051 mm/yr SLE and 0.74 +/- 0.18 mm/yr for the time period 2005 – 2016 (uncertainties are averaged). Different studies refer to different time periods. However, because of the probable low variability of global annual glacier changes, compared to other components of the sea-level budget, averaging trends for slightly different time periods is appropriate.

The main source of uncertainty is that the vast majority of glaciers are unmeasured, which makes interpolation or extrapolation necessary, whether for in situ or satellite measurements, and for glacier modeling. Other main contributions to uncertainty in the ensemble mean stem from methodological differences, such as the downscaling of atmospheric forcing required for glacier modeling, the separation of glacier mass change to other mass change in the spatial gravimetry signal and the derivation of observational estimates of mass change from different raw measurements (e.g. length and volume changes, mass balance measurements and geodetic methods) all with their specific uncertainties.

2.5 Greenland

Ice sheets are the largest potential source of future sea level rise (SLR) and represent the largest uncertainty in projections of future sea level. Almost all land ice (~99.5%) is locked in the ice sheets, with a volume in sea level equivalent/SLE terms of 7.4 m for Greenland, and 58.3 m for Antarctica. It has been estimated that approximately 25% to 30% of the total land ice contribution to sea level rise over the last decade came from the Greenland ice sheet (e.g. Dieng et al., 2017, Box and Colgan, 2017).

There are three main methods that can be used to estimate the mass balance of the Greenland ice sheet: (1) measurement of changes in elevation of the ice surface over time (dh/dt) either from imagery or altimetry; (2) the mass budget or Input-Output Method (IOM) which involves estimating the difference between the surface mass balance and ice discharge; and (3) consideration of the redistribution of mass via gravity anomaly measurements which only became viable with the launch of GRACE in 2002. Uncertainties due to the GIA correction are small in Greenland compared to Antarctica: on the order of ±20 Gt/yr mass equivalent (Khan et al., 2016). Prior to 2003, mass trends are reliant on IOM and altimetry. Both techniques have limited sampling in time and/or space for parts of the satellite era (1992-2002) and errors for this earlier period are, therefore, higher (van den Broeke et al., 2016, Hurkmans et al., 2014).

The consistency between the three methods mentioned above was demonstrated for Greenland by Sasgen et al. (2012) for the period 2003-2009. Ice sheet wide estimates showed excellent agreement although there was less consistency at a basin scale. We have, therefore, high confidence and relatively low uncertainties in the mass rates for the Greenland ice sheet in the satellite era (see also Bamber et al., 2018).

2.5.1 Datasets considered for the assessment

This assessment of sea level budget contribution from the Greenland ice sheet considers the following datasets:

Reference	**Time period**	**Method**
Update from Barletta et al. (2013)	2003-2016	GRACE
Groh and Horwath (2016)	2003-2015	GRACE
Update from Luthcke et al. (2013)	2003-2015	GRACE
Update from Sasgen et al. (2012)	2003-2016	GRACE
Update from Schrama et al. (2014)	2003-2016	GRACE
Update from (van den Broeke et al., 2016)	1993-2016	Input/output Method (IOM)
Wiese et al. (2016)	2003-2016	GRACE
Update from Wouters et al. (2008)	2003-2016	GRACE

Table 4. Datasets considered in the Greenland mass balance assessment, as well as covered time span and type of observations.

2.5.2. Methods and analyses

All but one of these datasets are based on GRACE data and therefore provide annual time series from ~2002 onwards. The one exception uses IOM (van den Broeke et al., 2016) to give an annual mass time series for a longer time period (1993 onwards).

Notwithstanding this, each group has chosen their own approach to estimate mass balance from GRACE observations. As the aim of this Global Sea Level Budget assessment is to compile existing results (rather than undertake new analyses), we have not imposed a specific methodology. Instead, we asked for the contributed datasets to reflect each group's 'best estimate' of annual trends for Greenland using the method(s) they have published.

Greenland contains glaciers and ice caps around the margins of the main ice sheet, often referred to as peripheral GIC (PGIC), which are a significant proportion of the total mass imbalance (circa 15-20%) (Bolch et al., 2013). Some studies consider the mass balance of the ice sheets and the PGIC separately but there has been, in general, no consistency in the treatment of PGIC and many studies do not specify if they are included or excluded from the total. The GRACE satellites have an approximate spatial resolution of 300 km and the large number of studies that use GRACE, by default, include all land ice within the domain of interest. For this reason, the results below for Greenland mass trends all include PGIC.

From these datasets, for each year from 1993 to 2015 (and 2016 where available), we have calculated an average change in mass (calculated as the weighted mean based on the stated error value for each year) and an error term. Prior to 2003, the results are based on just one dataset (van den Broeke et al., 2016).

2.5.3 Results

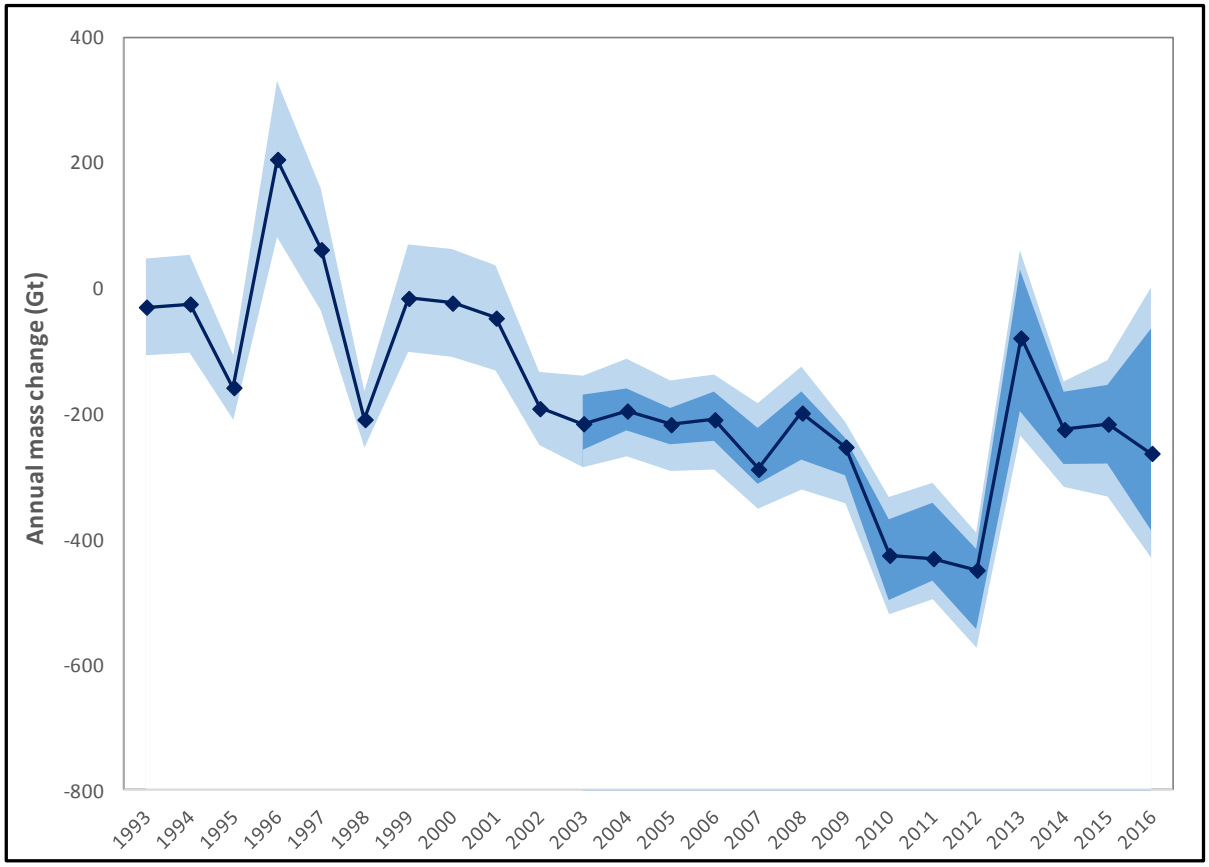

Figure 9. Greenland annual mass change from 1993 to 2016. The medium blue region shows the range of estimates from the datasets listed in Table 1. The lighter blue region shows the

range of estimates when stated errors are included, to provide upper and lower bounds. The dark blue line shows the mean mass trend.

Year	**Δ mass (Gt/yr)**	**Error (Gt/yr)**	**σ (Gt)**
1993	-30	76	
1994	-25	77	
1995	-159	51	
1996	205	123	
1997	61	97	
1998	-209	45	
1999	-16	85	
2000	-24	85	
2001	-48	83	
2002	-192	58	
2003	-216	13	28
2004	-196	12	24
2005	-218	13	21
2006	-210	12	29
2007	-289	10	31
2008	-199	11	39
2009	-253	11	21
2010	-426	9	42
2011	-431	9	47
2012	-450	10	41
2013	-80	13	76
2014	-225	13	38
2015	-217	13	48
2016	-263	23	123
Average estimate 1993-2015	-167	54	

Average estimate 1993-2016	-171	53	
Average estimate 2005-2015	-272	11	
Average estimate 2005-2016	-272	13	

Table 5. Annual time series of Greenland mass change (GT/yr, negative values mean decreasing mass). Δ mass is calculated as the weighted mean based on the stated error value for each year. The error for each year is calculated as the mean of all stated 1-sigma errors divided by sqrt(N) where N is the number of datasets available for that year, assuming that the errors are uncorrelated. The standard deviation (σ) is also given to illustrate the level of agreement between datasets for each year when multiple datasets are available (2003 onwards).

There is generally a good level of agreement between the datasets (Figure 9), and taken together they provide an average estimate of 171 Gt/yr of ice mass loss (or sea level budget contribution) from Greenland for the period 1993 to 2016, increasing to 272 Gt/yr for the period 2005 to 2016 (Table 5).

All the datasets illustrate the previously documented accelerating mass loss up to 2012 (Rignot et al., 2011, Velicogna, 2009) . In 2012, the ice sheet experienced exceptional surface melting reaching as far as the summit (Nghiem et al., 2012) and a record mass loss since, at least 1958, of over 400 Gt (van den Broeke et al., 2016) . The following years, however, show a reduced loss (not more than 270 Gt in any year). Inclusion of the years since 2012 in the 2005-2016 trend estimate reduces the overall rate of mass loss acceleration and its statistical significance. There is greater divergence in the GRACE time series for 2016. We associate this with the degradation of the satellites as they came towards the end of their mission. For 2005-2012, it might be inferred that there is a secular trend towards greater mass loss and from 2010-2012 the value is relatively constant. Inter-annual variability in mass balance of the ice sheet is driven, primarily, by the surface mass balance (i.e. atmospheric weather) and it is apparent that the magnitude of this year to year variability can be large: exceeding 360 Gt (or 1 mm sea level equivalent) between 2012 and 2013. Caution is required, therefore, in extrapolating trends from a short record such as this.

2.6 Antarctica

The annual turn over of mass of Antarctica is about 2,200 Gt/yr (over 6 mm/yr of SLE), 5 times larger than in Greenland (Wessem et al. 2017). In contrast to Greenland, ice and snow melt have a negligible influence on Antarctica's mass balance which is therefore completely controlled by the balance between snowfall accumulation in the drainage basins and ice discharge along the periphery. The continent is also 7 times larger than Greenland, which makes satellite techniques absolutely essential to survey the continent. Interannual variations in accumulation are large in Antarctica, showing decadal to multi-decadal variability, so that many years of data are required to extract trends, and missions limited to only a few years may produce misleading results (e.g. Rignot et al., 2011).

As in Greenland, the estimation of the mass balance has employed a variety of techniques, including 1) the gravity method with GRACE since April 2002 until the end of the mission in late 2016; 2) the IOM method using a series of Landsat and Synthetic-Aperture Radar (SAR) satellites for measuring ice motion along the periphery (Rignot et al., 2011), ice thickness from airborne depth radar sounders such as Operation IceBridge (Leuschen et al., 2014), and reconstructions of surface mass balance using regional atmospheric climate models constrained by re-analysis data (RACMO, MAR and others); and 3) radar/laser altimetry method which mix various satellite altimeters and correct ice elevation changes with density changes from firm models. The largest uncertainty in the GRACE estimate in Antarctica is the GIA which is larger than in Greenland and a large fraction of the observed signal. The IOM method compares two large numbers with large uncertainties to estimate the mass balance as the difference. In order to detect an imbalance at the 10% level, surface mass balance and ice discharge need to be estimated with a precision typically of 5 to 7%. The altimetry method is limited to areas of shallow slope, hence is difficult to use in the Antarctic Peninsula and in the deep interior of the Antarctic continent due to unknown variations of the penetration depth of the signal in snow/firn. The only method that expresses the partitioning of the mass balance between surface processes and dynamic processes is the IOM method (e.g. Rignot et al., 2011). The gravity method is an integrand method which does not suffer from the limitations of SMB models but is limited in spatial resolution (e.g. Velicogna et al., 2014). The altimetry method provides independent evidence of changes in ice dynamics, e.g. by revealing rapid ice thinning along the ice streams and glaciers revealed by ice motion maps, as opposed to large scale variations reflecting a variability in surface mass balance (McMillan et al., 2014).

All these techniques have improved in quality over time and have accumulated a decade to several decades of observations, so that we are now able to assess the mass balance of the Antarctic continent using methods with reasonably low uncertainties, and multiple lines of

838 evidence as the methods are largely independent, which increases confidence in the results
839 (see recent publication by the IMBIE Team, 2018). There is broad agreement in the mass loss
840 from the Antarctic Peninsula and West Antarctica; most residual uncertainties are associated
841 with East Antarctica as the signal is relatively small compared to the uncertainties, although
842 most estimates tend to indicate a low contribution to sea level (e.g. Shepherd et al., 2012).
843
844 **2.6.1 Datasets considered for the assessment**
845 This assessment considers the following datasets:
846

Reference	**Method**	**2005-2015 SLE Trend (mm/yr)**	**1993-2015 SLE Trend (mm/yr)**
Update from Martín-Español et al. (2016)	Joint inversion GRACE/altimetry /GPS	0.43±0.07	-
Update from Forsberg et al. (2017)	Joint inversion GRACE/CryoSat	0.31±0.02	-
Update from Groh and Horwath (2016)	GRACE	0.32±0.11	-
Update from Luthcke et al. (2013)	GRACE	0.36±0.06	-
Update from Sasgen et al. (2013)	GRACE	0.47±0.07	-
Update from Velicogna et al. (2014)	GRACE	0.33±0.08	-
Update from Wiese et al. (2016)	GRACE	0.39±0.02	-
Update from Wouters et al. (2013)	GRACE	0.41±0.05	-
Update from Rignot et al. 2011	Input/Output method (IOM)	0.46±0.05	0.25±0.1
Update from Schrama et al. (2014); version 1	GRACE ICE6G GIA model	0.47±0.03	
Update from Schrama et al. (2014); version 2	GRACE Updated GIA models	0.33±0.03	

Table 6. Datasets considered in this assessment of the Antarctica mass change, and associated trends for the 2005-2015 and 1993-2015 expressed in mm/yr SLE. Positive values mean positive contribution to sea level (i.e. sea level rise)

In Table 6, the negative trend estimate by Zwally et al. (2016) is not added. It is worth noting that including it would only slightly reduce the ensemble mean trend.

2.6.2 Methods and analyses

The datasets used in this assessment are Antarctica mass balance time series generated using different approaches. Two estimates are a joint inversion of GRACE/altimetry/GPS data (Martín-Español et al.,2016), and GRACE and CryoSat data (Forsberg et al.,2017). Two methods are mascon solutions obtained from the GRACE intersatellite range-rate measurements over equal-area spherical caps covering the Earth' surface (Luthcke et al., 2013; Wiese et al., 2016), three estimates use the GRACE spherical harmonics solutions (Velicogna et al., 2014; Wiese et al., 2016; Wouters et al., 2013) and one gridded GRACE products (Sasgen et. al., 2013).

All GRACE time series were provided as monthly time series except for the one using the Martín-Español et al. (2016) method that were provided as annual estimates. In addition, different groups use different GIA corrections, therefore the spread of the trend solutions represents also the error associated to the GIA correction which, in Antarctica, is the largest source of uncertainty. Sasgen et al. (2013) used their own GIA solution (Sasgen et al., 2017), Martín-Español et al. (2016) as well, Luthcke et al., (2013), Velicogna et al. (2014) and Groh and Horwath (2016) used IJ05-R2 (Ivins et al., 2013), Wouter et al. (2013) used Whitehouse et al. (2012), and Wise et al. (2016) used A et al. (2013). In addition, Groh and Horwath (2016) did not include the peripheral glaciers and ice caps, while all other estimates do.

Table 6 shows the Antarctic contribution to sea level during 2005-2015 from the different GRACE solutions, and for the input and output method (IOM).. There is a single IOM-based dataset that provides trends for the period 1993-2015 (update of Rignot et al., 2011). For the period 2005-2015, we calculated the annual sea level contribution from Antarctica using GRACE and IOM estimates (Table 7).

As we are interested in evaluating the long-term trend and inter-annual variability of the Antarctic contribution to sea level, for each GRACE datasets available in monthly time series, we first removed the annual and sub-annual components of the signal by applying a 13-month averaging filter and we then used the smoothed time series to calculate to annual mass

change. Figure 10 shows the annual sea level contribution from Antarctica calculated from the GRACE-derived estimates and for the Input-Output method. The GRACE mean annual estimates are calculated as the mean of the annual contributions from the different groups, and the associated error calculated as the sum of the spread of the annual estimates and the mean annual error.

2.6.3 Results

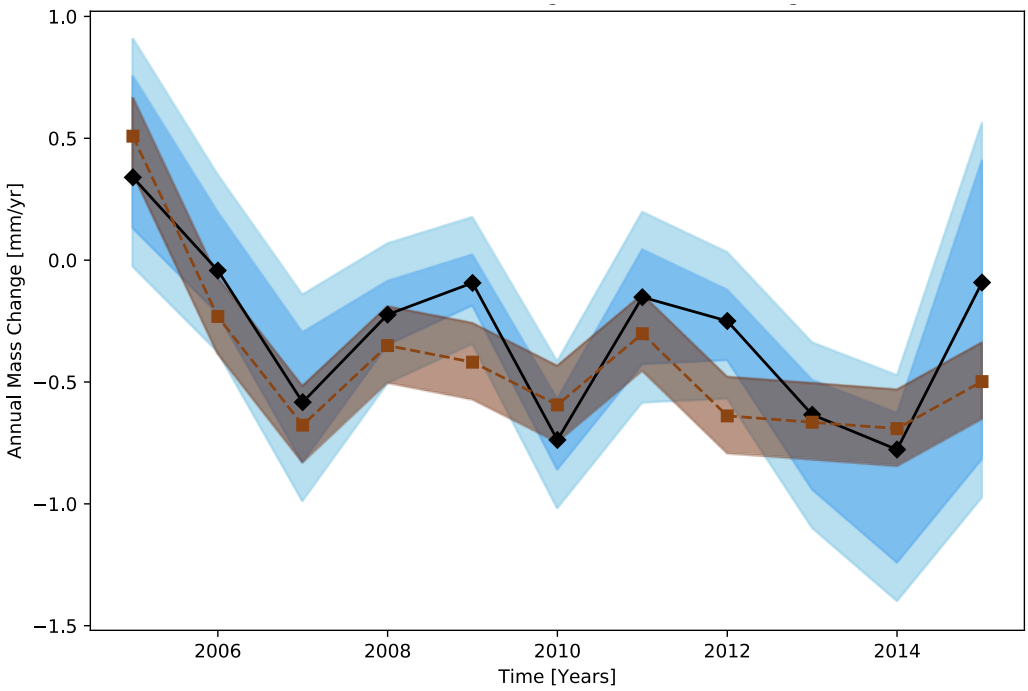

Figure 10. Antarctic annual sea level contribution during 2005 to 2015. The black squares are the mean annual sea level calculated using the GRACE datasets listed in Table 6. The darker blue band shows the range of estimates from the datasets. The light blue band account for the error in the different GRACE estimates. The brown squares are the annual sea level contribution calculated using the Input-Output method (updated from Rignot et al., 2011), the light brown band is the associated error.

Year	**GRACE** **mm/yr** **SLE**	**IOM** **mm/yr** **SLE**	**Mean** **mm/yr** **SLE**

2005	-0.34±0.47	-0.51±0.16	-0.42±0.31
2006	0.04±0.36	0.23±0.16	0.14±0.26
2007	0.58±0.42	0.68±0.16	0.63±0.29
2008	0.22±0.29	0.35±0.16	0.29±0.22
2009	0.09±0.26	0.42±0.16	0.26±0.21
2010	0.74±0.30	0.59±0.16	0.67±0.23
2011	0.15±0.39	0.30±0.16	0.23±0.27
2012	0.25±0.30	0.64±0.16	0.44±0.23
2013	0.63±0.38	0.67±0.16	0.65±0.27
2014	0.78±0.46	0.69±0.16	0.73±0.31
2015	0.09±0.77	0.50±0.16	0.29±0.46
Average estimate 2005-2015	0.38±0.06	0.46±0.05	0.42±0.06

Table 7. Annual sea level contribution from Antarctica during 2005-2015 from GRACE and Input-Output method (IOM) calculated as described above and expressed in mm/yr SLE. Also shown is the mean of the estimate from the two methods, associated errors are the mean of the two estimated errors. Positive values mean positive contribution to sea level (i.e. sea level rise)

There is generally broad agreement between the GRACE datasets (Figure 10), as most of the differences between GRACE estimates are caused by differences in the GIA correction. We find a reasonable agreement between GRACE and the IOM estimates although the IOM estimates indicate higher losses. Taken together, these estimates yield an average of 0.42 mm/yr sea level budget contribution from Antarctica for the period 2005 to 2015 (Table 7) and 0.25 mm/yr sea level for the time period 1993-2005, where the latter value is based on IOM only.

All the datasets illustrate the previously documented accelerating mass loss of Antarctica (Rignot et al., 2011, Velicogna, 2009). In 2005-2010, the ice sheet experienced ice mass loss driven by an increase in mass loss in the Amundsen Sea sector of West Antarctica (Mouginot et al., 2014). The following years showed a reduced increase in mass loss, as colder ocean conditions prevailed in the Amundsen Sea Embayment sector of West Antarctica in 2012-2013 which reduced the melting of the ice shelves in front of the glaciers (Dutrieux et al.,

2014). Divergence in the GRACE time series is observed after 2015 due to the degradation of the satellites towards the end of the mission.

The large inter-annual variability in mass balance in 2005-2015, characteristic of Antarctica, nearly masks out the trend in mass loss, which is more apparent in the longer time series than in short time series. The longer record highlights the pronounced decadal variability in ice sheet mass balance in Antarctica, demonstrating the need for multi-decadal time series in Antarctica, which have been obtained only by IOM and altimetry. The inter-annual variability in mass balance is driven almost entirely by surface mass balance processes. The mass loss of Antarctica, about 200 Gt/yr in recent years, is only about 10% of its annual turn over of mass (2,200 Gt/yr), in contrast with Greenland where the mass loss has been growing rapidly to nearly 100% of the annual turn over of mass. This comparison illustrates the challenge of detecting mass balance changes in Antarctica, but at the same time, that satellite techniques and their interpretation have made tremendous progress over the last 10 years, producing realistic and consistent estimates of the mass using a number of independent methods (Bamber et al., 2018; the IMBIE Team, 2018).

2.7 Terrestrial Water Storage

Human transformations of the Earth's surface have impacted the terrestrial water balance, including continental patterns of river flow and water exchange between land, atmosphere and ocean, ultimately affecting global sea level. For instance, massive impoundment of water in man-made reservoirs has reduced the direct outflow of water to the sea through rivers, while groundwater abstractions, wetland and lake storage losses, deforestation and other land use changes have caused changes to the terrestrial water balance, including changing evapotranspiration over land, leading to net changes in land-ocean exchanges (Chao et al., 2008; Wada et al., 2012a,b; Konikow 2011; Church et al., 2013; Doll et al., 2014a,b). Overall, the combined effects of direct anthropogenic processes have reduced land water storage, increasing the rate of sea level rise (SLR) by 0.3-0.5 mm/yr during recent decades (Church et al., 2013; Gregory et al., 2013; Wada et al., 2016). Additionally, recent work has shown that climate driven changes in water stores can perturb the rate of sea level change over interannual to decadal time scales, making global land mass budget closure sensitive to varying observational periods (Cazenave et al., 2014; Dieng et al., 2015; Reager et al., 2016; Rietbroek et al., 2016). Here we discuss each of the major component contributions from

964 land, with a summary in Table 8, and estimate the net terrestrial water storage (TWS)
965 contribution to sea level.
966
967 ***2.7.1 Direct anthropogenic changes in terrestrial water storage***
968
969 *Water impoundment behind dams*
970 Wada et al. (2016) built on work by Chao et al. (2008) to combine multiple global reservoir
971 storage data sets in pursuit of a quality-controlled global reservoir database. The result is a list
972 of 48064 reservoirs that have a combined total capacity of 7968 km^3. The time history of
973 growth of the total global reservoir capacity reflects the history of the human activity in dam
974 building. Applying assumptions from Chao et al. (2008), Wada et al. (2016) estimated that
975 humans have impounded a total of 10,416 km^3 of water behind dams, accounting for a
976 cumulative 29 mm drop in global mean sea level. From 1950 to 2000 when global dam-
977 building activity was at its highest, impoundment contributed to the average rate of sea level
978 change at -0.51 mm/year. This was an important process in comparison to other natural and
979 anthropogenic sources of sea level change over the past century, but has now largely slowed
980 due to a global decrease in dam building activity.
981
982 *Global groundwater depletion*
983 Groundwater currently represents the largest secular trend component to the land water
984 storage budget. The rate of groundwater depletion (GWD) and its contribution to sea level has
985 been subject to debate (Gregory et al., 2013; Taylor et al., 2013). In the IPCC AR4 (Solomon
986 et al., 2007), the contribution of non-frozen terrestrial waters (including GWD) to sea-level
987 variation was not considered due to its perceived uncertainty (Wada, 2016). Observations
988 from GRACE opened a path to monitor total water storage changes including groundwater in
989 data scarce regions (Strassberg et al., 2007; Rodell et al. 2009; Tiwari et al. 2009; Jacob et al.,
990 2012; Shamsudduha et al., 2012; Voss et al., 2013). Some studies have also applied global
991 hydrological models in combination with the GRACE data (see Wada et al., 2016 for a
992 review).
993 Earlier estimates of GWD contribution to sea level range from 0.075 mm yr^{-1} to 0.30 mm yr^{-1}
994 (Sahagian et al., 1994; Gornitz, 1995, 2001; Foster and Loucks, 2006). More recently, Wada
995 et al. (2012b), using hydrological modelling, estimated that the contribution of GWD to
996 global sea level increased from 0.035 (±0.009) to 0.57 (±0.09) mm/yr during the 20^{th} century
997 and projected that it would further increase to 0.82 (±0.13) mm/yr by 2050. Döll et al. (2014)

998 used hydrological modeling, well observations, and GRACE satellite gravity anomalies to
999 estimate a 2000–2009 global GWD of 113 km^3/yr (0.314 mm/yr SLE). This value represents
1000 the impact of human groundwater withdrawals only and does not consider the effect of
1001 climate variability on groundwater storage. A study by Konikow (2011) estimated global
1002 GWD to be 145 (±39) km^3/yr (0.41 ±0.1 mm/yrSLE) during 1991-2008 based on
1003 measurements of changes in groundwater storage from in situ observations, calibrated
1004 groundwater modelling, GRACE satellite data and extrapolation to unobserved aquifers.
1005 An assumption of most existing global estimates of GWD impacts on sea level change is that
1006 nearly 100% of the GWD ends up in the ocean. However, groundwater pumping can also
1007 perturb regional climate due to land-atmosphere interactions (Lo and Famiglietti, 2013). A
1008 recent study by Wada et al. (2016) used a coupled land-atmosphere model simulation to track
1009 the fate of water pumped from underground and found it more likely that ~80% of the GWD
1010 ends up in the ocean over the long-term, while 20% re-infiltrates and remains in land storage.
1011 They estimated an updated contribution of GWD to global sea level rise ranging from 0.02
1012 (±0.004) mm/yr in 1900 to 0.27 (±0.04) mm/yr in 2000 (Figure 11). This indicates that
1013 previous studies had likely overestimated the cumulative contribution of GWD to global SLR
1014 during the 20th century and early 21st century by 5-10 mm.
1015
1016 *Land cover and land-use change*
1017 Humans have altered a large part of the land surface, replacing 33% (Vitousek et al., 1997) or
1018 even 41 % (Sterling et al., 2013) of natural vegetation by anthropogenic land cover such as
1019 crop fields or pasture. Such land cover change can affect terrestrial hydrology by changing the
1020 infiltration-to-runoff ratio, and can impact subsurface water dynamics by modifying recharge
1021 and increasing groundwater storage (Scanlon et al., 2007). The combined effects of
1022 anthropogenic land cover changes on land water storage can be quite complex. Using a
1023 combined hydrological and water resource model, Bosmans et al. (2017) estimated that land
1024 cover change between 1850 and 2000 has contributed to a discharge increase of 1058 km^3 /yr,
1025 on the same order of magnitude as the effect of human water use. These recent model results
1026 suggest that land-use change is an important topic for further investigation in the future. So
1027 far, this contribution remains highly uncertain.
1028
1029 *Deforestation/afforestation*
1030 At present, large losses in tropical forests and moderate gains in temperate-boreal forests
1031 result in a net reduction of global forest cover (FAO, 2015; Keenan et al., 2015; MacDicken,

2015; Sloan and Sayer, 2015). Net deforestation releases carbon and water stored in both biotic tissues and soil, which leads to sea level rise through three primary processes: deforestation-induced runoff increases (Gornitz et al., 1997), carbon loss-related decay and plant storage loss, and complex climate feedbacks (Butt et al., 2011; Chagnon and Bras, 2005; Nobre et al., 2009; Shukla et al., 1990; Spracklen et al., 2012). Due to these three causes, and if uncertainties from the land-atmospheric coupling are excluded, a summary by Wada et al. (2016) suggests that the current net global deforestation leads to an upper-bound contribution of ~0.035 mm/yr SLE.

Wetland degradation

Wetland degradation contributes to sea level primarily through (i) direct water drainage or removal from standing inundation, soil moisture, and plant storage, and (ii) water release from vegetation decay and peat combustion. Wada et al. (2016) consider a recent wetland loss rate of 0.565% yr^{-1} since 1990 (Davidson, 2014) and a present global wetland area of 371 mha averaged from three databases: Matthews natural wetlands (Matthews and Fung, 1987), ISLSCP (Darras, 1999), and DISCover (Belward et al., 1999; Loveland and Belward, 1997). They assume a uniform 1-meter depth of water in wetlands (Milly et al., 2010), to estimate a contribution of recent global wetland drainage to sea level of 0.067 mm/yr. Wada et al. (2016) apply a wetland area and loss rate as used for assessing wetland water drainage, to determine the annual reduction of wetland carbon stock since 1990, if completely emitted, releases water equivalent to 0.003–0.007 mm/yr SLE. Integrating the impacts of wetland drainage, oxidation and peat combustion, Wada et al. (2016) suggest that the recent global wetland degradation results in an upper bound of 0.074 mm/yr SLE.

Lake storage changes

Lakes store the greatest mass of liquid water on the terrestrial surface (Oki and Kanae, 2006), yet, because of their "dynamic" nature (Sheng et al., 2016; Wang et al., 2012), their overall contribution to sea level remains uncertain. In the past century, perhaps the greatest contributor in global lake storage was the Caspian Sea (Milly et al., 2010), where the water level exhibits substantial oscillations attributed to meteorological, geological, and anthropogenic factors (Ozyavas et al., 2010, Chen et al., 2017). Assuming the lake level variation kept pace with groundwater changes (Sahagian et al., 1994), the overall contribution of the Caspian Sea, including both surface and groundwater storage variations through 2014, has been about 0.03 mm/yr SLE since 1900, 0.075 (±0.002) mm/yr since 1995, or 0.109

(±0.004) mm/yr since 2002. Additionally, between 1960 and 1990, the water storage in the Aral Sea Basin declined at a striking rate of 64 km^3/yr, equivalent to 0.18 mm/yr SLE (Sahagian, 2000; Sahagian et al., 1994; Vörösmarty and Sahagian, 2000) due mostly to upstream water diversion for irrigation (Perera, 1993), which was modeled by Pokhrel et al. (2012) to be ~500 km^3 during 1951–2000, equivalent to 0.03 mm/yr SLE. Dramatic decline in the Aral Sea continued in the recent decade, with an annual rate of 6.043 (±0.082) km^3/yr measured from 2002 to 2014 (Schwatke et al., 2015). Assuming that groundwater drainage has kept pace with lake level reduction (Sahagian et al., 1994), the Aral Sea has contributed 0.0358 (±0.0003) mm/yr to the recent sea level rise.

Water cycle variability

Natural changes in the interannual to decadal cycling of water can have a large effect on the apparent rate of sea level change over decadal and shorter time periods (Milly et al., 2003; Lettenmaier and Milly, 2009; Llovell et al., 2010). For instance, ENSO-driven modulations of the global water cycle can be important in decadal-scale sea level budgets and can mask underlying secular trends in sea level (Cazenave et al., 2014, Nerem et al., 2018).

Sea level variability due to climate-driven hydrology represents a super-imposed variability on the secular rates of global mean sea level rise. While this term can be large and is important in the interpretation of the sea level record, it is arguably the most difficult term in the land water budget to quantify.

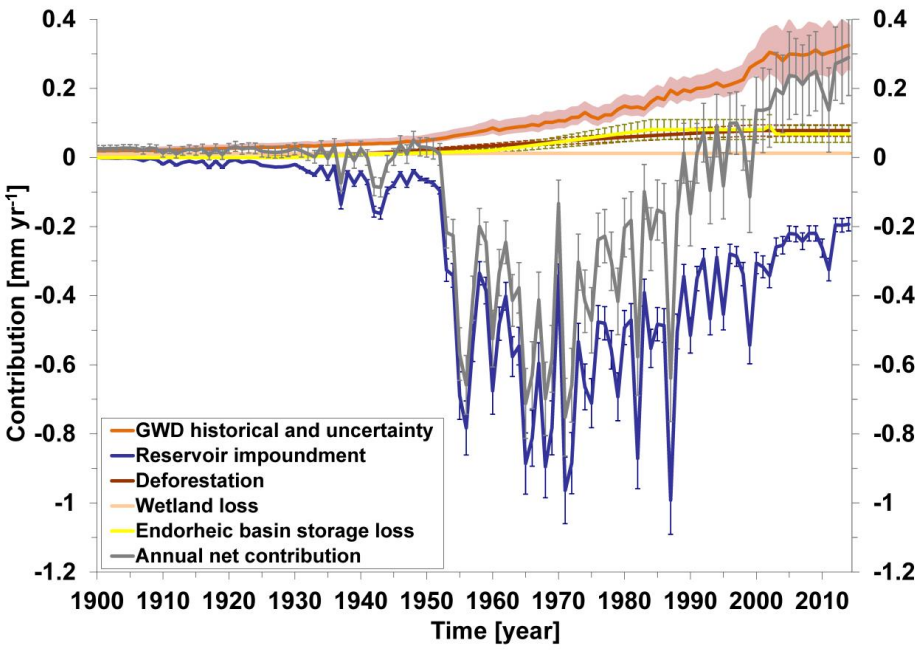

Figure 11: *Time series of the estimated annual contribution of terrestrial water storage change to global sea-level over the period 1900-2014 (rates in mm yr^{-1} SLE) (modified from Wada et al., 2016).*

2.7.2. Net terrestrial water storage

GRACE-based estimates

Measurements of non-ice-sheet continental land mass from GRACE satellite gravity have been presented in several recent studies (Jensen et al., 2013, Rietbroek et al., 2016; Reager et al., 2016, Scanlon et al., 2018), and can be used to constrain a global land mass budget. Note that these 'top-down' estimates contain both climate-driven and direct anthropogenic driven effects, which makes them most useful in assessing the total impact of land water storage changes and closing the budget of all contributing terms. GRACE observations, when averaged over the whole land domain following Reager et al. (2016), indicate a total TWS change (including glaciers) over the 2002-2014 study period of approximately +0.32 ± 0.13 mm/yr SLE (i.e., ocean gaining mass). Global mountain glaciers have been estimated to lose mass at a rate of 0.65 +/- 0.09 mm/yr (e.g. Gardner et al., 2013; Reager et al., 2016) during that period, such that a mass balance indicates that global glacier-free land gained water at a rate of -0.33 ± 0.16 mm/yr SLE (i.e., ocean losing mass; Figure 12). A roughly similar estimate was found from GRACE using glacier free river basins globally (-0.21 ± 0.09 mm/yr) (Scanlon et al., 2018). Thus, the GRACE-based net TWS estimates suggest a negative sea level contribution from land over the GRACE period (Table 8). However, mass change estimate from GRACE incorporates uncertainty from all potential error sources that arise in processing and post-processing of the data, including from the GIA model, and from the geocenter and mean pole corrections.

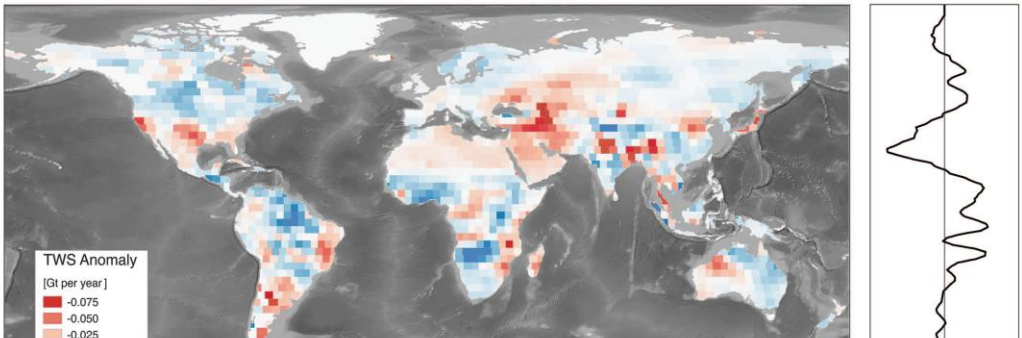

Figure 12: An example of trends in land water storage from GRACE observations, April 2002 to November 2014. Glaciers and ice sheets are excluded. Shown are the global map (gigatons per year), zonal trends, and full time series of land water storage (in mm/yr SLE). Following methods details in Reager et al., (2016), GRACE shows a total gain in land water storage during the 2002-2014 period, corresponding to a sea level trend of -0.33 ± 0.16 mm/yr[1] SLE (modified from Reager et al., 2016). These trends include all human-driven and climate-driven processes in Table 1, and can be used to close the land water budget over the study period.

Estimates based on global hydrological models

Global land water storage can also be estimated from global hydrological models (GHMs) and global land surface models. These compute water, or water and energy balances, at the Earth surface, yielding time variations of water storage in response to prescribed atmospheric data (temperature, humidity and wind) and the incident water and energy fluxes from the atmosphere (precipitation and radiation). Meteorological forcing is usually based on atmospheric model reanalysis. Model uncertainties result from several factors. Recent work has underlined the large differences among different state-of-the-art precipitation datasets (Beck et al., 2017) with large impacts on model results at seasonal (Schellekens et al., 2017) and longer time scales (Felfelani et al., 2017). Another source of uncertainty is the treatment of subsurface storage in soils and aquifers, as well as dynamic changes in storage capacity due to representation of frozen soils and permafrost, the complex effects of dynamic vegetation, atmospheric vapor pressure deficit estimation and an insufficiently deep soil column. A recent study by Scanlon et al. (2018) compared water storage trends from five global land surface models and two global hydrological models to GRACE storage trends, and found that models estimated the opposite trend in net land

water storage to GRACE over the 2002 – 2014 period. These authors attributed this discrepancy to model deficiencies, in particular soil depth limitations. These combined error sources are responsible for a range of storage trends across models of approximately 0.5 ± 0.2 mm/yr SLE. In terms of global land average, model differences can cause up to ~0.4 mm/yr SLE uncertainty.

Estimate Terrestrial Water Storage contribution to sea level		**2002-2014/15 (mm/yr) SLE** *(Positive values mean sea level rise)*
Human contributions by component		
Ground water depletion	*Wada et al. (2016)*	0.30 (± 0.1)
Reservoir impoundment	*Wada et al. (2017)*	-0.24 (± 0.02)
Deforestation (after 2010)	*Wada et al. (2017)*	0.035
Wetland loss (after 1990)	*Wada et al. (2017)*	0.074
Endorheic basin storage loss		
Caspian Sea	*Wada et al. (2017)*	0.109 (± 0.004)
Aral Sea	*Wada et al. (2017)*	0.036 (± 0.0003)
Aggregated human intervention (sum of above)	*Scanlon et al. (2018)*	0.15 to 0.24
Hydrological model-based estimates		
WGHM model *(natural variability plus human intervention; P. Döll, personal communication)*		0.15 +/- 0.14
ISBA-TRIP model *(natural variability only ; Decharme et al., 2016) + human intervention from Wada et al. (2016) (from Dieng et al., 2017)*		0.23 +/- 0.10
GRACE-based estimates of total land water storage (not including glaciers) *(Reager et al., 2016; Rietbroek et al., 2016; Scanlon et al., 2018)*		-0.20 to -0.33 (± 0.09 - 0.16)

Table 8. Estimates of TWS components due to human intervention and net TWS based on hydrological models and GRACE

2.7.3 Synthesis

Based on the different approaches to estimate the net land water storage contribution, we estimate that corresponding sea level rate ranges from -0.33 to 0.23 mm/yr during the period of 2002-2014/15 due to water storage changes (Table 8). According to GRACE, the net TWS change (i.e. not including glaciers) over the period 2002-2014 shows a negative contribution to sea level of -0.33 mm/yr and -0.21 mm/yr by Reager et al. (2016) and Scanlon et al. (2018) respectively. Such a negative signal is not currently reproduced by hydrological models which estimate slightly positive trends over the same period (see Table 8). It is to be noted however that looking at trends only over periods of the order of a decade may not be appropriate due the strong interannual variability of TWS at basin and global scales. For example, Figure 5 from Scanlon et al. (2018) (see also Figure S9 from their Supplementary Material), that compares GRACE TWS and model estimates over large river basins over 2002-2014, clearly show that the discrepancies between GRACE and models occur at the end of the record for the majority of basins. This is particularly striking for the Amazon basin (the largest contributor to TWS), for which GRACE and models agree reasonably well until 2011, and then depart significantly, with GRACE TWS showing strongly positive trend since then, unlike models. Such a divergence at the end of the record is also noticed for several other large basins (see Scanlon et al., Figure S9 SM). No clear explanation can be provided yet, even though one may questions the quality of the meteorological forcing used by hydrological models for the recent years. But this calls for some caution when comparing GRACE and models on the basis of trends only because of the dominant interannual variability of the TWS component. Much more work is needed to understand differences among models, and between models and GRACE. Of all components entering in the sea level budget, the TWS contribution currently appears as the most uncertain one.

2.8 Glacial Isostatic Adjustment

The Earth's dynamic response to the waxing and waning of the late-Pleistocene ice sheets is still causing isostatic disequilibrium in various regions of the world. The accompanying slow process of GIA is responsible for regional and global fluctuations in relative and absolute sea level, 3D crustal deformations and changes of the Earth's gravity field (for a review, see Spada, 2017). To isolate the contribution of current climate change, geodetic observations must be corrected for the effects of GIA (King et al., 2010). These are obtained by solving the "Sea Level Equation'' (Farrell and Clark 1976, Mitrovica and Milne 2003). The sea level can be expressed as $S=N-U$, where S is the rate of change of sea-level relative to the solid Earth, N

is the geocentric rate of sea-level change, and U is the vertical rate of displacement of the solid Earth. The sea level equation accounts for solid Earth deformational, gravitational and rotational effects on sea level, which are sensitive to the Earth's mechanical properties and to the melting chronology of continental ice. Forward GIA modeling, based on the solution of the sea level equation, provides predictions of unique spatial patterns (or *fingerprints,* see Plag and Juettner, 2001) of relative and geocentric sea-level change (e.g., Milne et al. 2009, Kopp et al. 2015). During the last decades, the two fundamental components of GIA modeling have been progressively constrained from the observed history of relative sea level during the Holocene (see *e.g.*, Lambeck and Chappell 2001, Peltier 2004). In the context of climate change, the importance of GIA has been recognized in the mid 1980s, when the awareness of global sea-level rise stimulated the evaluation of the isostatic contribution to tide gauge observations (see Table 1 in Spada and Galassi 2012). Subsequently, GIA models have been applied to the study of the pattern of sea level change from satellite altimetry (Tamisiea 2011), and since 2002 to the study of the gravity field variations from GRACE. Our primary goal here is to analyse GIA model outputs that have been used to infer global mean sea level change and ice sheet volume change from geodetic datasets during the altimetry era. These outputs are the sea-level variations detected by satellite altimetry across oceanic regions (n), the ocean mass change (w) and the modern ice sheets mass balance from GRACE. We also discuss the GIA correction that needs to be applied to GRACE-based land water storage changes. The GIA correction applied to tide gauge-based sea level observations at the coastlines is not discussed here. Since GIA evolves on time scales of millennia (e.g., Turcotte and Schubert, 2014), the rate of change of all the isostatic signals can be considered constant on the time scale of interest.

2.8.1 GIA correction to altimetry-based sea level

Unlike tide gauges, altimeters directly sample the sea surface in a geocentric reference frame. Nevertheless, GIA contributes significantly to the rates of absolute sea-level change observed over the "altimetry era'', which require a correction N_{gia} that is obtained by solving the SLE (e.g., Spada 2017). As discussed in detail by Tamisiea (2011), N_{gia} is sensitive to the assumed rheological profile of the Earth and to the history of continental glacial ice sheets. The variance of N_{gia} over the surface of the oceans is much reduced, being primarily determined by the change of the Earth's gravity potential, apart from a spatially uniform shift. As discussed by Spada and Galassi (2016), the GIA contribution N_{gia} is strongly affected by variations in the centrifugal potential associated with Earth rotation, whose fingerprint is

dominated by a spherical harmonic contribution of degree $l=2$ and order $m=\pm 1$. Since N_{gia} has a smooth spatial pattern, the global the GIA correction to altimetry data can be obtained by simply subtracting its average $n = < N_{gia} >$ over the ocean sampled by the altimetry missions. The computation of the GIA contribution N_{gia} has been the subject of various investigations, based on different GIA models. The estimate by Peltier (2001) of n equals -0.30 mm/yr, based on the ICE-4G (VM2) GIA model. Such a value has been adopted in the majority of studies estimating the GMSL rise from altimetry. Since n appears to be small compared to the global mean sea-level rise from altimetry (~3 mm/yr), a more precise evaluation has not been of concern until recently. However, it is important to notice that n is of comparable magnitude as the GMSL trend uncertainty, currently estimated to ~0.3 mm/yr (see sub section 2.2). In Table 9a, we summarize the values of n according to works in the literature where various GIA model models and averaging methods have been employed. Based on values in Table 9a for which a standard deviation is available, the average of n (weighted by the inverse of associated errors), assumed to represent the best estimate, is $n = (-0.29 \pm 0.02)$ mm/yr where the uncertainty corresponds to 2σ.

2.8.2 GIA correction to GRACE-based ocean mass

GRACE observations of present-day gravity variations are sensitive to GIA, due to the sheer amount of rock material that is transported by GIA throughout the mantle and the resulting changes in surface topography, especially over the formerly glaciated areas. The continuous change in the gravity field results in a nearly linear signal in GRACE observations. Since the gravity field is determined by global mass redistribution, GIA models used to correct GRACE data need to be global as well, especially when the region of interest is represented by all ocean areas. To date, the only global ice reconstruction publicly available is provided by the University of Toronto. Their latest product, named ICE-6G, has been published and distributed in 2015 (Peltier et al., 2015); note that the ice history has been simultaneously constrained with a specific Earth model, named VM5a. During the early period of the GRACE mission, the available Toronto model was ICE-5G (VM2) (Peltier, 2004). However, different groups have independently computed GIA model solutions based on the Toronto ice history reconstruction, by using different implementations of GIA codes and somehow different Earth models. The most widely used model is the one by Paulson et al. (2007), later updated by A et al. (2013). Both studies use a deglaciation history based on ICE-5G, but differ for the viscosity profile of the mantle: A et al. use a 3D compressible Earth with VM2 viscosity profile and a PREM-based elastic structure used by Peltier (2004), whereas Paulson

et al. (2007) use an incompressible Earth with self-gravitation, and a Maxwell 1-D multi-layer mantle. Over most of the oceans, the GIA signature is much smaller than over the continents. However, once integrated over the global ocean, the signal *w* due to GIA is about -1 mm/yr of equivalent sea level change (Chambers et al., 2010), which is of the same order of magnitude as the total ocean mass change induced by increased ice melt (Leuliette and Willis, 2011). The main uncertainty in the GIA contribution to ocean mass change estimates, apart from the general uncertainty in ice history and Earth mechanical properties, originates from the importance of changes in the orientation of the Earth's rotation axis (Chambers et al., 2010, Tamisiea, 2011). Different choices in implementing the so-called "rotational feedback" lead to significant changes in the resulting GIA contribution to GRACE estimates. The issue of properly accounting from rotational effects has not been settled yet (Mitrovica et al., 2005, Peltier and Luthcke, 2009, Mitrovica and Wahr, 2011, Martinec and Hagedoorn, 2014). Table 9b summarizes the values of the mass-rate GIA contribution *w* according to the literature, where various models and averaging methods are employed. The weighed average of the values in Table 9b for which an assessment of the standard deviation is available, is w = (-1.44 ± 0.36) mm/yr (the uncertainty is 2σ), which we assume to represent the preferred estimate.

2.8.3 GIA correction to GRACE-based terrestrial water storage

As discussed in the previous section, the GIA correction to apply to GRACE over land is significant, especially in regions formerly covered by the ice sheets (Canada and Scandinavia). Over Canada, GIA models significantly differ. This is illustrated in Figure 13 that shows difference between two models of GIA correction to GRACE over land, the A et al. (2013) and Peltier et al. (2009) models. We see that over the majority of the land areas, differences are small, except over north Canada, in particular around the Hudson Bay, where differences larger than +/- 20 mm/yr SLE are noticed. This may affect GRACE-based TWS estimates over Canadian river basins.

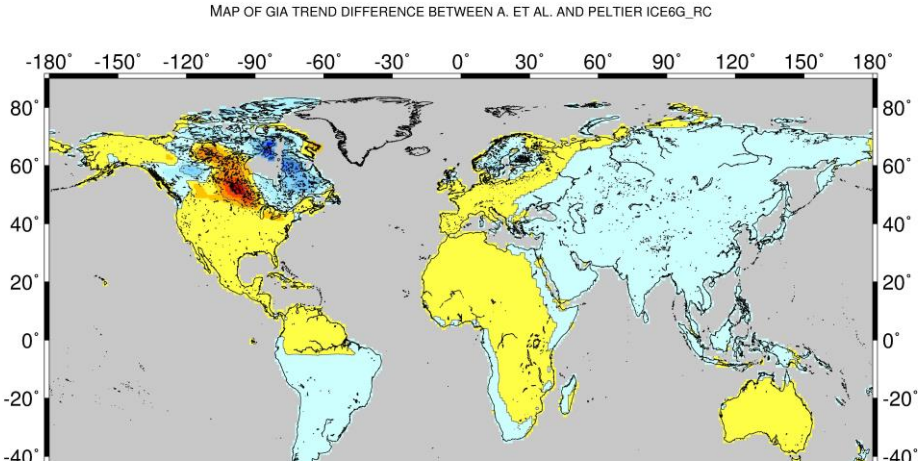

Figure 13: Difference map between two models of GIA correction to GRACE over land: A et al. (2013) versus Peltier et al. (2015), the units in mm/yr SLE.

When averaged over the whole land surface as done in some studies to estimate the combined effect of land water storage and glacier melting from GRACE (e.g., Reager et al., 2015; see section 2.7), the GIA correction ranges from ~ 0.5 to 0.7 mm/yr (in mm/yr SLE). Values for different GIA models are given in Table 9c.

2.8.4 GIA correction to GRACE-based ice sheet mass balance

The GRACE gravity field observations allow the determination of mass balances of ice sheets and large glacier systems with inaccuracy similar or superior to the input-output method or satellite laser and radar altimetry (Shepherd et al., 2012). However, GRACE ice-mass balances rely on successfully separating and removing the apparent mass change related to GIA. While the GIA correction is small compared to the mass balance for Greenland ice sheet (ca. < 10%), its magnitude and uncertainty in Antarctica is of the order of the ice-mass balance itself (*e.g.* Martín-Español et al., 2016). Particularly for today's glaciated areas, GIA remains poorly resolved due to the sparse data constraining the models, leading to large uncertainties in the climate history, the geometry and retreat chronology of the ice sheet, as well as the Earth structure. The consequences are ambiguous GIA predictions, despite fitting the same observational data. There are two principal approaches towards resolving GIA underneath the ice sheets. Empirical estimates can be derived making use of the different sensitivities of satellite observations to ice-mass changes and GIA (e.g. Riva et al., 2009, Wu et al., 2010). Alternatively, GIA can be modeled numerically by forcing an Earth model with a fixed ice retreat scenario (e.g., Peltier 2009, Whitehouse et al., 2012) or with output from a thermodynamic ice sheet model (Gomez et al., 2013, Konrad et al., 2015). Values of GIA-induced apparent mass change for Greenland and Antarctica as listed in the literature should be applied with caution (Table 9d) when applying them to GRACE mass balances. Each of

these estimates may rely on a different GRACE post-processing strategy and may differ in the approach used for solving the gravimetric inverse problem (mascon analysis, forward-modeling, averaging kernels). Of particular concern is the modeling and filtering of the pole tide correction caused by the rotational variations related to GIA, affecting coefficients of harmonic degree $l=2$ and order $m=\pm1$. As mentioned above, agreement on the modeling of the rotational feedback has not been reached within the GIA community. Furthermore, the pole tide correction applied during the determination gravity-field solutions differs between the GRACE processing centres and may not be consistent with the GIA correction listed. This inconsistency may introduce a significant bias in the ice-mass balance estimates (e.g. Sasgen et al., 2013, Supplementary Material). Wahr et al. (2015) presented recommendations on how to treat the pole tides in GRACE analysis. However, a systematic inter-comparison of the GIA predictions in terms of their low-degree coefficients and their consistency with the GRACE processing standards still need to be done.

Table 9. *Estimated contributions of GIA to the rate of absolute sea level change observed by altimetry (a), to the rate of mass change observed by GRACE over the global oceans (b), to the rate of mass change observed by GRACE over land (c), and to Greenland and Antarctic ice sheets (c), during the altimetry era. The GIA corrections are expressed in mm/yr SLE except over Greenland and Antarctica where values are given in Gt/yr (ice mass equivalent). Most of the GIA contributions are expressed as a value ± one standard deviation; a few others are given in terms of a plausible range, for some the uncertainties are not specified.*

(a) GIA correction to absolute sea level measured by altimetry

Reference	*GIA (mm/yr)*	*Notes*
Peltier (2009) (Table 3)	-0.30 ± 0.02 -0.29 ± 0.03 -0.28 ± 0.02	Average of 3 groups of 4 values obtained by variants of the analysis procedure, using ICE-5G(VM2), over a global ocean, in the range of latitudes 66°S to 66°N and 60°S to 60°N, respectively.
Tamisiea (2011) (Figure 2)	-0.15 to -0.45 -0.20 to -0.50	Simple average over the oceans for a range of estimates obtained varying the Earth model parameters, over a

		global ocean and between latitudes 66°S and 66°N.
Huang (2013) (Table 3.6)	-0.26 ± 0.07 -0.27 ± 0.08	Average from an ensemble of 14 GIA models over a global ocean and between latitude from 66°S to 66°N.
Spada (2017) (Table 1)	-0.32 ± 0.08	Based on four runs of the Sea Level Equation solver SELEN (Spada and Stocchi, 2007) using model ICE-5G(VM2), with different assumptions in solving the SLE.

(b) GIA contribution to GRACE mass-rate of change over the oceans

Reference	*GIA (mm/yr SLE)*	*Notes*
Peltier (2009) (Table 3)	-1.60 ± 0.30	Average of values from 12 corrections for variants of the analysis procedure, using ICE-5G (VM2).
Chambers (2010) (Table 1)	-1.45 ± 0.35	Average over the oceans for a range of estimates produced by varying the Earth models.
Tamisiea (2011) (Figures 3 and 4)	-0.5 to -1.9 -0.9 to −1.5	Ocean average of a range of estimates varying the Earth model, and based on a restricted set, respectively.
Huang (2013) (Table 3.7)	-1.31 ± 0.40 -1.26 ± 0.43	Average from an ensemble of 14 GIA models over a global ocean and between latitude from 66°S to 66°N, respectively.

(c) GIA contribution to GRACE-based terrestrial water storage change

Reference	*GIA correction (mm/yr SLE) (without Greenland, Antarctica, Iceland, Svalbard, Hudson Bay and Black Sea*
A et al. (2013)	0.63
Peltier ICE5G	0.68
Peltier ICE6G_rc	0.71

ANU_ICE6G	0.53

(d) GIA contribution to GRACE mass-rate of the ice sheets

	Greenland	
Reference	*GIA (Gt/yr)*	*Notes*
Simpson et al. (2009) [r]	-3 ± 12 [m]	Thermodynamic sheet / solid Earth model, 1D (uncoupled); constrained by geomorphology; inversion results in Sutterley *et al.* (2014).
Peltier (2009) (ICE-5G) [g]	-4 [f]	Ice load reconstruction / solid Earth model, 1D (ICE-5G / similar to VM2); Greenland component of ICE-5G (13 Gt/yr) + Laurentide component of ICE-5G (-17 Gt/yr); inversion results in Khan *et al.* 2016, Discussion.
Khan *et al.* (2016) (GGG-1D) [r]	15 ± 10 [f]	Ice load reconstruction / solid Earth model, 1D (uncoupled); constrained with geomorphology & GPS; Greenland component (+32 Gt/yr) + Laurentide component of ICE-5G (-17 Gt/yr); inversion results in Khan *et al.* (2016), Discussion.
Fleming *et al.* (2004) [r] (Green1)	3 [f]	Ice load reconstruction / solid Earth model, 1D (uncoupled); constrained with geomorphology; Greenland component (+ 20 Gt/yr) + Laurentide component of ICE-5G (-17 Gt/yr); inversion in Sasgen *et al.* (2012, supplement).
Wu *et al.* (2010) [g]	-69 ± 19 [m]	Joint inversion estimate based on GPS, satellite laser ranging, and very long baseline interferometry, and bottom pressure from ocean model output; inversion results in Sutterley *et al.* (2014).
	Antarctica	
Reference	*GIA (Gt/yr)*	*Notes*

Whitehouse *et al.* (2012) (W12a) [r]	60 [n]	Thermodynamic sheet / solid Earth model, 1D (uncoupled); constrained by geomorphology; inversion results in Shepherd *et al.* 2012, supplement (Fig. S8).
Ivins *et al.* (2013) (IJ05_R2) [r]	40-65 [n]	Ice load reconstruction / solid Earth model, 1D; constrained by geomorphology and GPS uplift rates; Ivins et al. 2013; inversion results in Shepherd *et al.* 2012, supplement (Fig. S8).
Peltier (2009) (ICE-5G) [g]	140-180 [n]	Ice load reconstruction / solid Earth model ICE-5G(VM2); constrained by geomorphology; inversion results in Shepherd *et al.* 2012, supplement (Fig. S8).
Argus *et al.* (2014) (ICE-6G) [g]	107 [n]	Ice load reconstruction / solid Earth model ICE-6G(VM5a); constrained by geomorphology and GPS; theory recently corrected by Purcell *et al.* 2016; inversion results in Argus *et al.* (2014), conclusion 7.8.
Sasgen *et al.* (2017) (REGINA) [r]	55 ± 22 [f]	Joint inversion estimate based on GRACE, altimetry, GPS and viscoelastic response functions; lateral heterogeneous Earth model parameters; inversion results in Sasgen *et al.* (2017), Table 1.
Gunter *et al.* (2014) (G14) [r]	ca. 64 ± 40 [a] (multimodel uncert.)	Joint inversion estimate based on GRACE, altimetry, GPS and regional climate model output; conversion of uplift to mass using average rock density; inversion results in, Gunter *et al.* (2014) Table 1.
Martin-Español *et al.* (2016) (RATES) [r]	55 ± 8 45 ± 7*	Joint inversion estimate based on GRACE, altimetry, GPS and regional climate model output; inversion results in Sasgen *et al.* (2017), * is improved for GIA of smaller spatial scales; inversion results in Martin-Español *et al.* (2016), Fig. 6.

[r] regional model; [g] global model; [m] mascon inversion; [f] forward modeling inversion; [a] averaging kernel inversion; [n] inversion method not specified.

The GRACE-based ocean mass, Antarctica mass and terrestrial water storage changes are much model dependent. As these GIA corrections cannot be assessed from independent information, they represent a large source of uncertainties to the sea level budget components based on GRACE.

2.9 Ocean mass change from GRACE

Since 2002, GRACE satellite gravimetry has provided a revolutionary means for measuring global mass change and redistribution at monthly intervals with unprecedented accuracy, and offered the opportunity to directly estimate ocean mass change due to water exchange between the ocean and other components of the Earth (e.g., ice sheets, mountain glaciers, terrestrial water). GRACE time-variable gravity data have been successfully applied in a series of studies of ice mass balance of polar ice sheets (e.g., Velicogna and Wahr, 2006; Luthcke et al., 2006) and mountain glaciers (e.g., Tamisiea et al., 2005; Chen et al., 2007) and their contributions to global sea level change. GRACE data can also be used to directly study long-term oceanic mass change or non-steric sea level change (e.g., Willis et al., 2008; Leuliette et al., 2009; Cazenave et al., 2009), and provide a unique opportunity to study interannual or long-term TWS change and its potential impacts on sea level change (Richey et al., 2015; Reager et al., 2016).

GRACE time-variable gravity data can be used to quantify ocean mass change from three different main approaches. One is through measuring ice mass balance of polar ice sheets and mountain glaciers and variations of TWS, and their contributions to the GMSL (e.g., Velicogna and Wahr, 2005; Schrama et al., 2014). The second approach is to directly quantify ocean mass change using ocean basin mask (kernel) (e.g., Chambers et al., 2004; Llovel et al., 2010; Johnson and Chambers, 2013). In the ocean basin kernel approach, coastal ocean areas within certain distance (e.g., 300 or 500 km) from the coast are excluded, in order to minimize contaminations from mass change signal over the land (e.g., glacial mass loss and TWS change). The third approach solves mass changes on land and over ocean at the same time via forward modeling (e.g., Chen et al., 2013; Yi et al., 2015). The forward modeling is a global inversion to reconstruct the “true” mass change magnitudes over land and ocean with geographical constraint of locations of the mass change signals, and can help effectively reduce leakage between land and ocean (Chen et al., 2015).

Estimates of ocean mass changes from GRACE are subject to a number of major error sources. These include : (1) leakage errors from the larger signals over ice sheets and land hydrology due to GRACE's low spatial resolution (of at least a few to several hundred km) and the need of coastal masking, (2) spatial filtering of GRACE data to reduce spatial noise, (3) errors and biases in geophysical model corrections (e.g., GIA, atmospheric mass) that need to be removed from GRACE observations to isolate oceanic mass change and/or polar ice sheets and mountain glaciers mass balance, and (4) residual measurement errors in GRACE gravity measurements, especially those associated with GRACE low-degree gravity changes. In addition, how to deal with the absent degree-1 terms, i.e., geocenter motion in GRACE gravity fields, is expected to affect estimates of GRACE-basedoceanic mass rates and ice mass balances.

Data sources	**Time Period**	**Ocean mass trends (mm/yr)**
Chen et al. (2013) (A13 GIA)	2005.01-2011.12	1.80 ± 0.47
Johnson and Chambers (2013) (A13 GIA)	2003.01-2012.12	1.80 ± 0.15
Purkey et al. (2014) (A13 GIA)	2003.01-2013.01	1.53 ± 0.36
Dieng et al. (2015a) (Paulson07 GIA)	2005.01-2012.12	1.87 ± 0.11
Dieng et al. (2015b) (Paulson07 GIA)	2005.01-2013.12	2.04 ± 0.08
Yi et al. (2015) (A13 GIA)	2005.01-2014.07	2.03 ± 0.25
Rietbroek et al. (2016)	2002.04-2014.06	1.08 ± 0.30
Chambers et al. (2017)	2005.0 – 2015.0	2.11 ± 0.36

Table 10. Recently published (since 2013) estimates of GRACE-based ocean mass rates (GIA corrected). Most of the listed studies use either the A13 (A et al., 2013) or Paulson07 (Paulson et al., 2007) GIA model.

With a different treatment of the GRACE land-ocean signal leakage effect through global forward modeling, Chen et al. (2013) estimated ocean mass rates using GRACE RL05 time-variable gravity solutions over the period 2005-2011. They demonstrated that the ocean mass change contributes to 1.80 ± 0.47 mm/yr (over the same period), which is significantly larger than previous estimates over about the same period. Yi et at. (2015) further confirmed that correct calibration of GRACE data and appropriate treatment of GRACE leakage bias are critical to improve the accuracy of GRACE estimated ocean mass rates. Table 10 summarizes different estimates of GRACE ocean mass rates. The uncertainty estimates of the listed studies (Table 10) are computed from different methods, with different considerations of error sources into the error budget, and represent different confidence levels.

As demonstrated in Chen et al. (2013), different treatments of just the degree-2 spherical harmonics of GRACE gravity solution alone can lead to substantial differences in GRACE estimated ocean mass rates (ranging from 1.71 to 2.17 mm/yr). Similar estimates from GRACE gravity solutions from different data processing centers can also be different. In the meantime, long-term degree-1 spherical harmonics variation, representing long-term geocenter motion and neglected in some of the previous studies (due to the lack of accurate observations) are also expected to have non-negligible effect on GRACE derived ocean mass rates (Chen et al., 2013). Different methods for computing ocean mass change using GRACE data may also lead to different estimates (Chen et al., 2013; Johnson and Chambers, 2013, Jensen et al., 2013).

To help better understand the potential and uncertainty of GRACE satellite gravimetry in quantification of the ocean mass rate, Table 11 provides a comparison of GRACE-estimated ocean mass rates over the period January 2005 to December 2016 based on different GRACE data products and different data processing methods, including the CSR, GFZ and JPL GRACE RL05 spherical harmonic solutions (i.e., the so-called GSM solutions), and CSR, JPL, and GSFC mascon solutions (the available GSFC mascons only cover the period up to July 2016). The three GRACE GSM results (CSR, GFZ, and JPL) are updates from Johnson and Chambers (2013), with degree-2 zonal term replaced by satellite laser ranging results

(Cheng and Ries, 2012), geocenter motion from Swenson et al. (2008), GIA model from A et al. (2013), an averaging kernel with a land mask that extends out 300 km, and no destriping or smoothing, as described in Johnson and Chambers (2013). An update of GRACE ocean mass rate from Chen et al. (2013) is also included for comparisons, which is based on the CSR GSM solutions using forward modeling (a global inversion approach), with similar treatments of the degree-2 zonal term, geocenter motion, and GIA effects.

The JPL mascon ocean mass rate is computed from all mascon grids over the ocean, and the GSFC mascon ocean mass rate is computed from all ocean mascons, with the Mediterranean, Black and Red Seas excluded. A coastline resolution improvement (CRI) filter is already applied in the JPL mascons to reduce leakage (Wiese et al., 2016), and in both the GSFC and JPL mascon solutions, the ocean and land are separately defined (Luthcke et al., 2013; Watkins et al., 2015). For the CSR mascon results, an averaging kernel with a land mask that extends out 200 km is applied to reduced leakage (Chen et al., 2017). Similar treatments or corrections of degree-2 zonal term, geocenter motion, and GIA effects are also applied in the three mascon solutions. When solving GRACE mascon solutions, the GRACE GAD fields (representing ocean bottom pressure changes, or combined atmospheric and oceanic mass changes) have been added back to the mascon solutions. To correctly quantify ocean mass change using GRACE mascon solutions, the means of the GAD fields over the oceans, which represents mean atmospheric mass changes over the ocean (as ocean mass is conserved in the GAD fields) need to be removed from GRACE mascon solutions. The removal of GAD average over the ocean in GRACE mascon solutions has very minor or negligible effect (of ~ 0.02 mm/yr) on ocean mass rate estimates, but is important for studying GMSL change at seasonal time scales.

Over the 12-year period (2005-2016), the three GRACE GSM solutions show pretty consistent estimates of ocean mass rate, in the range of 2.3 to 2.5 mm/yr. Greater differences are noticed for the mascon solutions. The GSFC mascons show the largest rate of 2.61mm/yr. The CSR and JPL mascon solutions show relatively smaller ocean mass rates of 1.76 and 2.02 mm/yr, respectively, over the studied period. Based on the same CSR GSM solutions, the forward modeling and basin kernel estimates agree reasonably well (2.52 vs. 2.44 mm/yr). In addition to the degree-2 zonal term, geocenter motion, and GIA correction, the degree-2, order-1 spherical harmonics of the current GRACE RL05 solutions are affected by the definition of the reference mean pole in GRACE pole tide correction (Wahr et al., 2015). This mean pole correction, excluded in all estimates listed in Table 11 (for fair comparison), is estimated to contribute ~ - 0.11 mm/yr to GMSL. How to reduce errors from the different

sources play a critical role in estimating ocean mass change from GRACE time-variable gravity data.

Data sources	Ocean mass trend (mm/yr)
GSM CSR Forward Modeling (update from Chen et al., 2013)	2.52±0.17
GSM CSR (update from Johnson and Chambers, 2013)	2.44±0.15
GSM GFZ (update from Johnson and Chambers, 2013)	2.30±0.15
GSM JPL (update from Johnson and Chambers, 2013)	2.48±0.16
Mascon CSR (200 km)	1.76±0.16
Mascon JPL	2.02±0.16
Mascon GSFC (update from Luthcke et al., 2013)	2.61±0.16
Ensemble mean	2.3 ± 0.19

Table 11. Ocean mass trends (in mm/yr) estimated from GRACE for the period January 2005 – December 2016 (the GSFC mascon solutions cover up to July 2016). The uncertainty is based on 2 times the sigma of least-squares fitting.

GRACE satellite gravimetry has brought a completely new era for studying global ocean mass change. Owing to the extended record of GRACE gravity measurements (now over 15 years), improved understanding of GRACE gravity data and methods for addressing GRACE limitations (e.g., leakage and low-degree spherical harmonics), and improved knowledge of background geophysical signals (e.g., GIA), GRACE-derived ocean mass rates from different studies in recent years show clearly increased consistency (Table 11). Most of the results agree well with independent observations from satellite altimeter and Argo floats, although the uncertainty ranges are still large. The GRACE Follow-On (FO) mission has been launched in May 2018. The GRACE and GRACE-FO together are expected to provide at least over two (or even three) decades of time-variable gravity measurements. Continuous improvements of GRACE data quality (in future releases) and background geophysical models are also expected, which will help improve the accuracy GRACE observed ocean mass change.

For the sea level budget assessment over the GRACE period, we will use the ensemble mean.

3. Sea Level Budget results

In section 2, we have presented the different terms of the sea level budget equation, mostly based on published estimates (and in some cases, from their updates). We now use them to examine the closure of the sea level budget. For all terms, we only consider ensemble mean values.

3.1 Entire altimetry era (1993-Present)

3.1.1 Trend estimates over 1993-Present

Because it is now clear that the GMSL and some components are accelerating (e.g., Nerem et al., 2018), we propose to characterize the long term variations of the time series by both a trend and an acceleration. We start looking at trends. Table 12 gathers the trends estimated in section 2. The end year is not always the same for all components (see section 2). Thus the word 'present' means either 2015 or 2016 depending on the component. As no trend estimate is available for the entire altimetry era for the terrestrial water storage contribution, we do not consider this component. The residual trend (GMSL minus sum of components trend) may then provide some constraint on the TWS contribution.

Component	**Trends (mm/yr)** **1993-Present**
1.GMSL (TOPEX-A drift corrected)	3.07 +/- 0.37
2. Thermosteric sea level (full depth)	1.3 +/- 0.4
3. Glaciers	0.65 +/- 0.15
4. Greenland	0.48 +/- 0.10
5. Antarctica	0.25 +/- 0.10
6. TWS	/
7. Sum of components (without TWS→ 2.+3.+4.+5.)	2.7 +/- 0.23
8. GMSL minus sum of components (without TWS)	0.37 +/- 0.3

Table 12: Trend estimates for individual components of the sea level budget, sum of components and GMSL minus sum of components over 1993-present. Uncertainties of the

sum of components and residuals represent rooted mean squares of components errors, assuming that errors are independent.

Results presented in Table 12 are discussed in detail in section 4.

3.1.2 Acceleration

The GMSL acceleration estimated in section 2.2 using Ablain et al. (2017b)'s TOPEX-A drift correction amounts to 0.10 mm/yr^2 for the 1993-2017 time span. This value is in good agreement with Nerem et al. (2018) estimate (of 0.084 +/- 0.025 mm/yr^2) over nearly the same period, after removal of the interannual variability of the GMSL. In Nerem et al. (2018), acceleration of individual components are also estimated as well as acceleration of the sum of components. The latter agrees well with the GMSL acceleration. Here we do not estimate the acceleration of the component ensemble means because time series are not always available. We leave this for a future assessment.

3.2 GRACE and Argo period (2005- Present)

3.2.1 Sea level budget using GRACE-based ocean mass

If we consider the ensemble mean trends for the GMSL, thermosteric and ocean mass components given in sections 2.2, 2.3 and 2.9 over 2005-present, we find agreement (within error bars) between the observed GMSL (3.5 +/- 0.2 mm/yr) and the sum of Argo-based thermosteric plus GRACE-based ocean mass (3.6 +/- 0.4 mm/yr) (see Table 13). The residual (GMSL minus sum of components) trend amounts to -0.1 mm/yr. Thus in terms of trends, the sea level budget appears closed over this time span within quoted uncertainties.

3.2.2 Trend estimates over 2005-Present from estimates of individual contributions

Table 13 gathers trends of individual components of the sea level budget over 2005-present, as well sum of components and residuals (GMSL minus sum of components) trend. As for the longer period, ensemble mean values are considered for each component.

Component	**Trend (mm/yr) 2005-Present**

1. GMSL	3.5 +/- 0.2
2. Thermosteric sea level (full depth)	1.3 +/- 0.4
3. Glaciers	0.74 +/- 0.1
4. Greenland	0.76 +/- 0.1
5. Antarctica	0.42 +/- 0.1
6. TWS from GRACE (mean of Reager et al. and Scanlon et al.)	-0.27 +/- 0.15
7. Sum of components (2.+3.+4.+5.+6.)	2.95 +/- 0.21
8. Sum of components (thermosteric full depth + GRACE-based ocean mass)	3.6 +/- 0.4
9. GMSL minus sum of components (including GRACE-based TWS→2.+3.+4.+5.+6.)	0.55 +/- 0.3
10.GMSL minus sum of components (without GRACE-based TWS→ 2.+3.+4.+5.)	0.28 +/- 0.2
11. GMSL minus sum of components (thermosteric full depth + GRACE-based ocean mass)	-0.1 +/- 0.3

Table 13: Trend estimates for individual components of the sea level budget, sum of components and GMSL minus sum of components over 2005-present.

As for Table 12, the results presented in Table 13 are discussed in detail in section 4.

3.2.3 Year-to-year budget over 2005-Present using GRACE-based ocean mass

We now examine the year-to-year sea level and mass budgets. Table 14 provides annual mean values for the ensemble mean GMSL, GRACE-based ocean mass and Argo-based thermosteric component. The components are expressed as anomalies and their reference is arbitrary. So to compare with the GMSL, a constant offset for all years was applied to the thermosteric and ocean mass annual means. The reference year (where all values are set to zero) is 2003.

Year	Ensemble mean GMSL mm	Sum of components mm	GMSL minus sum of components mm
2005	7.00	8.78	-0.78
2006	10.25	10.78	-0.53
2007	10.51	11.35	-0.85
2008	15.33	15.07	0.25
2009	18.78	18.88	-0.10
2010	20.64	20.53	0.11
2011	20.91	21.38	-0.48
2012	31.10	29.33	1.77
2013	33.40	33.87	-0.47
2014	36.65	36.22	0.43
2015	46.34	45.69	0.65

Table 14. Annual mean values for the ensemble means GMSL and sum of components (GRACE-based ocean mass and Argo-based thermosteric, full depth). Constant offset applied to the sum of components. The reference year (where all values are set to zero) is 2003.

Figure 14 shows the sea level budget over 2005-2015 in terms of annual bar chart using values given in Table 14. It compares for years 2005 to 2016 the annual mean GMSL (blue bars) and annual mean sum of thermosteric and GRACE-based ocean mass (red bars). Annual residuals are also shown (green bars). These are either positive or negative depending on years. The trend of these annual residuals is estimated to 0.135 mm/yr.

In Figure 15 is also shown the annual sea level budget over 2005-2015 but now using the individual components for the mass terms. As we have no annual estimates for TWS, we ignore it, so that the total mass includes only glaciers, Greenland and Antarctica. The annual residuals thus include the TWS component in addition to the missing contributions (e.g., deep ocean warming). For years 2006 to 2011, the residuals are negative, an indication of a negative TWS to sea level as suggested by GRACE results (Reager et al., 2016, Scanlon et al.,

2018). But as of 2012, the residuals become positive and on average over 2005-2015, the residual trend amounts +0.28 mm/yr, a value larger than when using GRACE ocean mass.

Finally, Figure 16 presents the mass budget. It compares annual GRACE-based ocean mass to the sum of the mass components, without TWS as in Figure 15. The residual trends over 2005-2015 time span is 0.14 mm/yr. It may dominantly represent the TWS contribution. From one year to another residuals can be either positive or negative, suggesting important interannual variability in the TWS or even in the deep ocean.

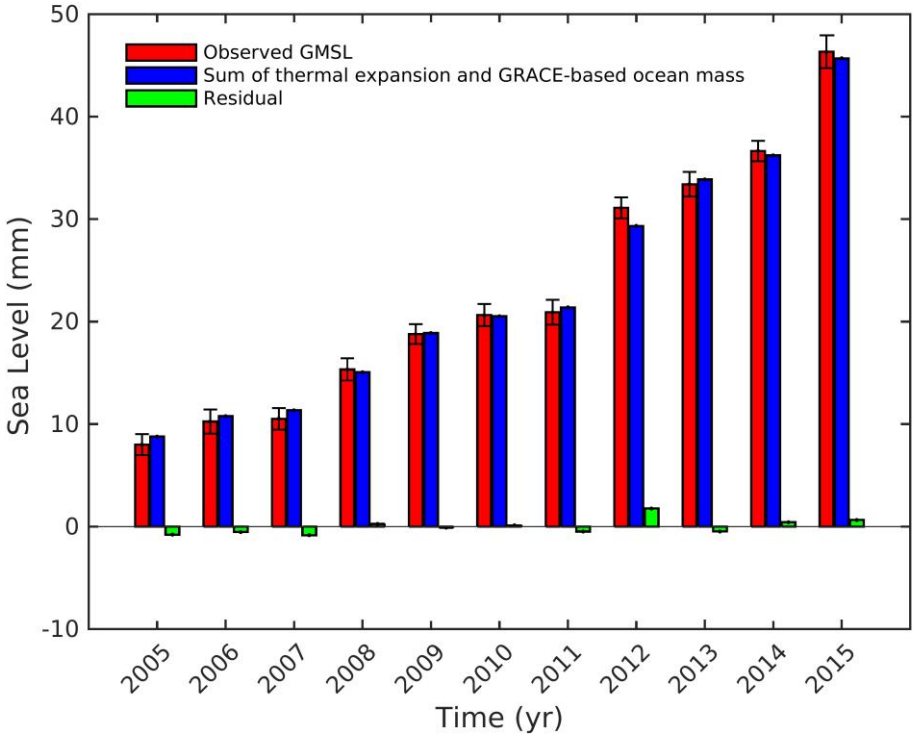

Figure 14: Annual sea level (blue bars) and sum of thermal expansion (full depth) and GRACE ocean mass component (red bars). Black vertical bars are associated uncertainties. Annual residuals (green bars) are also shown.

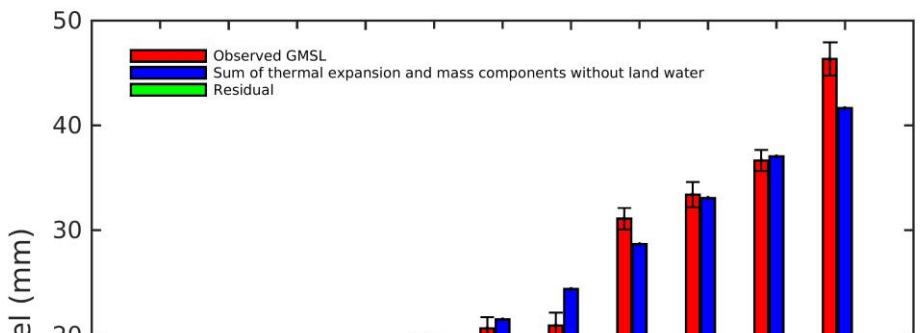

Figure 15: Annual global mean sea level (blue bars) and sum components without TWS (full depth thermal expansion+ glaciers + Greenland + Antarctica) (red bars). Black vertical bars are associated uncertainties. Annual residuals (green bars) are also shown.

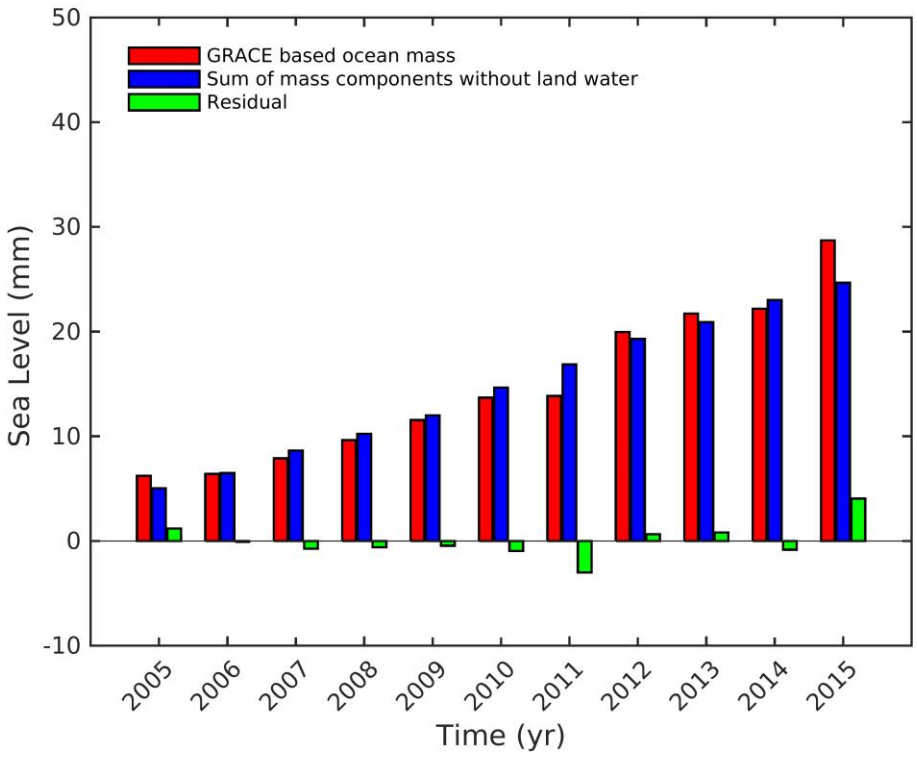

Figure 16: Annual GRACE-based ocean mass (red bars) and sum components without TWS (full depth thermal expansion+ glaciers + Greenland + Antarctica) (blue bars). Annual residuals (green bars) are also shown.

4. Discussion

The results presented in section 2 for the components of the sea level budget are based on syntheses of the recently published literature. When needed, the time series have been updated. In section 3, we considered ensemble means for each component to average out random errors of individual estimates. We examined the closure/non closure of the sea level budget using these ensemble mean values, for 2 periods: 1993-present and 2005-present (Argo and GRACE period). Because of the lack of observation-based TWS estimate for the 1993-present time span, we compared the observed GMSL trend to the sum of components excluding TWS. We found a positive residual trend of 0.37 +/- 0.3 mm/yr, supposed to include the TWS contribution, plus other imperfectly known contributions (deep ocean warming) and data errors.

For the 2005-present time span, we considered both GRACE-based ocean mass and sum of individual mass components, allowing us to also look at the mass budget. For TWS, as discussed in section 2.7, GRACE provides a negative trend contribution to sea level over the last decade (i.e., increase on water storage on land) attributed to internal natural variability (Reager et al., 2016), unlike hydrological models that lead to a small (possible not significantly different from zero) positive contribution to sea level over the same period . Assuming that GRACE observations are perfect, such discrepancies could be attributed to the inability of models to correctly account for uncertainties in meteorological forcing and inadequate modeling of soil storage capacity (see discussion in section 2.7). However, when looking at the sea level budget over the GRACE time span and using the GRACE-based TWS, we find a rather large positive residual trend (> 0.5 mm/yr) that needs to be explained. Since GRACE-based ocean mass is supposed to represent all mass terms, one may want to attribute this residual trend to an additional contribution of the deep ocean to the abyssal contribution already taken into account here, but possibly underestimated because of incomplete monitoring by current observing systems. If such a large positive contribution from the deep ocean (meaning ocean warming) is real (which is unlikely, given the high implied heat storage), this has to be confirmed by independent approaches e.g., using ocean reanalysis, and eventually model-based and top-of-the-atmosphere estimates of the Earth Energy Imbalance.

In addition to mean trends over the period, we also looked at the annual budget for all years starting in 2005. For most components, annual mean values are provided during the Argo-GRACE era, except for the terrestrial water storage component. However, the sea level

budget based on GRACE ocean mass (plus ocean thermal expansion; Figure 14) includes the TWS contribution. As shown in Figure 14, yearly residuals are small, suggesting near closure of the sea level budget. The residual trend amounts to 0.13 mm/yr. It could be interpreted as an additional deep ocean contribution not accounted by the SIO estimate (see section 2.3). However, when looking at Figure 14, we note that yearly residuals are either positive or negative, an indication of interannual variability that can hardly be explained by a deep ocean contribution. The residual trend derived from the difference (GMSL minus sum of components) (Table 13) amounts -0.1 +/- 0.3 mm/yr, suggesting a sea level budget closed within 0.3 mm/yr over 2005-present, with no substantial deep ocean contribution.

Figure 16 compares GRACE ocean mass to the sum of mass components (excluding TWS, for the reasons mentioned above). In principle, this mass budget may provide a constraint on the TWS contribution. The corresponding residual trend amounts to 0.14 mm/yr over the GRACE period, a value that disagrees with the above quote GRACE-based TWS estimates. However, it is worth noting that the GRACE-based TWS trend is much dependent on the considered time span because of the strong interannual variability; a recent study by Palanisamy et al. (in preparation), based on 347 land river basins, found zero GRACE-based TWS trend over 2005-2015. Given the remaining data uncertainties, any robust conclusion can hardly be reached so far. That being said, more work is needed to clarify the sign discrepancy between GRACE-based and model-based TWS estimates.

5. Concluding Remarks

As mentioned in the introduction, the global mean sea level budget has been the object of numerous previous studies, including successive IPCC assessments of the published literature. What is new in the effort presented here, is that it involves the international community currently studying present-day sea level and its components. Moreover, it relies on a large variety of datasets derived from different space-based and in situ observing systems. Near closure of the sea level budget as reported here over the GRACE and Argo era suggests that no large systematic errors affect these independent observing systems, including the satellite altimetry system. Study of the sea level budget allows improved understanding of the different processes causing sea level rise, such as ocean warming and land ice melt. When accuracy increases, it will offer an integrative view of the response of the Earth system to natural & anthropogenic forcing and internal variability, and provide an independent constraint on the current Earth Energy Imbalance. Validation of climate models against

observations is another important application of this kind of assessment (e.g., Slangen et al., 2017).

However, important uncertainties still remain, that affect several terms of the budget; for example the GIA correction applied to GRACE data over Antarctica or the net land water storage contribution to sea level. The latter results from a variety of factors but is dominated by ground water pumping and natural climate variability. Both terms are still uncertain and accurately quantifying them remains a challenge.

Several ongoing international projects related to sea level should provide in the near future improved estimates of the components of the sea level budget. This is the case, for example, of the ice sheet mass balance inter-comparison exercise (IMBIE, 2nd assessment), a community effort supported by NASA (National Aeronautics and Space Administration) and ESA, dedicated to reconcile satellite measurements of ice sheet mass balance (The IMBIE Team, 2018). This is also the case for the ongoing ESA Sea level Budget Closure project (Horwath et al., 2018) that uses a number of space-based Essential Climate Variables (ECVs) reprocessed during the last few years in the context of the ESA Climate Change Initiative project. The recently launched GRACE follow-on mission will lengthen the current mass component time series, with hopefully increased precision and resolution. Finally, the deep Argo project, still in an experimental phase, will provide important information on the deep ocean heat content in the coming years. Availability of this new data set will be open new insight on the total thermosteric component of the sea level budget, allowing constraining other missing or poorly known contributions, from the evaluation of the budget.

The sea level budget assessment discussed here essentially relies on trend estimates. But annual budget estimates have been proposed for the first time over the GRACE-Argo era. It is planned to provide updates of the global sea level budget every year, as done for more than a decade for the global carbon budget (Le Queré et al., 2018). In the next assessments, updates of all components will be considered, accounting for improved evaluation of the raw data, improved processing and corrections, use of ocean reanalysis, etc. Need for additional information where gaps exist should also be considered. As a closing remark, study of the sea level budget in terms of time series, not just trends as done here, will be required.

List of authors and affiliations:

Anny Cazenave (LEGOS, France & ISSI, Switzerland), Benoit Meyssignac (LEGOS, France);

Michael Ablain (CLS, France), Jonathan Bamber (U. Bristol, UK), Valentina Barletta (DTU-SPACE, Denmark), Brian Beckley (SGT Inc./NASA GSFC, USA), Jérôme Benveniste (ESA/ESRIN, Italy), Etienne Berthier (LEGOS, France), Alejandro Blazquez (LEGOS, France), Tim Boyer (NOAA, USA), Denise Caceres (Goethe U., Germany), Don Chambers (U. South Florida, USA), Nicolas Champollion (U. Bremen, Germany), Ben Chao (IES-AS, Taiwan), Jianli Chen (U. Texas, USA), Lijing Cheng (IAP-CAS, China), John A. Church (U. New South Wales, Australia), Stephen Chuter (U. Bristol, UK), J. Graham Cogley (Trent U., Canada), Soenke Dangendorf (U. Siegen, Germany), Damien Desbruyères (IFREMER, France), Petra Döll (Goethe U., Germany), Catia Domingues (CSIRO, Australia), Ulrike Falk (U. Bremen, Germany), James Famiglietti (JPL/Caltech, USA), Luciana Fenoglio-Marc (U. Bonn, Germany), Rene Forsberg (DTU-SPACE, Denmark), Gaia Galassi (U. Urbino, Italy), Alex Gardner (JPL/Caltech, USA), Andreas Groh (TU-Dresden, Germany), Benjamin Hamlington (Old Dominion U., USA), Anna Hogg (U. Leeds, UK), Martin Horwath (TU-Dresden, Germany), Vincent Humphrey (ETHZ, Switzerland), Laurent Husson (U. Grenoble, France), Masayoshi Ishii (MRI-JMA, Japan), Adrian Jaeggi (U. Bern, Switzerland), Svetlana Jevrejeva (NOC, UK), Gregory Johnson (NOAA/PMEL, USA), Jürgen Kusche (U. Bonn, Germany), Kurt Lambeck (ANU, Australia & ISSI, Switzerland), Felix Landerer (JPL/Caltech, USA), Paul Leclercq (UIO, Norway), Benoit Legresy (CSIRO, Australia), Eric Leuliette (NOAA, USA), William Llovel (LEGOS, France), Laurent Longuevergne (U. Rennes, France), Bryant D. Loomis (NASA GSFC, USA), Scott B. Luthcke (NASA GSFC, USA), Marta Marcos (UIB, Spain), Ben Marzeion (U. Bremen, Germany), Chris Merchant (U. Reading, UK), Mark Merrifield (UCSD, USA), Glenn Milne (U. Ottawa, Canada), Gary Mitchum (U. South Florida, USA), Yara Mohajerani (UCI, USA), Maeva Monier (Mercator-Ocean, France), Steve Nerem (U. Colorado, USA), Hindumathi Palanisamy (LEGOS, France), Frank Paul (UZH, Switzerland), Begoña Perez (Puertos del Estados, Spain), Christopher G. Piecuch (WHOI, USA), Rui M. Ponte (AER inc., USA), Sarah G. Purkey (SIO/UCSD, USA), John T. Reager (JPL/Caltech, USA), Roelof Rietbroek (U. Bonn, Germany), Eric Rignot (UCI and JPL, USA), Riccardo Riva (TU Delft, The Netherlands), Dean H. Roemmich (SIO/UCSD USA), Louise Sandberg Sørensen (DTU-SPACE, Denmark), Ingo Sasgen (AWI, Germany), E.J.O. Schrama (TU Delft, The Netherlands), Sonia I. Seneviratne (ETHZ, Switzerland), C.K. Shum (Ohio State U., USA), Giorgio Spada (U.

Urbino, Italy), Detlef Stammer (U. Hamburg, Germany), Roderic van de Wal (U. Utrecht, The Netherlands), Isabella Velicogna (UCI and JPL, USA), Karina von Schuckmann (Mercator-Océan, France), Yoshihide Wada (U. Utrecht, The Netherlands), Yiguo Wang (NERSC/BCCR, Norway), Christopher Watson (U. Tasmania, Australia), David Wiese (JPL/Caltech, USA), Susan Wijffels (CSIRO, Australia), Richard Westaway (U. Bristol, UK), Guy Woppelmann (U. La Rochelle, France), Bert Wouters (U. Utrecht, The Netherlands)

Acknowledgements and author contributions:

This community assessment was initiated by A. Cazenave and B. Meyssignac as a contribution to the Grand Challenge 'Regional Sea Level and Coastal Impacts' of the World Climate Research Programme (WCRP). The results presented in this paper were prepared by 9 different teams dedicated to the various terms of the sea level budget (i.e., altimetry-based sea level, tide gauges, thermal expansion, glaciers, Greenland, Antarctica, terrestrial water storage, glacial isostatic adjustment, ocean mass from GRACE). Thanks to the team leaders (in alphabetic order), M. Ablain, J. Bamber, N. Champollion, J. Chen, C. Domingues, S. Jevrejeva, J.T. Reager, K. von Schuckmann, G. Spada, I. Velicogna and R. van de Wal, who interacted with their team members, collected all needed information, provided a synthetized assessment of the literature and when needed, updated the published results. The coordinators A.C. and B.M. collected those materials and prepared a first draft of the manuscript, but all authors contributed to its refinement and to the discussion of the results. Special thanks are addressed to J. Benveniste, E. Berthier, G. Cogley, J. Church, G. Johnson (PMEL Contribution Number 4776), B. Marzeion, F. Paul, R. Ponte, and E. Schrama for improving the successive versions of the manuscript, and to H. Palanisamy for providing all figures presented in section 3.

The views, opinions, and findings contained in this paper are those of the authors and should not be construed as an official NOAA, U.S. Government or other institutions position, policy, or decision.

We are grateful to the anonymous reviewer for his/her thorough comments that helped to improve the manuscript.

References

1. A G., Chambers, D. P., Calculating trends from GRACE in the presence of large changes in continental ice storage and ocean mass. *Geophys. J. Int.*, pp. 272, doi:10.1111/j.1365-246X.2008.04012.x, 2008.
2. A G., Wahr J. and Zhong S., Computations of the viscoelastic response of a 3-D compressible Earth to surface loading: an application to Glacial Isostatic Adjustment in Antarctica and Canada, *Geophysical Journal International*, 192.2, 557-572, 2013.
3. Ablain M., A. Cazenave, G. Valladeau, and S. Guinehut, "A New Assessment of the Error Budget of Global Mean Sea Level Rate Estimated by Satellite Altimetry over 1993–2008." *Ocean Science*, doi:10.5194/os-5-193-2009, 2009.
4. Ablain, M., S. Philipps, M. Urvoy, N. Tran, and N. Picot, "Detection of Long-Term Instabilities on Altimeter Backscatter Coefficient Thanks to Wind Speed Data Comparisons from Altimeters and Models." *Marine Geodesy* 35 (sup1):258–75, doi:10.1080/01490419.2012.718675, 2012.
5. Ablain M., A. Cazenave, G. Larnicol, M. Balmaseda, P. Cipollini, Y. Faugère, M. J. Fernandes, et al., "Improved Sea Level Record over the Satellite Altimetry Era (1993–2010) from the Climate Change Initiative Project." *Ocean Science*, doi:10.5194/os-11-67-2015, 2015.
6. Ablain M., J. F. Legeais, P. Prandi, M. Marcos, L. Fenoglio-Marc, H. B. Dieng, J. Benveniste, and A. Cazenave, "Satellite Altimetry-Based Sea Level at Global and Regional Scales." *Surveys in Geophysics*, doi:10.1007/s10712-016-9389-8, 2017a.
7. Ablain M., R. Jugier, L. Zawadki, and N. Taburet, "The TOPEX-A Drift and Impacts on GMSL Time Series." AVISO Website. October 2017. https://meetings.aviso.altimetry.fr/fileadmin/user_upload/tx_ausyclsseminar/files/Poster_OSTST17_GMSL_Drift_TOPEX-A.pdf, 2017b.
8. Abraham J. P., et al., A review of global ocean temperature observations: Implications for ocean heat content estimates and climate change, *Rev. Geophys*., 51, 3, 450-483, doi:10.1002/rog.20022, 2013.
9. Adrian R et al., Lakes as sentinels of climate change *Limnology and Oceanography* 54:2283-2297 doi:10.4319/lo.2009.54.6_part_2.2283, 2009.
10. Ahmed M, Sultan M, Wahr J, Yan E, The use of GRACE data to monitor natural and anthropogenic induced variations in water availability across Africa *Earth-Science Reviews* 136:289-300, 2014.
11. Argus D.F. Peltier, W. R., Drummond, R., The Antarctica component of postglacial rebound model ICE-6G_C (VM5a) based on GPS positioning, exposure age dating of ice thicknesses, and relative sea level histories. *Geophysical Journal International* 198, 1, 537-563, 2014.
12. Armentano TV, Menges ES, Patterns of Change in the Carbon Balance of Organic Soil-Wetlands of the Temperate Zone *J Ecol*, 74:755-774, doi:10.2307/2260396, 1986.
13. Awange J.L., Sharifi M.A., Ogonda G., Wickert J., Grafarend E.W., Omulo M., The falling Lake Victoria water level: GRACE, TRIMM and CHAMP satellite analysis of the lake basin, *Water Resources Management* 22:775-796, 2008.
14. Bahr, D. and Radic, V., Significant contribution to total mass from very small glaciers, *The Cryosphere*, 6, 763-770, 2012.
15. Bahr, D., Pfeffer, W., Sassolas, C. and Meier, M., Response time of glaciers as a function of size and mass balance: 1. Theory, *Journal of Geophysical Research: Solid Earth*, 103, 9777-9782, 1998.
16. Balmaseda M.A,. K. Mogensen, A. Weaver (2013b). Evaluation of the ECMWF Ocean Reanalysis ORAS4. *Q. J. R. Meteorol. Soc.*, doi:10.1002/qj.2063, 2013.

17. Bamber J.L., R.M. Westaway, B. Marzeion and B. Wouters, The land ice contribution to sea level during the satellite era, *Environ. Res. Lett*., 13, 063008, doi:10.1088/1748-9326/aac2f0, 2018.
18. Barletta, V. R., Sørensen, L. S. & Forsberg, R. Scatter of mass changes estimates at basin scale for Greenland and Antarctica, *The Cryosphere*, 7, 1411-1432, 2013.
19. Bartnett, T.P.. The estimation of "global" sea level change: A problem of uniqueness. J. Geophys. Res., 89 (C5), 7980-7988, 1984.
20. Beck, H. E., van Dijk, A. I., de Roo, A., Dutra, E., Fink, G., Orth, R., & Schellekens, J., Global evaluation of runoff from 10 state-of-the-art hydrological models. *Hydrology and Earth System Sciences*, *21*, 6, 2881, 2017.
21. Becker M, LLovel W, Cazenave A, Güntner A, Crétaux J-F, Recent hydrological behavior of the East African great lakes region inferred from GRACE, satellite altimetry and rainfall observations, *C. R. Geosci* 342:223-233, 2010.
22. Beckley, B. D., P. S. Callahan, D. W. Hancock, G. T. Mitchum, and R. D. Ray. "On the 'Cal-Mode' Correction to TOPEX Satellite Altimetry and Its Effect on the Global Mean Sea Level Time Series." *Journal of Geophysical Research, C: Oceans* 122 (11):8371–84. https://doi.org/10.1002/2017jc013090, 2017.
23. Belward AS, Estes JE, Kline KD, The IGBP-DIS global 1-km land-cover data set DISCover: A project overview *Photogrammetric Engineering and Remote Sensing* 65:1013-1020, 1999.
24. Bindoff, N., J. Willebrand, V. Artale, et al., Observations: Oceanic climate and sea level. In *Climate Change 2007: The Physical Science Basis; Contribution of Working Group I to the Fourth Assessment Report of the Intergovernmental Panel on Climate Change*. Edited by S. Solomon, D. Qin, M. Manning, et al., 386–432. Cambridge, UK, and New York: Cambridge Univ. Press, 2007.
25. Boening, C., J. K. Willis, F. W. Landerer, R. S. Nerem, and J. Fasullo, The 2011 La Niña: So strong, the oceans fell, *Geophys. Res. Lett*., 39(19), n/a-n/a, doi:10.1029/2012GL053055, 2012.
26. Bosmans, J. H. C., van Beek, L. P. H., Sutanudjaja, E. H., and Bierkens, M. F. P.: Hydrological impacts of global land cover change and human water use, *Hydrol. Earth Syst. Sci.*21, 5603–5626, doi.org/10.5194/hess-21-5603-2017, 2017.
27. Boyer, T., C. Domingues, S. Good, G. C. Johnson, J. M. Lyman, M. Ishii, V. Gouretski, J., Antonov, N. Bindoff, J. Church, R. Cowley, J. Willis, and S. Wijffels. 2015. Sensitivity of global ocean heat content estimates to mapping methods, XBT bias corrections, and baseline climatology, *Journal of Climate*, 29, 4817–4842, doi:10.1175/JCLI-D-15-0801.1., 2016.
28. Bredehoeft, J. D., The water budget myth revisited: why hydrogeologists model?, *Ground Water*, 40, 340–345, doi:10.1111/j.1745-6584.2002.tb02511.x, 2002.
29. Butt N, de Oliveira PA, Costa MH, Evidence that deforestation affects the onset of the rainy season in Rondonia, Brazil *Journal of Geophysical Research-Atmospheres* 116: D11120 doi:10.1029/2010jd015174, 2011.
30. Bolch, T., Sandberg Sørensen, L., Simonsen, S. B., Mölg, N., Machguth, H., Rastner, P. & Paul, F. Mass loss of Greenland's glaciers and ice caps 2003–2008 revealed from ICESat laser altimetry data. *Geophysical Research Letters*, 40, 875-881, 2013.
31. Box, J. E. & Colgan, W. T., Sea level rise contribution from Arctic land ice: 1850-2100. Snow, Water, Ice and Permafrost in the Arctic (SWIPA) 2017. Oslo, Norway: Arctic Monitoring and Assessment Programme (AMAP), 2017.
32. Brun, F., Berthier, E., Wagnon, P., Kääb, A. and Treichler, D., A spatially resolved estimate of High Mountain Asia mass balances from 2000 to 2016, *Nature Geoscience*, 2017.

33. Cao, G., C. Zheng, B. R. Scanlon, J. Liu, and W. Li, Use of flow modeling to assess sustainability of groundwater resources in the North China Plain, *Water Resour. Res*., 49, doi:10.1029/2012WR011899, 2013.
34. Calafat, F.M., Chambers, D.P., and M.N. Tsimplis. On the ability of global sea level reconstructions to determine trends and variability. *J. Geophys. Res*., 119, 1572-1592, 2014.
35. Cazenave, A., Dominh, K., Guinehut, S., Berthier, E., Llovel, W., Ramillien, G., Ablain, M., and Larnicol, G., 2009. Sea level budget over 2003–2008: A reevaluation from GRACE space gravimetry, satellite altimetry and Argo, *Glob. Planet. Change* **65**:83–88, doi:10.1016/j/gloplacha.2008.10.004, 2009.
36. Cazenave, A., Llovel, W., Contemporary Sea Level Rise, *Annu. Rev. Mar. Sci*. 2:145–73, 10.1146/annurev-marine-120308-081105, 2010.
37. Cazenave, A., Champollion, N., Paul, F. and Benveniste, J. Integrative Study of the Mean Sea Level and Its Components, *Space Science Series of ISSI - Spinge*r, 416 pp, vol 58., 2017.
38. Cazenave, A, H.B. Dieng, B. Meyssignac, K. von Schuckmann, B. Decharme, and E. Berthier. "The Rate of Sea-Level Rise." *Nature Climate Change* 4 (5):358–61. https://doi.org/10.1038/nclimate2159, 2014.
39. Chagnon FJF, Bras RL (2005) Contemporary climate change in the Amazon *Geophysical Research Letters* 32:L13703 doi:10.1029/2005gl022722, 2005.
40. Chao, B. F., Y. H. Wu, and Y. S. Li, Impact of artificial reservoir water impoundment on global sea level, *Science*, 320, 212-214, doi:10.1126/science.1154580, 2008.
41. Cheema, M. J., W. W. Immerzeel, and W. G. Bastiaanssen, Spatial quantification of groundwater abstraction in the irrigated Indus basin, *Ground Water*, 52, 25-36, doi:10.1111/gwat.12027, 2014.
42. Chambers, D. P**.,** J. Wahr, M. E. Tamisiea, and R. Steven Nerem, Reply to Comments by Peltier et al., 2012 ("Concerning the Interpretation of GRACE Time Dependent Gravity Observations and the Influence Upon them of Rotational Feedback in Glacial Isostatic Adjustment.") *J. Geophys. Res., 117*, doi: 10.1029/2012JB009441, 2012.
43. Chambers, D. P., Wahr, J., Tamisiea, M. E., and Nerem, R. S., Ocean mass from GRACE and glacial isostatic adjustment. *Journal of Geophysical Research* (Solid Earth), 115(B14): L11415, doi:10.1029/2010JB007530, 2010.
44. Chambers, D. P., A. Cazenave, N. Champollion, H. Dieng, W. Llovel, R. Forsberg, K. von Schuckmann, and Y. Wada, Evaluation of the Global Mean Sea Level Budget between 1993 and 2014, *Surv. Geophys. 38*, 309-327, doi: 10.1007/s10712-016-9381-3, 2017.
45. Chen, Xianyao, Xuebin Zhang, John A. Church, Christopher S. Watson, Matt A. King, Didier Monselesan, Benoit Legresy, and Christopher Harig. "The Increasing Rate of Global Mean Sea-Level Rise during 1993–2014." *Nature Climate Change* 7, 492–95. https://doi.org/10.1038/nclimate3325, 2017.
46. Chen, J. L., Wilson, C. R., and Tapley, B. D., Contribution of ice sheet and mountain glacier melt to recent sea level rise, *Nature Geoscience*, doi: 10.1038/NGEO1829, 2013.
47. Chen, J. L., Wilson, C. R., Tapley, B. D., Blankenship, D. D., and Ivins, E. R., Patagonia Icefield Melting Observed by GRACE, *Geophys. Res. Lett*., Vol. 34, No. 22, L22501, 10.1029/2007GL031871, 2007.
48. Chen, J. L., Wilson, C. R., Tapley, B. D., Save, H., and Cretaux, J.-F., Long-term and seasonal Caspian Sea level change from satellite gravity and altimeter measurements. *Journal of Geophysical Research (Solid Earth)*, 122:2274–2290, doi:10.1002/2016JB013595, 2017.

49. Chen, J. L., C. R. Wilson, and B. D. Tapley (2010), The 2009 exceptional Amazon flood and interannual terrestrial water storage change observed by GRACE, *Water Resour. Res.*, 46, W12526, doi:10.1029/2010WR009383.
50. Chen, J., J. S. Famiglietti, B. R. Scanlon, and M. Rodell, Groundwater Storage Changes: Present Status from GRACE Observations, *Surveys in Geophysics*, 37, 397–417, doi:10.1007/s10712-015-9332-4, 2017.
51. Cheng, M.K., and Ries, J.R., Monthly estimates of C20 from 5 SLR satellites based on GRACE RL05 models, GRACE Technical Note 07, The GRACE Project, Center for Space Research, University of Texas at Austin, 2012.
52. Cheng L., Trenberth K., Fasullo J., Boyer T., Abraham J. and Zhu J., Improved estimates of ocean heat content from 1960-2015, *Science Advances*, 3, e1601545, 2017.
53. Choblet, G., Husson, L., Bodin, T., Probabilistic surface re- construction of coastal sea level rise during the twentieth century *J. Geophys. Res*., 119, 9206-9236, 2014.
54. Church, J. et al., Sea level change, in Stocker, T. et al. (eds.) Climate Change 2013: The Physical Science Basis. Contribution of Working Group I to the Fifth Assessment Report of the Intergovernmental Panel on Climate Change (Cambridge University Press, Cambridge, United Kingdom and New York, NY, USA), 2013.
55. Church, John, Jonathan Gregory, Neil White, Skye Platten, and Jerry Mitrovica. "Understanding and Projecting Sea Level Change." *Oceanography* 24 (2):130–43. https://doi.org/10.5670/oceanog.2011.33, 2011.
56. Church, J. A., and N. J. White. A 20th century acceleration in global sea-level rise, Geophys. Res. Lett., 33, L01602, doi:10.1029/2005GL024826, 2006.
57. Church, J. A., and N. J. White, Sea-Level Rise from the Late 19th to the Early 21st Century, *Surveys in Geophysics*, *32*(4-5), 585-602, doi:10.1007/s10712-011-9119-1., 2011.
58. Ciais P et al., Carbon and other biogeochemical cycles. In: Stocker TF et al. (eds) Climate change 2013: the physical science basis. Contribution of working group I to the fifth assessment report of the Intergovernmental Panel on Climate Change. Cambridge University Press, Cambridge, United Kingdom and New York, NY, USA, pp 465-570, 2013.
59. Cretaux JF et al., SOLS: A lake database to monitor in the Near Real Time water level and storage variations from remote sensing data *Adv Space Res* 47:1497-1507 doi:10.1016/j.asr.2011.01.004, 2011.
60. Cogley, J., Geodetic and direct mass-balance measurements: comparison and joint analysis, *Annals of Glaciology*, 50, 96-100, 2009.
61. Couhert, Alexandre, Luca Cerri, Jean-François Legeais, Michael Ablain, Nikita P. Zelensky, Bruce J. Haines, Frank G. Lemoine, William I. Bertiger, Shailen D. Desai, and Michiel Otten. "Towards the 1mm/y Stability of the Radial Orbit Error at Regional Scales." *Advances in Space Research: The Official Journal of the Committee on Space Research* 55 (1):2–23. https://doi.org/10.1016/j.asr.2014.06.041, 2015.
62. Dangendorf, S., M. Marcos, A. Müller, E. Zorita, R. Riva, K. Berk, and J. Jensen, Detecting anthropogenic footprints in sea level rise. Nature Communications, 6, 7849, 2015.
63. Dangendorf, Sönke, Marta Marcos, Guy Wöppelmann, Clinton P. Conrad, Thomas Frederikse, and Riccardo Riva. "Reassessment of 20th Century Global Mean Sea Level Rise." *Proceedings of the National Academy of Sciences* 114 (23):5946–51. https://doi.org/10.1073/pnas.1616007114, 2017.

64. Davaze, L., Rabatel, A., Arnaud, Y., Sirguey, P., Six, D., Letreguilly, A. and Dumont, M., Monitoring glacier albedo as a proxy to derive summer and annual mass balances from optical remote-sensing data, *The Cryosphere*, 12, 271-286, 2018.
65. Darras S, IGBP-DIS wetlands data initiative, a first step towards identifying a global delineation of wetalnds. IGBP-DIS Office, Toulouse, France, 1999.
66. Davidson NC, How much wetland has the world lost? Long-term and recent trends in global wetland area *Marine and Freshwater Research* 65:934-941 doi:10.1071/Mf14173, 2014.
67. DeAngelis, A., F. Dominguez, Y. Fan, A. Robock, M. D. Kustu, and D. Robinson, Evidence of enhanced precipitation due to irrigation over the Great Plains of the United States, *J. Geophys. Res*., 115, D15115, doi:10.1029/2010JD013892, 2010.
68. Decharme B., R. Alkama, F. Papa, S. Faroux, H. Douville and C. Prigent, Global off−line evaluation of the ISBA−TRIP flood model, *Climate Dynamics*, 38, 1389-1412, doi:10.1007/s00382−011−1054−9, 2012.
69. Decharme, B., Brun, E., Boone, A., Delire, C., Le Moigne, P., and Morin, S. (2016), Impacts of snow and organic soils parameterization on northern Eurasian soil temperature profiles simulated by the ISBA land surface model, *The Cryosphere*, 10, 853-877, doi:10.5194/tc-10-853-2016.
70. Dieng, H. B., N. Champollion, A. Cazenave, Y. Wada, E. Schrama, and B. Meyssignac, Total land water storage change over 2003-2013 estimated from a global mass budget approach, *Environ. Res. Lett*., 10, 124010, doi:10.1088/1748-9326/10/12/124010, 2015a.
71. Dieng, H. B., Cazenave, A., von Schuckmann, K., Ablain, M., and Meyssignac, B., 2015b. Sea level budget over 2005-2013: missing contributions and data errors. *Ocean Science*, 11:789–802, doi:10.5194/os-11-789-2015, 2015b.
72. Dieng, H. B., Palanisamy, H., Cazenave, A., Meyssignac, B., and von Schuckmann, K., The Sea Level Budget Since 2003: Inference on the Deep Ocean Heat Content. *Surveys in Geophysics*, 36:209–229, doi:10.1007/s10712-015-9314-6, 2015c.
73. Dieng, H.B, A.Cazenave, B.Meyssignac, M.Ablain, New estimate of the current rate of sea level rise from a sea level budget approach, *Geophysical Research Letters*, 44, doi:10.1002/ 2017GL073308, 2017.
74. Döll, P., H. Hoffmann-Dobrev, F. T. Portmann, S. Siebert, A. Eicker, M. Rodell, and G. Strassberg, Impact of water withdrawals from groundwater and surface water on continental water storage variations, *J. Geodyn*., 59-60, 143-156, doi:10.1016/j.jog.2011.05.001, 2012.
75. Döll, P., M. Fritsche, A. Eicker, and S. H. Mueller, Seasonal water storage variations as impacted by water abstractions: Comparing the output of a global hydrological model with GRACE and GPS observations, *Surv. Geophys*., doi:10.1093/gji/ggt485, 2014a.
76. Döll, P., H. Müller Schmied, C. Schuh, F. T. Portmann, and A. Eicker, Global-scale assessment of groundwater depletion and related groundwater abstractions: Combining hydrological modeling with information from well observations and GRACE satellites, *Water Resour. Res*., 50, 5698–5720, doi:10.1002/2014WR015595, 2014b.
77. Döll, P., H. Douville, A. Güntner, H. Müller Schmied, and Y. Wada, Modelling freshwater resources at the global scale: Challenges and prospects, *Surv. Geophys*., 37, 195–221, Special Issue: ISSI Workshop on Remote Sensing and Water Resources, 2017.

78. Domingues C, Church J, White N, Gleckler PJ, Wijffels SE, et al. 2008. Improved estimates of upper ocean warming and multidecadal sea level rise. *Nature* 453:1090–93, doi:10.1038/nature07080, 2008.
79. Douglas B., Global sea level rise, *Journal of Geophysical Research: Oceans* 96(C4):6981-6992, 1991.
80. Douglas B., Global sea rise: a redetermination, *Surveys in Geophysics* 18(2-3):279-292, 1997.
81. Douglas, B.C., Sea level change in the era of recording tide gauges, in Sea Level Rise, History and Consequences, pp. 37–64, eds Douglas, B.C., Kearney, M.S. & Leatherman, S.P., Academic Press, San Diego, CA, 2001.
82. Durack P., Gleckler, P., Landerer, F., and Taylor, K., Quantifying underestimates of long-term upper-ocean warming, *Nature Climate Change* 4, 999–1005, doi:10.1038/nclimate2389, 2014.
83. Dutrieux P et al., Strong sensitivity of Pine Island ice shelf melting to climatic variability, *Science* 343(6167), 2014.
84. Escudier et al., Satellite radar altimetry: principle, accuracy and precision, in 'Satellite altimetry over oceans and land surfaces, D.L Stammer and A. Cazenave edts., 617 pages, CRC Press, Taylor and Francis Group, Boca Raton, New York, London, ISBN: 13: 978-1-4987-4345-7, 2018.
85. Famiglietti, J. S., The global groundwater crisis, *Nature Clim. Change*, 4, 945-948, doi:10.1038/nclimate2425, 2014.
86. FAO, Global forest resources assessment 2015: how have the world's forests changed? Rome, 2015.
87. Farinotti, D. et al. (2017). How accurate are estimates of glacier ice thickness ?, *The Cryosphere*, 11, 949-970, 2004.
88. Farrell W., Clark J., On postglacial sea level, *Geophysical Journal International* 46.3:647-667, 1976.
89. Fasullo, J. T., C. Boening, F. W. Landerer, and R. S. Nerem, Australia's unique influence on global sea level in 2010–2011, *Geophys. Res. Lett.*, 40, 4368–4373, doi:10.1002/grl.50834, 2013.
90. Felfelani, F., Wada, Y., Longuevergne, L., & Pokhrel, Y. N., Natural and human-induced terrestrial water storage change: A global analysis using hydrological models and GRACE. *Journal of Hydrology*, *553*, 105-118, 2017.
91. Feng, W., M. Zhong, J.-M. Lemoine, R. Biancale, H.-T. Hsu, and J. Xia, Evaluation of groundwater depletion in North China using the Gravity Recovery and Climate Experiment (GRACE) data and ground-based measurements, *Water Resour. Res.*, 49, 2110–2118, doi:10.1002/wrcr.20192, 2013.
92. Fleming K., Lambeck K., Constraints on the Greenland Ice Sheet since the Last Glacial Maximum from sea-level observations and glacial-rebound models, *Quaternary Science Reviews*23(9), 1053-1077, 2004.
93. Forsberg, R., Sørensen, L. & Simonsen, S: Greenland and Antarctica Ice Sheet Mass Changes and Effects on Global Sea Level. *Surveys in Geophysics*, 38, 89. doi:10.1007/s10712-016-9398-7, 2017.
94. Foster, S. and D. P. Loucks (eds.), Non-Renewable Groundwater Resources: A guidebook on socially-sustainable management for water-policy makers, IHP-VI, Series on Groundwater No. 10, UNESCO, Paris, France, 2006.
95. Frederikse et al, A consistent sea-level reconstruction and its budget on basin and global scales over 1958-2014, Journal of Climate, https://doi.org/10.1175/JCLI-D-17-0502.1, 2017.

96. Frey, H., Machguth, H., Huss, M., Huggel, C., Bajracharaya, S., Bolch, T., Kulkarni, A., Linsbauer, A., Salzmann, N. and Stoffel, M., Estimating the volume of glaciers in the Himalayan-Karakoram region using different methods, *The Cryosphere*, 2014.
97. Gardner, A.S., G. Moholdt, J.G. Cogley, B. Wouters, A.A. Arendt, J. Wahr, E. Berthier, R. Hock, W.T. Pfeffer, G. Kaser, S.R.M. Ligtenberg, T.Bolch, M.J. Sharp, J.O. Hagen, M.R. van den Broeke, and F. Paul, A reconciled estimate of glacier contributions to sea level rise: 2003 to 2009. *Science*, 340, 852-857, doi:10.1126/science.1234532, 2013.
98. Gleick, P. H., Global Freshwater Resources: Soft-Path Solutions for the 21st Century, *Science*, 302, 1524-1528, doi:10.1126/science.1089967, 2003.
99. Golytsyn GS, Panin GN, Once more on the water level changes of the Caspian Sea Vestnik Akademii Nauk SSSR 9:59-63 (in Russian), 1989.
100. Gomez N., Pollard D., Mitrovica J.X., A 3-D coupled ice sheet–sea level model applied to Antarctica through the last 40 ky, *Earth and Planetary Science Letters* 384, 88-99, 2013.
101. Gornitz V, Rosenzweig C, Hillel D, Effects of anthropogenic intervention in the land hydrologic cycle on global sea level rise *Global and Planetary Change* 14:147-161 doi:10.1016/s0921-8181(96)00008-2, 1997.
102. Gornitz, V., Sea-level rise: A review of recent past and near-future trends. *Earth Surf. Process. Landforms*, 20, 7–20. doi: 10.1002/esp.3290200103, 1995.
103. Gornitz, V., In Sea Level Rise: History and Consequences, Douglas, B. C., M. S. Kearney, and S. P. Leatherman (eds.), 97-119, Academic Press, San Diego, CA, USA, 2001.
104. Gornitz, V., Lebedeff, S. and Hansen, J., Global sea level trend in the past century, Science, 215, 1611–1614, 1982.
105. Gouretski, V. and K. Peter Koltermann. How much is the ocean really warming? *Geophysical Research Letters*, 34, L01610, doi:10.1029/2006GL027834, 2007.
106. Gregory, J. M., and J. A. Lowe. Predictions of global and regional sea-level rise using AOGCMs with and without flux adjustment. *Geophys. Res. Lett.*, **27**, 3069–3072, 2000..
107. Gregory, J. M., N. J. White, J. A. Church, M. F. P. Bierkens, J. E. Box, M. R. van den Broeke, J. G. Cogley, X. Fettweis, E. Hanna, P. Huybrechts, L. F. Konikow, P. W. Leclercq, B. Marzeion, J. Oerlemans, M. E. Tamisiea, Y. Wada, L. M.Wake, R. S. W. van de Wal, Twentieth-Century Global-Mean Sea Level Rise: Is the Whole Greater than the Sum of the Parts? J. *Climate*, 26, 4476–4499, doi:10.1175/JCLI-D-12-00319.1, 2013.
108. Grinsted, A., An estimate of global glacier volume, *The Cryosphere*, 7, 141–151, 2013.
109. Groh, A., & Horwath, M., The method of tailored sensitivity kernels for GRACE mass change estimates. *Geophysical Research Abstracts*, 18, EGU2016-12065, 2016.
110. Gunter B.C., Didova O., Riva R.E.M., Ligtenberg S.R.M., Lenaerts J.T.M., King M.A., Van den Broeke M.R., Urban T., and others, Empirical estimation of present-day Antarctic glacial isostatic adjustment and ice mass change, *The Cryosphere* 8(2), 743-760, 2014.
111. Haeberli, W. and Linsbauer, A., Brief communication: global glacier volumes and sea level; small but systematic effects of ice below the surface of the ocean and of new local lakes on land, *The Cryosphere*, 7, 817-821, 2013.

112. Hamlington, B. D., R. R. Leben, R. S. Nerem, W. Han, and K.-Y. Kim, Reconstructing sea level using cyclostationary empirical orthogonal functions, J. Geophys. Res., 116, C12015, doi:10.1029/2011JC007529, 2011.
113. Hamlington, B.D., Thompson, P., Hammond, W.C., Blewitt, G., and R.D. Ray, Assessing the impact of vertical land motion on twentieth century global mean sea level estimates, Journal of Geophysical Research: Oceans, 121(7), 4980-4993. doi: 10.1002/2016JC011747, 2016.
114. Hay, Carling C., Eric Morrow, Robert E. Kopp, and Jerry X. Mitrovica. "Probabilistic Reanalysis of Twentieth-Century Sea-Level Rise." *Nature* 517, 7535, 481–84, doi:10.1038/nature14093, 2015.
115. Henry, O., M.Ablain, B. Meyssignac, A. Cazenave, D. Masters, S. Nerem, and G. Garric. "Effect of the Processing Methodology on Satellite Altimetry-Based Global Mean Sea Level Rise over the Jason-1 Operating Period." *Journal of Geodesy* 88, 4, 351-361, doi: 10.1007/s00190-013-0687-3, 2014.
116. Horwath, M., Novotny K, Cazenave, A., Palanisamy, H., Marzeion, B., Paul, F., Döll, P., Cáceres, D., Hogg, A., Shepherd, A., Forsberg, R., Sørensen, L., Barletta, V.R., Andersen, O.B., Ranndal, H., Johannessen, J., Nilsen, J.E., Gutknecht, B.D., Merchant, Ch.J., MacIntosh, C.R., von Schuckmann, K., *ESA Climate Change Initiative (CCI) Sea Level Budget Closure (SLBC_cci) Sea Level Budget Closure Assessment Report D3.1*. Version 1.0, 2018.
117. Hosoda, S., T. Ohira and T. Nakamura. A monthly mean dataset of global oceanic temperature and salinity derived from Argo float observations. JAMSTEC Rep. Res. Dev., Volume 8, November 2008, 47–59, 2008.
118. Khan, S. A., Sasgen, I., Bevis, M., Van Dam, T., Bamber, J. L., Wahr, J., Willis, M., Kjær, K. H., Wouters, B., Helm, V., Csatho, B., Fleming, K., Bjørk, A. A., Aschwanden, A., Knudsen, P. & Munneke, P. K., Geodetic measurements reveal similarities between post–Last Glacial Maximum and present-day mass loss from the Greenland ice sheet. *Science Advances*, 2, 2016.
119. Huang, Z., Y. Pan, H. Gong, P. J. Yeh, X. Li, D. Zhou, and W. Zhao, Subregional-scale groundwater depletion detected by GRACE for both shallow and deep aquifers in North China Plain, *Geophys. Res. Lett*., 42, 1791–1799. doi: 10.1002/2014GL062498, 2015.
120. Huang Z., The Role of glacial isostatic adjustment (GIA) process on the determination of present-day sea level rise, Report n° 505, Geodetic Science, The Ohio State University, 2013.
121. Huntington TG, Can we dismiss the effect of changes in land-based water storage on sea-level rise? *Hydrological Processes* 22:717-723 doi:10.1002/hyp.7001, 2008.
122. Hurkmans, R. T. W. L., Bamber, J. L., Davis, C. H., Joughin, I. R., Khvorostovsky, K. S., Smith, B. S. & Schoen, N., Time-evolving mass loss of the Greenland Ice Sheet from satellite altimetry. *The Cryosphere*, 8, 1725-1740, 2014.
123. Huss, M. and Hock, R., A new model for global glacier change and sea-level rise, *Front Earth Science*, 2015.
124. IMBIE Team (the), Mass balance of the Antarctic ice sheet from 1992 to 2017, *Nature*, 558, 219-222, doi:10.1038/s41586-018-0179-y, 2018.
125. Ishii, M., and M. Kimoto, Reevaluation of Historical Ocean Heat Content Variations with Time-varying XBT and MBT Depth Bias Corrections. *Journal of Oceanography* 65 (3) (June 1): 287–299. doi:10.1007/s10872-009-0027-7., 2009.
126. Ivins, E. R., T. S. James, J. Wahr, E. J. O Schrama, F. W. Landerer, and K. M. Simon, Antarctic contribution to sea level rise observed by GRACE with improved

GIA correction, *J. Geophys. Res. Solid Earth*, 118, 3126–3141, doi:10.1002/jgrb.50208, 2013.

127. Jacob, T., J. Wahr, W. T. Pfeffer, and S. Swenson, Recent contributions of glaciers and ice caps to sea level rise, *Nature* 482, 514–518, doi:10.1038/nature10847, 2012.

128. Jensen, L., R. Rietbroek, and J. Kusche, Land water contribution to sea level from GRACE and Jason-1 measurements, *J. Geophys. Res. Oceans*, 118, 212–226, doi:10.1002/jgrc.20058, 2013.

129. Jevrejeva S et al.. Nonlinear trends and multi-year cycle in sea level records, *Journal of Geophysical Research*, 111, 2005JC003229, 2006.

130. Jevrejeva, S., J. C. Moore, A. Grinsted, A. P. Matthews, and G. Spada, "Trends and Acceleration in Global and Regional Sea Levels since 1807." *Global and Planetary Change* 113:11–22. https://doi.org/10.1016/j.gloplacha.2013.12.004, 2014.

131. Johannesson, T., Raymond, C. and Waddington, E., Time-Scale for Adjustment of Glaciers to Changes in Mass Balance, *Journal of Glaciology*, 35, 355-369, 1989.

132. Johnson, G. C. and Chambers, D. P., Ocean bottom pressure seasonal cycles and decadal trends from GRACERelease-05: Ocean circulation implications, *J. Geophys. Res*. Oceans, 118, 4228–4240, doi:10.1002/jgrc.20307, 2013.

133. Johnson, G. C., and A. N. Birnbaum. 2017. As El Niño builds, Pacific Warm Pool expands, ocean gains more heat. *Geophysical Research Letters***,** 44, 438-445, doi:10.1002/2016GL071767, 2017.

134. Khan, S. A., Sasgen, I., Bevis, M., Van Dam, T., Bamber, J. L., Wahr, J., Willis, M., Kjær, K. H., Wouters, B., Helm, V., Csatho, B., Fleming, K., Bjørk, A. A., Aschwanden, A., Knudsen, P. and Munneke, P. K., Geodetic measurements reveal similarities between post–Last Glacial Maximum and present-day mass loss from the Greenland ice sheet. *Science Advances*, 2., 2016.

135. Kääb, A., Treichler, D.,Nuth, C. and Berthier, E., Brief communication: contending estimates of 2003–2008 glacier mass balance over the Pamir–Karakoram–Himalaya, *The Cryosphere*, 9, 557–564, 2015.

136. Kaser, G., Cogley, J., Dyurgerov, M., Meier, M. and Ohmura, A., Mass balance of glaciers and ice caps: Consensus estimates for 1961-2004, *Geophysical Research Letters*, 33, L19501, 2006.

137. Keenan RJ, Reams GA, Achard F, de Freitas JV, Grainger A, Lindquist E., Dynamics of global forest area: Results from the FAO Global Forest Resources Assessment 2015 *Forest Ecol Manag* 352:9-20 doi:10.1016/j.foreco.2015.06.014, 2015.

138. Kemp, A. C., B. Horton, J. P. Donnelly, M. E. Mann, M. Vermeer, and S. Rahmstorf, Climate related sea level variations over the past two millennia. *PNAS* 108.27: 11017–11022, 2011.

139. Khatiwala S, Primeau F, Hall T., Reconstruction of the history of anthropogenic CO2 concentrations in the ocean *Nature* 462:346-U110 doi:10.1038/nature08526, 2009.

140. King M.A., Altamimi Z., Boehm J., Bos M., Dach R., Elosegui P., and others, Improved constraints on models of glacial isostatic adjustment: a review of the contribution of ground-based geodetic observations, *Surveys in geophysics* 31(5):465, 2010.

141. Klige RK, Myagkov MS, Changes in the water regime of the Caspian Sea, *Geol. Journal* 27:299-307, 1992.

142. Konikow, L. F., Contribution of global groundwater depletion since 1900 to sea-level rise, *Geophys. Res. Lett*., 38, L17401, doi:10.1029/2011GL048604, 2011.
143. Konrad H., Sasgen I., Pollard D., Klemann V., Potential of the solid-Earth response for limiting long-term West Antarctic Ice Sheet retreat in a warming climate, *Earth and Planetary Science Letters* 432, 254-264, 2015.
144. Kopp R.E., Hay C.C., Little C.M., Mitrovica J.X., Geographic variability of sea-level change, *Current Climate Change Reports* 1(3):192, 2015.
145. Kustu, M., Y. Fan, and A. Robock, Large-scale water cycle perturbation due to irrigation pumping in the US High Plains: A synthesis of observed streamflow changes, *J. Hydrol*., 390, 222–244, doi:10.1016/j.jhydrol.2010.06.045, 2010.
146. Kustu, M. D., Y. Fan, and M. Rodell, Possible link between irrigation in the U.S. High Plains and increased summer streamflow in the Midwest, *Water Resour. Res*., 47, W03522, doi:10.1029/2010WR010046, 2011.
147. Lambeck K, Chappell J., *Science* 292(5517):679, 2001.
148. Lambeck K., Sea-level change from mid-Holocene to recent time: An Australian example with global implications, In: Ice Sheets, Sea Level and the Dynamic Earth, JX Mitrovica and LLA Vermeersen, Eds., Geodynamics Series, 29:33-50, 2002.
149. Lambeck K. et al., Paleoenvironmental records, geophysical modelling and reconstruction of sea level trends and variability on centennial and longer time scales, *In Understanding sea level rise and variability*, JA Church et al ed., Wiley-Blackwell, 2010.
150. Leclercq, P., Oerlemans, J. and Cogley, J., Estimating the glacier contribution to sea-level rise for the period 1800–2005, *Surveys in Geophysics*, 32, 519–535, 2011.
151. Legeais, J-F, Michaël Ablain, Lionel Zawadzki, Hao Zuo, Johnny A. Johannessen, Martin G. Scharffenberg, Luciana Fenoglio-Marc, et al., "An Accurate and Homogeneous Altimeter Sea Level Record from the ESA Climate Change Initiative." *Earth System Science Data Discussions*, 1–35, doi:10.5194/essd-2017-116, 2018.
152. Lehner, B., C. Reidy Liermann, C. Revenga, C. Vörösmarty, B. Fekete, P. Crouzet, P. Döll, M. Endejan, K. Frenken, J. Magome, C. Nilsson, J. C. Robertson, R. Rödel, N. Sindorf, and D. Wisser, High-resolution mapping of the world's reservoirs and dams for sustainable river-flow management, *Fron. Ecol. Environ*., 9, 494-502, doi:10.1890/100125, 2011.
153. Le Queré et al., Global Carbon Budget 2017, *Earth Syst. Sci. Data*, 10, 405-448, 2018, doi.org/10.5194/essd-10-405-2018, 2018.
154. Lettenmaier, D. P., and P. C. D. Milly, Land waters and sea level, *Nat. Geosci*., 2, 452-454, doi:10.1038/ngeo567, 2009.
155. Leuliette, E. W., and Miller, L.,Closing the sea level rise budget with altimetry, Argo, and GRACE, *Geophys. Res. Lett*., 36, L04608, doi:10.1029/2008GL036010, 2009.
156. Leuliette, E.W., and Willis, J.K., Balancing the sea level budget, *Oceanography* 24 (2): 122–129, doi:10.5670/oceanog.2011.32, 2011.
157. Leuschen, C.: IceBridge Geolocated Radar Echo Strength Profiles, Boulder, Colorado, NASA DAAC at the National Snow and Ice Data Center, http://dx.doi.org/10.5067/ FAZTWP500V70, last access: 15 June 2014
158. Levitus S., J.I. Antonov, T.P. Boyer, O.K. Baranova, H.E. Garcia, R.A. Locarnini, A.V. Mishonov, J.R. Reagan, D. Seidov, E.S. Yarosh and M.M. Zweng, World ocean heat content and thermosteric sea level change (0-2000 m), 1955-2010, *Geophys. Res. Lett*., 39, L10603, doi:10.1019/2012GL051106, 2012.

159. Llovel, W., J. K. Willis, F. W. Landerer, and I. Fukumori, Deep-ocean contribution to sea level and energy budget not detectable over the past decade, *Nature Clim. Change* 4, 1031–1035, doi:10.1038/nclimate2387, 2014.
160. Llovel, W., M. Becker, A. Cazenave, J.-F. Crétaux, and G. Ramillien, *C. R. Geosci.* 342, 179–188, doi :10.1016/j.crte.2009.12.004, 2010.
161. Lo, M.-H., and J. S. Famiglietti, Irrigation in California's Central Valley strengthens the southwestern U.S. water cycle, *Geophys. Res. Lett.*, 40, doi:10.1002/grl.50108, 2013.
162. Loriaux, T. and Casassa, G., Evolution of glacial lakes from the Northern Patagonia Icefield and terrestrial water storage in a sea-level rise context, *Global and Planetory Change*, 102, 33-40, 2013.
163. Lovel TR, Belward AS, The IGBP-DIS global 1 km land cover data set, DISCover: first results *International Journal of Remote Sensing* 18:3291-3295, 1997.
164. Luthcke, S. B., Sabaka, T. J., Loomis, B. D., Arendt, A. A., McCarthy, J. J., and Camp, J., Antarctica, Greenland and Gulf of Alaska land-ice evolution from an iterated GRACE global mascon solution. *Journal of Glaciology*, 59:613–631, doi:10.3189/2013JoG12J147, 2013.
165. Luthcke, S. B., Zwally, H. J., Abdalati, W., Rowlands, D. D., Ray, R. D., Nerem, R. S., Lemoine, F. G., McCarthy, J. J., and Chinn, D. S., Recent Greenland Ice Mass Loss by Drainage System from Satellite Gravity Observations. *Science*, 314:1286–1289, doi:10.1126/science.1130776, 2006.
166. Luthcke, S. B., Sabaka, T., Loomis, B., Arendt, A., Mccarthy, J. & Camp, J., Antarctica, Greenland and Gulf of Alaska land-ice evolution from an iterated GRACE global mascon solution. *Journal of Glaciology*, 59, 613-631, 2013.
167. Lyman, J. M., S. A. Godd, V. V. Gouretski, et al., Robust warming of the global upper ocean. *Nature* 465:334–337, 2010.
168. MacDicken KG, Global Forest Resources Assessment, What, why and how? *Forest Ecol Manag* 352:3-8 doi:10.1016/j.foreco.2015.02.006, 2015.
169. Martín-Español, A., Zammit-Mangion, A., Clarke, P. J., Flament, T., Helm, V., King, M. A., and Wouters, B., Spatial and temporal Antarctic Ice Sheet mass trends, glacio-isostatic adjustment, and surface processes from a joint inversion of satellite altimeter, gravity, and GPS data. *Journal of Geophysical Research*: Earth Surface, 121(2), 182-200, 2016.
170. Martinec Z., Hagedoorn J.,The rotational feedback on linear-momentum balance in glacial isostatic adjustment, *Geophysical Journal International* 199, 3, 1823-1846, 2014.
171. Merrifield MA et al., An anomalous recent acceleration of global sea level rise. J. Clim. 22: 5772–5781. doi:10.1175/2009JCLI2985.1., 2009.
172. Meyssignac B., M. Becker, W. Llovel, and A. Cazenave, An Assessment of Two-Dimensional Past Sea Level Reconstructions Over 1950–2009 Based on Tide-Gauge Data and Different Input Sea Level Grids, *Surveys in Geophysics*, doi:10.1007/s10712-011-9171-x, 2011.
173. Milne G.A., Gehrels W.R., Hughes C.W., Tamisiea M.E., Identifying the causes of sea-level change, *Nature Geoscience* 2.7:471, 2009.
174. Mitrovica J.X., Milne G.A., On the origin of late Holocene sea-level highstands within equatorial ocean basins, *Quaternary Science Reviews* 21, 20-22, 2179-2190, 2002.
175. Mitrovica J.X., Milne G.A., On post-glacial sea level: I. General theory, *Geophysical Journal International* 154, 2, 253, 2003.

176. Mitrovica J.X., Wahr J., Matsuyama I., Paulson A., The rotational stability of an ice-age earth, *Geophysical Journal International*, 161.2, 491-506, 2005.

177. Mitrovica J.X., Wahr J., Matsuyama I., Paulson A., and Tamisiea M.E., Reanalysis of ancient eclipse, astronomic and geodetic data: A possible route to resolving the enigma of global sea-level rise. *Earth and Planetary Science Letters, 243, 3-4,* 390-399, doi: 10.1016/j.epsl.2005.12.029, 2006.

178. Mitrovica J.X., Wahr J., Ice age Earth rotation, *Annual Review of Earth and Planetary Sciences* 39, 577-616, 2011.

179. Marzeion, B., Jarosch, A., Hofer, M., Past and future sea-level change from the surface mass balance of glaciers, *The Cryosphere*, 6, 1295–1322, 2012.

180. Marzeion, B., Cogley, J., Richter, K. and Parkes, D., Attribution of global glacier mass loss to anthropogenic and natural causes, *Science*, 345, 919–92, 2014.

181. Marzeion, B., Champollion, N., Haeberli, W., Langley, K., Leclercq, P. and Paul, F., Observation-Based Estimates of Global Glacier Mass Change and Its Contribution to Sea-Level Change, *Surveys in Geophysics*, 28, 105-130, 2017.

182. Marzeion, B., Kaser, G., Maussion, F. and Champollion, N., Limited influence of climate change mitigation on short-term glacier mass loss, Nature Climate Change, doi:10.1038/s41558-018-0093-1, 2018.

183. Masters, D., R. S. Nerem, C. Choe, E. Leuliette, B. Beckley, N. White, and M. Ablain., "Comparison of Global Mean Sea Level Time Series from TOPEX/Poseidon, Jason-1, and Jason-2." *Marine Geodesy* 35 (sup1):20–41. https://doi.org/10.1080/01490419.2012.717862, 2012.

184. Matthews E, Fung I, Methane emission from natural wetlands: Global distribution, area, and environmental characteristics of sources Global Biogeochemical Cycles 1:61-86, 1987.

185. Matthews GVT, The Ramsar Convention on wetlands: its history and development. Ramsar Convention Bureau, Gland, Switzerland, 1993.

186. Maussion, F, Butenko, A., Eis, J., Fourteau, K., Jarosch, A., Landmann, J., Oesterle, J., Recinos, B., Rothenpieler, T., Vlug, A., Wild, C. and Marzeion; B., The Open Global Glacier Model (OGGM) v1.0, *subm. to The Cryosphere,* 2018.

187. McMillan M. et al. Increased ice losses from Antarctica detected by Cryosat-2, *Geophys. Res. Lett*., 41(11), 3899-3905, 2014.

188. Meherhomji VM, Probable Impact of Deforestation on Hydrological Processes Climatic Change 19:163-173 doi:10.1007/Bf00142223, 1991.

189. Micklin PP, The Aral Crisis - Introduction to the Special Issue Post-Sov Geogr 33:269-282, 1992.

190. Milly P. C. D. et al., Terrestrial water-storage contributions to sea-level rise and variability , in Understanding Sea-Level Rise and Variability:226-255, 2010.

191. Milly, P. C. D., A. Cazenave, and M. C. Gennero, Contribution of climate-driven change in continental water storage to recent sea-level rise. *Proc. Natl. Acad. Sci.*, 100, 13158–13161, 2003.

192. Mitra S, Wassmann R, Vlek PLG, An appraisal of global wetland area and its organic carbon stock *Curr Sci India* 88:25-35, 2005.

193. Mitsch WJ, Gosselink JG, Wetlands, 2nd ed. Van Nostrand Reinhold, New York, 1993.

194. Mouginot J., E. Rignot, B. Scheuchl, Sustained increase in ice discharge from the Amundsen Sea Embayment, West Antarctica, from 1973 to 2013, *Geophys. Res. Lett.* 41, 1576-1584, 2014.

195. Munk W., Twentieth century sea level: An enigma, *PNAS*, 99, 10, 6550-6555, doi/10.1073/pnas092704599, 2002.

196. Natarov, S. I., M. A. Merrifield, J. M. Becker, and P. R. Thompson, Regional influences on reconstructed global mean sea level, Geophys. Res. Lett., 44, 3274-3282, 2017.
197. Nerem, R. S., D. P. Chambers, C. Choe, and G. T. Mitchum. "Estimating Mean Sea Level Change from the TOPEX and Jason Altimeter Missions." *Marine Geodesy* 33 (sup1):435–46. https://doi.org/10.1080/01490419.2010.491031, 2010.
198. Nerem R.S., Beckley B.D., Fasullo J., Hamlington B.D., Masters D. and Mitchum G.T., Climate Change Driven Accelerated Sea Level Rise Detected In The Altimeter Era, *PNAS*, 2018.
199. Nghiem, S., Hall, D., Mote, T., Tedesco, M., Albert, M., Keegan, K., Shuman, C., Digirolamo, N. & Neumann, G., The extreme melt across the Greenland ice sheet in 2012. *Geophysical Research Letters*, 39, 2012.
200. Nobre P, Malagutti M, Urbano DF, de Almeida RAF, Giarolla E, Amazon Deforestation and Climate Change in a Coupled Model Simulation *J Climate* 22:5686-5697 doi:10.1175/2009jcli2757.1, 2009.
201. Oki, T. and S. Kanae, Global hydrological cycles and world water resources, *Science*, 313, 1068-1072, doi:10.1126/science.1128845, 2006.
202. Ozyavas A, Khan SD, Casey JF, A possible connection of Caspian Sea level fluctuations with meteorological factors and seismicity *Earth Planet Sc Lett* 299:150-158 doi:10.1016/j.epsl.2010.08.030, 2010.
203. Pala, C., Once a Terminal Case, the North Aral Sea Shows New Signs of Life, *Science*, 312, 183, doi:10.1126/science.312.5771.183, 2006.
204. Pala, C., In Northern Aral Sea, Rebound Comes With a Big Catch, Science, 334, 303, doi:10.1126/science.334.6054.303, 2011.
205. Palmer M. et al., 2016.
206. Paul, F., Huggel, C. and Kääb, Combining satellite multispectral image data and a digital elevation model for mapping of debris-covered glaciers, *Remote Sensing of Environment*, 89, 510–518, 2004.
207. Paulson, A., Zhong, S., and Wahr, J., Inference of mantle viscosity from GRACE and relative sea level data. *Geophysical Journal International*, 171:497–508, doi:10.1111/j.1365-246X.2007.03556.x, 2007.
208. Peltier W.R., Global glacial isostatic adjustment and modern instrumental records of relative sea level history, in: B.C. Douglas, M.S. Kearney, S.P. Leatherman (Eds.), *Sea-Level Rise: History and Consequences*, vol. 75, Academic Press, San Diego, 2001, pp. 65–95.
209. Peltier W.R., Luthcke S.B., On the origins of Earth rotation anomalies: New insights on the basis of both "paleogeodetic" data and Gravity Recovery and Climate Experiment (GRACE) data, *Journal of Geophysical Research: Solid Earth* 114, B11405, 2009.
210. Peltier W.R., Global glacial isostasy and the surface of the ice-age Earth: the ICE-5G (VM2) model and GRACE, *Annual Review of Earth and Planetary Sciences* 32, 111, 2004.
211. Peltier W.R., Argus D.F., Drummond R., Space geodesy constrains ice age terminal deglaciation: The global ICE-6G_C (VM5a) model, *Journal of Geophysical Research: Solid Earth* 120, 1, 450-487, 2015.
212. Peltier W.R., Closure of the budget of global sea level rise over the GRACE era: the importance and magnitudes of the required corrections for global glacial isostatic adjustment. *Quaternary Science Reviews*, 28, 1658-1674, 2009.

213. Peltier, W. R., R. Drummond, and K. Roy, Comment on "Ocean mass from GRACE and glacial isostatic adjustment" by D. P. Chambers et al. *Journal of Geophysical Research-Solid Earth*, **117**, B11403, 2012.
214. Perera J, A Sea Turns to Dust *New Sci* 140:24-27, 1993.
215. Pfeffer, W., Arendt, A., Bliss, A., Bolch, T., Cogley, J., Gardner, A., Hagen, J.-O., Hock, R., Kaser, G., Kienholz, C., Miles, E., Moholdt, G., Mölg, N., Paul, F., Radić, V., Rastner, P., Raup, B., Rich, J. and Sharp, M., The Randolph Glacier Inventory: a globally complete inventory of glaciers., *Journal of Glaciology*, 60, 537–552, 2014.
216. Plag H.P., Juettner H.U., Inversion of global tide gauge data for present-day ice load changes, *Memoirs of National Institute of Polar Research* 54:301, 2001.
217. Pokhrel, Y. N., N. Hanasaki, P. J.-F. Yeh, T. Yamada, S. Kanae, and T. Oki, Model estimates of sea level change due to anthropogenic impacts on terrestrial water storage, *Nat. Geosci*., 5, 389–392, doi:10.1038/ngeo1476, 2012.
218. Pokhrel, Y. N., S. Koirala, P. J.-F. Yeh, N. Hanasaki, L. Longuevergne, S. Kanae, and T. Oki, Incorporation of groundwater pumping in a global Land Surface Model with the representation of human impacts, *Water Resour. Res*., 51, 78–96, doi:10.1002/2014WR015602, 2015.
219. Postel, S. L., Pillar of Sand: Can the Irrigation Miracle Last? W.W. Norton, New York USA, ISBN 0-393-31937-7, 1999.
220. Purcell A.P., Tregoning P., Dehecq A., An assessment of the ICE6G_C (VM5a) glacial isostatic adjustment model, *Journal of Geophysical Research: Solid Earth* 121, 5, 3939-3950, 2016.
221. Purkey, S. G., Johnson, G. C., and Chambers, D. P., Relative contributions of ocean mass and deep steric changes to sea level rise between 1993 and 2013, *J. Geophys. Res. Oceans*, 119, 7509–7522, doi:10.1002/2014JC010180, 2014.
222. Purkey, S., and G. C. Johnson, Warming of global abyssal and deep southern ocean waters between the 1990s and 2000s: Contributions to global heat and sea level rise budget, *J. Clim.*, *23*, 6336–6351, doi:10.1175/2010JCLI3682.1, 2010.
223. Radic, V. and Hock, R., Regional and global volumes of glaciers derived from statistical upscaling of glacier inventory data, *Journal of Geophysical Research Earth Surface*, 115, F01010, 2010.
224. Radic, V. and Hock, R., Regionally differentiated contribution of mountain glaciers and ice caps to future sea-level rise, *Nature Geoscience*, 4, 91-94, 2011.
225. Ramillien G, Frappart F, Seoane L, Application of the regional water mass variations from GRACE Satellite Gravimetry to large-scale water management in Africa *Remote Sensing* 6:7379-7405, 2014.
226. Ray, R.D. and B.C. Douglas, Experiments in reconstructing twentieth-century sea levels, Prog. Oceanogr. 91, 495–515, 2011.
227. Reager, J. T., Gardner, A. S., Famiglietti, J. S., Wiese, D. N., Eicker, A., & Lo, M. H., A decade of sea level rise slowed by climate-driven hydrology. *Science*, *351*(6274), 699-703, doi:10.1126/science.aad8386, 2016.
228. Reager, J. T., Thomas, B. F., and Famiglietti, J. S., River basin flood potential inferred using GRACE gravity observations at several months lead time. *Nature Geoscience*, 7:588–592, doi:10.1038/ngeo2203, 2014.
229. Rhein, M., S.R. Rintoul, S. Aoki, E. Campos, D. Chambers, R.A. Feely, S. Gulev, G.C. Johnson, S.A. Josey, A. Kostianoy,C. Mauritzen, D. Roemmich, L.D. Talley and F. Wang: Observations: Ocean. In: Climate Change 2013: The Physical Science Basis. Contribution of Working Group I to the Fifth Assessment Report of the Intergovernmental Panel on Climate Change [Stocker, T.F., D. Qin, G.-K. Plattner, M.

Tignor, S.K. Allen, J. Boschung, A. Nauels, Y. Xia, V. Bex and P.M. Midgley (eds.)]. Cambridge University Press, Cambridge, United Kingdom and New York, NY, USA., 2013.

230. Richey, A. S., B. F. Thomas, M.-H. Lo, J. T. Reager, J. S. Famiglietti, K. Voss, S. Swenson, and M. Rodell, Quantifying renewable groundwater stress with GRACE, *Water Resour. Res*., 51, 5217–5238, doi:10.1002/2015WR017349, 2015.

231. Rietbroek, R., Brunnabend, S.-E., Kusche, J. and Schröter, J., Resolving sea level contributions by identifying fingerprints in time-variable gravity and altimetry, *J. Geodyn*., 59-60, 72-81, 2012.

232. Rietbroek, R., Brunnabend, S.-E., Kusche, J., Schröter, J., and Dahle, C., Revisiting the contemporary sea-level budget on global and regional scales. *Proceedings of the National Academy of Sciences*, 113(6):1504–1509, doi:10.1073/pnas.1519132113, 2016.

233. Rignot, E. J., I. Velicogna, M. R. van den Broeke, A. J. Monaghan, and J. T. M. Lenaerts, Acceleration of the contribution of the Greenland and Antarctic ice sheets to sea level rise, *Geophys. Res. Lett*., 38, L05503, doi:10.1029/2011GL046583, 2011.

234. Rignot, E., J. Mouginot, and B. Scheuchl, Ice flow of the Antarctic Ice Sheet, *Science*, **333**(6048), 1427–1430, doi:10.1126/science.1208336, 2011.

235. Riva R.E., Gunter B.C., Urban T.J., Vermeersen B.L., Lindenbergh R.C., Helsen M.M., and others, Glacial isostatic adjustment over Antarctica from combined ICESat and GRACE satellite data, *Earth and Planetary Science Letters* 288(3), 516-523, 2009.

236. Riva, R. E. M., J. L. Bamber, D. A. Lavallée, and B. Wouters, Sea-level fingerprint of continental water and ice mass change from GRACE, *Geophys. Res. Lett*., 37, L19605, doi:10.1029/2010GL044770, 2010.

237. Rodell, M., I. Velicogna, and J. S. Famiglietti, Satellite-based estimates of groundwater depletion in India, *Nature*, 460, 999-1002, doi:10.1038/nature08238, 2009.

238. Roemmich, D., Owens, W.B., The ARGO project: global ocean observations for understanding for understanding and prediction of climate variability. *Oceanography* 13 (2), 45–50, 2000.

239. Roemmich, D., W. J. Gould, and J. Gilson, 135 years of global ocean warming between the Challenger expedition and the Argo Programme, *Nature Climate Change*, *2*(6), 425-428, doi:10.1038/nclimate1461, 2012.

240. Roemmich, D, Gilson J, Sutton P, Zilberman N. 2016. Multidecadal change of the South Pacific gyre circulation. Journal of Physical Oceanography. 46:1871-1883. 10.1175/jpo-d-15-0237.1 , 2016.

241. Roemmich, D. and J. Gilson. The 2004–2008 mean and annual cycle of temperature, salinity, and steric height in the global ocean from the Argo Program, Progress in Oceanography, Volume 82, Issue 2, August 2009, Pages 81-100, 2009.

242. Rohrig E, Biomass and productivity. In: Rohrig E (edt.) Ecosystems of the world. Elsevier, New York, pp 165-174, 1991.

243. Sabine C.L. et al., The oceanic sink for anthropogenic CO2 *Science* 305:367-371 doi:10.1126/science.1097403, 2004.

244. Sahagian D., Global physical effects of anthropogenic hydrological alterations: sea level and water redistribution *Global and Planetary Change* 25:39-48 doi:10.1016/S0921-8181(00)00020-5, 2000.

245. Sahagian, D. L., F. W. Schwartz, and D. K. Jacobs, Direct anthropogenic contributions to sea level rise in the twentieth century, *Nature*, 367, 54-57, doi:10.1038/367054a0, 1994.
246. Sasgen I., Konrad H., Ivins E.R., Van den Broeke M.R., Bamber J.L., Martinec Z., Klemann V., Antarctic ice-mass balance 2003 to 2012: regional reanalysis of GRACE satellite gravimetry measurements with improved estimate of glacial-isostatic adjustment based on GPS uplift rates, *The Cryosphere*, 7, 1499-1512, 2013.
247. Sasgen I., Martín-Español A., Horvath A., Klemann V., Petrie E.J., Wouters B., and others Joint inversion estimate of regional glacial isostatic adjustment in Antarctica considering a lateral varying Earth structure (ESA STSE Project REGINA), *Geophysical Journal International* 211, 3, , 1534-1553, 2017.
248. Sasgen, I., Van Den Broeke, M., Bamber, J. L., Rignot, E., Sørensen, L. S., Wouters, B., Martinec, Z., Velicogna, I. & Simonsen, S. B., Timing and origin of recent regional ice-mass loss in Greenland. *Earth and Planetary Science Letters*, 333, 293-303, 2012.
249. Sasgen, I., Konrad, H., Ivins, E. R., Van den Broeke, M. R., Bamber, J. L., Martinec, Z., & Klemann, V., Antarctic ice-mass balance 2003 to 2012: regional reanalysis of GRACE satellite gravimetry measurements with improved estimate of glacial-isostatic adjustment based on GPS uplift rates. *The Cryosphere*, 7, 1499- 1512, 2013.
250. Sasgen, I., Martín-Español, A., Horvath, A., Klemann, V., Petrie, E. J., Wouters, B., & Konrad, Joint inversion estimate of regional glacial isostatic adjustment in Antarctica considering a lateral varying Earth structure (ESA STSE Project REGINA). *Geophysical Journal International*, 211, 3, 1534-1553, 2017.
251. Scanlon, B. R., I. Jolly, M. Sophocleous, and L. Zhang, Global impacts of conversions from natural to agricultural ecosystems on water resources: Quantity versus quality, *Water Resources Res.*, 43, 3, W03437, 2007.
252. Scanlon, B. R., C. C. Faunt, L. Longuevergne, R. C. Reedy, W. M. Alley, V. L. McGuire, and P. B. McMahon, Groundwater depletion and sustainability of irrigation in the U.S. High Plains and Central Valley, *PNAS*, 109, 9320-9325, doi:10.1073/pnas.1200311109, 2012a.
253. Scanlon, B. R., L. Longuevergne, and D. Long, Ground referencing GRACE satellite estimates of groundwater storage changes in the California Central Valley, USA, *Water Resour. Res.*, 48, W04520, doi:10.1029/2011WR011312, 2012b.
254. Scanlon, B. R., Zhang, Z., Save, H., Sun, A. Y., Schmied, H. M., van Beek, L. P., & Longuevergne, L., Global models underestimate large decadal declining and rising water storage trends relative to GRACE satellite data. *PNAS*, 201704665, 2018.
255. Schrama, E. J., Wouters, B. & Rietbroek, R., A mascon approach to assess ice sheet and glacier mass balances and their uncertainties from GRACE data. *Journal of Geophysical Research: Solid Earth*, 119, 6048-6066, 2014.
256. Schellekens, J., Dutra, E., Martínez-de la Torre, A., Balsamo, G., van Dijk, A., Weiland, F. S., & Fink, G., A global water resources ensemble of hydrological models: the eartH2Observe Tier-1 dataset. *Earth System Science Data*, *9*(2), 389, 2017.
257. Schwatke C, Dettmering D, Bosch W, Seitz F, DAHITI – an innovative approach for estimating water level time series over inland waters using multi-mission satellite altimetry, *Hydrol. Earth Syst. Sci*., 19, 4345-4364, 2015.
258. Shamsudduha, M., R. G. Taylor, and L. Longuevergne, Monitoring groundwater storage changes in the highly seasonal humid tropics: Validation of

GRACE measurements in the Bengal Basin, *Water Resour. Res.*, 48, W02508, doi:10.1029/2011WR010993, 2012.

259. Sheng Y, Song C, Wang J, Lyons EA, Knox BR, Cox JS, Gao F., Representative lake water extent mapping at continental scales using multi-temporal Landsat-8 imagery *Remote Sensing of Environment* in press:doi:10.1016/j.rse.2015.1012.1041, 2016.
260. Shepherd, A., Ivins E.R., Geruo A., Barletta V.R., Bentley M.J., Bettadpur S., and others, A reconciled estimate of ice-sheet mass balance. *Science,* 338(6111), 1183-1189, doi:10.1126/science.1228102, 2012.
261. Shukla J, Nobre C, Sellers P., Amazon Deforestation and Climate Change *Science* 247:1322-1325 doi:10.1126/science.247.4948.1322, 1990.
262. Singh A, Seitz F, Schwatke C., Inter-annual water storage changes in the Aral Sea from multi-mission satellite altimetry, optical remote sensing, and GRACE satellite gravimetry *Remote Sens Environ* 123:187-195, 2012.
263. Slangen, A.B.A., Meyssignac, B., Agosta, C., Champollion, N., Church, J.A., Fettweis, X., Ligtenberg, S.R.M., Marzeion, B., Melet, A., Palmer, M.D., Richter, K., Roberts, C.D., Spada, G., Evaluating model simulations of 20th century sea-level rise. Part 1: global mean sea-level change. *J. Clim. 30*, 21, 8539–8563. https://dx.doi.org/10.1175/jcli-d-17-0110.1, 2017.
264. Sloan S, Sayer JA., Forest Resources Assessment of 2015 shows positive global trends but forest loss and degradation persist in poor tropical countries, *Forest Ecol Manag*, 352:134-145 doi:10.1016/j.foreco.2015.06.013, 2015.
265. Smith LC, Sheng Y, MacDonald GM, Hinzman LD, Disappearing Arctic lakes *Science* 308:1429-1429 doi:10.1126/science.1108142, 2005.
266. Solomon, S. et al. (eds.), Climate Change 2007: The Physical Science Basis. Contribution of Working Group I to the Fourth Assessment Report of the Intergovernmental Panel on Climate Change, Cambridge Univ. Press, Cambridge, UK., 2007.
267. Song C, Huang B, Ke L., Modeling and analysis of lake water storage changes on the Tibetan Plateau using multi-mission satellite data *Remote Sens Environ* 135:25-35 doi:10.1016/j.rse.2013.03.013, 2013.
268. Spada G,. Stocchi P., SELEN: A Fortran 90 program for solving the "sea-level equation", *Computers & Geosciences* 33.4, 538-562, 2007.
269. Spada G., Galassi G., New estimates of secular sea level rise from tide gauge data and GIA modelling, *Geophysical Journal International* 191(3): 1067-1094, 2012.
270. Spada G., Galassi G., Spectral analysis of sea level during the altimetry era, and evidence for GIA and glacial melting fingerprints, *Global and Planetary Change* 143:34-49, 2016.
271. Spada G.,Glacial isostatic adjustment and contemporary sea level rise: An overview. *Surveys in Geophysics* 38(1), 153-185, 2017.
272. Spracklen DV, Arnold SR, Taylor CM., Observations of increased tropical rainfall preceded by air passage over forests *Nature* 489:282-U127 doi:10.1038/nature11390, 2012.
273. Sutterley T.C., Velicogna I., Csatho B., van den Broeke M., Rezvan-Behbahani S., Babonis G., Evaluating Greenland glacial isostatic adjustment corrections using GRACE, altimetry and surface mass balance data *Environmental Research Letters* 9(1), 014004, 2014.
274. Strassberg, G., B. R. Scanlon, and M. Rodell, Comparison of seasonal terrestrial water storage variations from GRACE with groundwater-level

measurements from the High Plains Aquifer (USA), *Geophys. Res. Lett*., 34, L14402, doi:10.1029/2007GL030139, 2007.

275. Swenson S, Wahr J., Monitoring the water balance of Lake Victoria, East Africa, from space *J Hydro* 370:163-176, 2009.

276. Syed, T. H., J. S. Famiglietti, D. P. Chambers, J. K. Willis, and K. Hilburn, Satellite-based global ocean mass balance reveals water cycle acceleration and increasing continental freshwater discharge, 1994–2006, *Proc. Natl. Acad. Sci*. U. S. A., 107, 17,916–17,921, doi:10.1073/pnas.1003292107, 2010.

277. Stammer, D., and Cazenave A., *Satellite Altimetry Over Oceans and Land Surfaces*, 617 pp., CRC Press, Taylor and Francis Group, Boca Raton, New York, London, ISBN: 13: 978-1-4987-4345-7, 2018.

278. Tamisiea, M. E., Leuliette, E. W., Davis, J. L., and Mitrovica, J. X., Constraining hydrological and cryospheric mass flux in southeastern Alaska using space-based gravity measurements. *Geophysical Research Letters*, 32:L20501, doi:10.1029/2005GL023961, 2005.

279. Tamisiea M.E., Ongoing glacial isostatic contributions to observations of sea level change, *Geophysical Journal International* 186(3):1036, 2011.

280. Tapley, B. D., S. Bettadpur, J. C. Ries, P. F. Thompson, and M. M. Watkins, GRACE measurements of mass variability in the Earth system. *Science* 305, 503–505, doi: 10.1126/science.1099192, 2004.

281. Tapley, B. D., Bettadpur, S., Ries, J. C., Thompson, P. F., and Watkins, M. M., The Gravity Recovery and Climate Experiment; Mission Overview and Early Results, *Geophy. Res. Lett*., Vol. 31, No. 9, L09607, 10.1029/2004GL019920, 2004.

282. Taylor, R. G., B. Scanlon, P. Döll, M. Rodell, R. van Beek, Y. Wada, L. Longuevergne, M. LeBlanc, J. S. Famiglietti, M. Edmunds, L. Konikow, T. R. Green, J. Chen, M. Taniguchi, M. F. P. Bierkens, A. MacDonald, Y. Fan, R. M. Maxwell, Y. Yechieli, J. J. Gurdak, D. M. Allen, M. Shamsudduha, K. Hiscock, P. J.-F. Yeh, I, Holman and H. Treidel, Groundwater and climate change, *Nature Clim. Change*, 3, 322-329, doi:10.1038/nclimate1744, 2013.

283. Thompson, P.R., and M.A. Merrifield, A unique asymmetry in the pattern of recent sea level change, Geophys. Res. Lett., 41, 7675-7683, 2014.

284. Tiwari, V. M., J. Wahr, and S. Swenson, Dwindling groundwater resources in northern India, from satellite gravity observations, *Geophys. Res. Lett*., 36, L18401, doi:10.1029/2009GL039401, 2009.

285. Tourian M, Elmi O, Chen Q, Devaraju B, Roohi S, Sneeuw N, A spaceborne multisensor approach to monitor the desiccation of Lake Urmia in Iran *Remote Sens Environ* 156:349-360, 2015.

286. Turcotte DL, Schubert G, Geodynamics. Cambridge University Press, Cambridge, 2014.

287. Valladeau, G., J. F. Legeais, M. Ablain, S. Guinehut, and N. Picot, "Comparing Altimetry with Tide Gauges and Argo Profiling Floats for Data Quality Assessment and Mean Sea Level Studies." *Marine Geodesy* 35 (sup1):42–60. https://doi.org/10.1080/01490419.2012.718226, 2012.

288. Van Den Broeke, M. R., Enderlin, E. M., Howat, I. M., Kuipers Munneke, P., Noël, B. P. Y., Van De Berg, W. J., Van Meijgaard, E. & Wouters, B., On the recent contribution of the Greenland ice sheet to sea level change. *The Cryosphere*, 10, 1933-1946, 2016.

289. Velicogna, I., Increasing rates of ice mass loss from the Greenland and Antarctic ice sheets revealed by GRACE. *Geophysical Research Letters*, 36, 2009.

290. van der Werf GR et al., Global fire emissions and the contribution of deforestation, savanna, forest, agricultural, and peat fires (1997-2009) *Atmos Chem Phys* 10:11707-11735 doi:10.5194/acp-10-11707-2010, 2010.
291. Van Dijk, A. I. J. M., L. J. Renzullo, Y. Wada, and P. Tregoning, A global water cycle reanalysis (2003–2012) merging satellite gravimetry and altimetry observations with a hydrological multi-model ensemble, *Hydrol. Earth Syst. Sci*., 18, 2955-2973, doi:10.5194/hess-18-2955-2014, 2014.
292. Velicogna, I., Sutterley, T. C., & Van Den Broeke, M. R., Regional acceleration in ice mass loss from Greenland and Antarctica using GRACE time-variable gravity data. *Geophysical Research Letters*, 41(22), 8130-8137, 2014.
293. Velicogna, I., Wahr, J., Measurements of Time-Variable Gravity Show Mass Loss in Antarctica, *Science*, DOI: 10.1126/science.1123785, 2006.
294. von Schuckmann, K., J.-B. Sallée, D. Chambers, P.-Y. Le Traon, C. Cabanes, F. Gaillard, S. Speich, and M. Hamon, Monitoring ocean heat content from the current generation of global ocean observing systems, *Ocean Science*, *10*, 547-557, DOI:10.5194/os-10-547-2012, 2014.
295. von Schukmann K., Palmer M.D., Trenberth K.E., Cazenave A., D. Chambers, Champollion N. et al., Earth's energy imbalance: an imperative for monitoring, *Nature Climate Change*, 26, 138-144, 2016.
296. Vörösmarty CJ, Sahagian D, Anthropogenic disturbance of the terrestrial water cycle *Bioscience* 50:753-765 doi:10.1641/0006-3568(2000)050[0753:Adottw]2.0.Co;2, 2000.
297. Voss, K. A., J. S. Famiglietti, M. Lo, C. de Linage, M. Rodell, and S. C. Swenson, Groundwater depletion in the Middle East from GRACE with implications for transboundary water management in the Tigris-Euphrates-Western Iran region, *Water Resour. Res.*, 49, doi:10.1002/wrcr.20078, 2013.
298. Watson, Christopher S., Neil J. White, John A. Church, Matt A. King, Reed J. Burgette, and Benoit Legresy, "Unabated Global Mean Sea-Level Rise over the Satellite Altimeter Era." *Nature Climate Change* 5 (6):565–68. https://doi.org/10.1038/nclimate2635, 2015.
299. Wada, Y., L. P. H. van Beek, C. M. van Kempen, J. W. T. M. Reckman, S. Vasak, and M. F. P. Bierkens, Global depletion of groundwater resources, *Geophys. Res. Lett*., 37, L20402, doi:10.1029/2010GL044571, 2010.
300. Wada, Y., Modelling groundwater depletion at regional and global scales: Present state and future prospects, *Surv. Geophys*., 37, 419-451, doi:10.1007/s10712-015-9347-x, Special Issue: ISSI Workshop on Remote Sensing and Water Resources, 2017.
301. Wada, Y., L. P. H. van Beek, and M. F. P. Bierkens, Nonsustainable groundwater sustaining irrigation: A global assessment, *Water Resour. Res*., 48, W00L06, doi:10.1029/2011WR010562, Special Issue: Toward Sustainable Groundwater in Agriculture, 2012a.
302. Wada, Y., L. P. H. van Beek, F. C. Sperna Weiland, B. F. Chao, Y.-H. Wu, and M. F. P. Bierkens, Past and future contribution of global groundwater depletion to sea-level rise, *Geophys. Res. Lett*., 39, L09402, doi:10.1029/2012GL051230, 2012b.
303. Wada, Y., M.-H. Lo, P. J.-F. Yeh, J. T. Reager, J. S. Famiglietti, R.-J. Wu, and Y.-H. Tseng, Fate of water pumped from underground causing sea level rise, *Nature Clim. Change*, doi:10.1038/nclimate3001, early online, 2016.
304. Wada, Y., Reager, J. T., Chao, B. F., Wang, J., Lo, M. H., Song, C. and Gardner, A. S., Satellite Altimetry-Based Sea Level at Global and Regional Scales. In

Integrative Study of the Mean Sea Level and Its Components (pp. 133-154). Springer International Publishing, 2017.

305. Wang J, Sheng Y, Hinkel KM, Lyons EA, Drained thaw lake basin recovery on the western Arctic Coastal Plain of Alaska using high-resolution digital elevation models and remote sensing imagery *Remote Sensing of Environment* 119:325-336 doi:10.1016/j.rse.2011.10.027, 2012.
306. Wang J, Sheng Y, Tong TSD, Monitoring decadal lake dynamics across the Yangtze Basin downstream of Three Gorges Dam *Remote Sensing of Environment* 152:251-269 doi:10.1016/j.rse.2014.06.004, 2014.
307. Wahr J., ,Nerem R.S. and Bettadpur S.V., The pole tide and its effect on GRACE time-variable gravity measurements: Implications for estimates of surface mass variations. *Journal of Geophysical Research: Solid Earth* 120(6), 4597-4615, 2015.
308. Watkins, M. M., Wiese, D. N., Yuan, D.-N., Boening, C., and Landerer, F. W., Improved methods for observing Earth's time variable mass distribution with GRACE using spherical cap mascons. *Journal of Geophysical Research (Solid Earth),* 120:2648–2671, doi:10.1002/2014JB011547, 2015.
309. Wenzel M and J Schroter, Reconstruction of regional mean sea level anomalies from tide gauges using neural networks, J. Geophys. Res. 115. doi:10.1029/2009JC005630, 2010.
310. Wessem J. M. et al., Modeling the climate and surface mass balance of polar ice sheets using RACMO2, part 2: Antarctica, *the Cryosphere*, 2017.
311. Whitehouse, P. L., et al., A new glacial isostatic adjustment model for Antarctica: calibrating the deglacial model using observations of relative sea-level and present-day uplift rates, *Geophys Journal Int*., 190, 1464-1482, 2012.
312. Wiese, D. N., Landerer, F. W., and Watkins, M. M., Quantifying and reducing leakage errors in the JPL RL05M GRACE mascon solution. *Water Resources Research*, 52:7490–7502, doi:10.1002/2016WR019344, 2016.
313. Willis, J.K., Chambers, D.T., Nerem, R.S., Assessing the globally averaged sea level budget on seasonal to interannual time scales, *J. Geophys. Res.* 113, C06015. doi:10.1029/2007JC004517, 2008.
314. Wisser, D., S. Frolking, S. Hagen, and M. F. P. Bierkens, Beyond peak reservoir storage? A global estimate of declining water storage capacity in large reservoirs, *Water Resour. Res.*, 49, 5732–5739, doi:10.1002/wrcr.20452, 2013.
315. Whitehouse, P.L., Bentley M.J., Milne G.A., King M.A., Thomas I.D., A new glacial isostatic adjustment model for Antarctica: calibrating the deglacial model using observations of relative sea-level and present-day uplift rates, *Geophysical Journal International* 190, 1464-1482, 2012.
316. Wiese, D., Yuan, D., Boening, C., Landerer, F. & Watkins, M., JPL GRACE Mascon Ocean, Ice, and Hydrology Equivalent Water Height RL05M. 1 CRI Filtered, Ver. 2, PO. DAAC, CA, USA. Dataset provided by Wiese in Nov/Dec 2017, 2016.
317. Wijffels, S. E., D. Roemmich, D. Monselesan, J. Church, J. Gilson, Ocean temperatures chronicle the ongoing warming of Earth. *Nature Climate Change*, (6),116-118,bdoi:10.1038/nclimate2924, 2016.
318. Wöppelmann, G., and M. Marcos, Vertical land motion as a key to understanding sea level change and variability, *Rev. Geophys*., 54, 64–92, doi:10.1002/2015RG000502, 2016.
319. Wouters, B., Bamber, J. Á., Van den Broeke, M. R., Lenaerts, J. T. M., & Sasgen, I., Limits in detecting acceleration of ice sheet mass loss due to climate variability. *Nature Geoscience*, 6(8), 613, 2013.

320. Wouters, B., R. E. M. Riva, D. A. Lavallée, and J. L. Bamber, Seasonal variations in sea level induced by continental water mass: First results from GRACE, *Geophys. Res. Lett.*, 38(3), doi:10.1029/2010GL046128, 2011.
321. Wouters, B., Chambers, D. & Schrama, E., GRACE observes small-scale mass loss in Greenland. *Geophysical Research Letters*, 35, 2008.
322. Wu X., Heflin M.B., Schotman H., Vermeersen B.L., Dong D., Gross R. S., and .others, Simultaneous estimation of global present-day water transport and glacial isostatic adjustment. *Nature Geoscience* 3.9: 642-646, 2010.
323. Yi, S., Sun, W., Heki, K., and Qian, A., An increase in the rate of global mean sea level rise since 2010. *Geophysical Research Letters*, 42:3998–4006, doi:10.1002/2015GL063902, 2015.
324. Zawadzki L., M. Ablain, Estimating a drift in TOPEX-A Global Mean Sea Level using Poseidon-1 measurements, paper presented at the OSTST meeting, La Rochelle, 2016.
325. Zhang G, Yao T, Xie H, Kang S, Lei Y, Increased mass over the Tibetan Plateau: From lakes or glaciers? *Geophys Res Lett*:1-6, 2013.
326. Zemp, M., Frey, H., Gärtner-Roer, I., Nussbaumer, S., Hoelzle, M., Paul, F., Haeberli, W., Denzinger, F., Ahlstrøm, A., Anderson, B., Bajracharya, S., Baroni, C., Braun, L., Cáceres, B., Casassa, G., Cobos, G., Dávila, L., Delgado Granados, H., Demuth, M., Espizua, L., Fischer, A., Fujita, K., Gadek, B., Ghazanfar, A., Hagen, J., Holmlund, P., Karimi, N., Li, Z., Pelto, M., Pitte, P., Popovnin, V., Portocarrero, C., Prinz, R., Sangewar, C., Severskiy, I., Sigurðsson, O., Soruco, A., Usubaliev, R. and Vincent, C., Historically unprecedented global glacier decline in the early 21st century, *Journal of Glaciology*, 61, 745–762, 2015.
327. Zwally, J.H., J. Li, J.W. Robbins, J.L. Saba, D.H. Yi, A.C. Brenner, 2016, Mass gains of the Antarctic ice sheet exceed losses, *Journal of Glaciology*, 61, 1013-1036, doi :10.3189/2015JoG15J071.